ALMA MATER STUDIORUM
UNIVERSITÀ DEGLI STUDI DI BOLOGNA

Dottorato di Ricerca in Scienze Ambientali:

Tutela e Gestione delle Risorse Naturali

XIX Ciclo

Curriculum: Sistemi Ambientali Marini

BIO/04

Phytoplankton physiological responses under changing environmental conditions

Tesi presentata da: Dott.ssa FRANCESCA RONCARATI

Relatore:
Dott.ssa Rossella Pistocchi

Coordinatore:
Prof: Carlo Ferrari

Correlatore:
Dott. Jan Willem Rijstenbil

ANNO ACCADEMICO 2006-2007

INDEX

INTRODUCTION

1. GLOBAL CLIMATE CHANGE: EFFECTS ON MICROALGAE

1.1 WHY AND TO WHAT EXTENT THE GLOBAL CLIMATE IS CHANGING?

Human activities are often the main cause of impacts on the environment, leading to changes on global climate. Even if the planet has experienced significant variations in climate, it seems that the rate at which the present changes are occurring is of a greater importance.

Increase CO_2 concentration. One of the main changes concerns the atmospheric CO_2 concentration, whose levels are rising at an unprecedented rate. Some 5.5 $\pm$ 0.5 Pg C (1 Pg = 10^{15} g.) is released annually from fossil fuel combustion, and land-use changes and deforestation release a further 1.6 $\pm$ 1 Pg C yr^{-1}. The major sink for anthropogenic CO_2 emissions is represented by oceans, accounting for up to 30% of emissions since the Industrial Revolution 3.8 Pg yr^{-1} of anthropogenic C released has been removed by oceans trough a combination of photosynthesis (~ 1.8 Pg yr^{-1}) and abiotic absorption of CO_2 (~ 2 Pg yr^{-1}), (Behrenfeld *et al*., 2002). Despite these activities the atmospheric CO_2 pool is currently increasing by ~ 3.3 Pg C yr^{-1} (Beherefeld *et al*., 2002). This rapid increase has occurred over the last 200 years from a value of 280 ppm (28 Pa) in 1800 to ~ 370 ppm (37 Pa) at present, with most of the increase occurring over the last 100 years (Houghton *et al*., 1990). Finally, the most likely scenario is for a two to threefold increase in atmospheric CO_2 concentration over the next century, even if it is dependent on the inputs for growth in the CO_2 emissions used, (Beardall *et al*.,1998). The algal components of oceans and freshwater ecosystems are responsible for a high proportion of the net global primary productivity; of the net 111-117 Pg C assimilated annually, oceanic phytoplankton account for up to 59 Pg or 50% of the global total (Behrenfeld *et al*., 2001). Due to the importance of algal photosynthesis in the global carbon budget, it is thus necessary to understand how algae will react to the changes, in atmospheric CO_2, predicted to take place over the next century and beyond, (Beardall and Raven, 2004). As a consequence of the predicted increase in gaseous CO_2 (100 Pa in 2100) there will be an increase in dissolved CO_2

leading to a decrease in pH. The equilibria between the DIC species will shift, so that there will be only minor changes in bicarbonate and carbonate concentrations (Stumm and Morgan, 1981). The fact that the CO_2 concentration will change but without variations in HCO_3 concentration may have repercussions for the ability of aquatic plants to acquire inorganic carbon under elevated CO_2, (Beardall and Raven, 2004). Most of the aquatic plants are C_3 plants using ribulose bisphosphate carboxylase-oxygenase (RUBISCO) as primary CO_2-fixing enzyme in carbon assimilation. This enzyme has a poor affinity for CO_2 and at present-day CO_2 levels is less than half saturated. The poor efficiency of RUBISCO is increased by its dual role as an oxygenase and the extent to which the two competitive reactions of RUBISCO occur is related to the O_2 and CO_2 concentrations at the RUBISCO active site. Due to these characteristics of RUBISCO enzyme, some organisms have evolved active systems to transport and accumulate inorganic carbon and hence increase the CO_2 concentration at the active site of RUBISCO, (CCMs, CO_2 Concentrating Mechanisms). CCMs utilization suppresses the oxygenase and stimulates the carboxylase activity of the enzyme. The activity of CCMs is driven by adenosine triphosphate (ATP) derived from photosynthesis and it is energetically demanding (Raven *et al*., 2000). Moreover, CCMs are regulated by a number of factors, including light intensity and spectral quality, nutrients status and environmental factors that affect the availability of CO_2. Experiments based on measurements on the effects of changing CO_2 concentration for growth on CO_2 and HCO_3^- transport, have reported results specie-dependent, (Burkhardt *et al.*, 2001). In any case Burkhardt speculated that CO_2 transport may be less energetically demanding than that of HCO_3^-, so that cells may save energy for growth, for instance, using the active CO_2 transport system as external CO_2 levels rise. It is clear that organisms with different photosynthesis responses to inorganic carbon concentration are likely to respond differently to current and future changes in CO_2. Several experiments address the question of changes in species composition in relation to bicarbonate use and CCM capacity, (Talling, 1985; Tortell, *et al*., 2002).

Temperature Increase. Increases in CO_2 have been predicted to result in an increase of 2-3 °C in average surface oceanic temperature. At higher latitudes the temperature rise is predicted to be even larger, (Houghton *et al.*,

1990, 2001). Higher water temperature will lead to a stimulation of metabolic activity and growth, provided that the algae concerned are adapted or acclimated to an optimal higher than the current water temperature and that growth is not limited by other factors. Suzuki and Takahashi (1995) studied the response of a range of diatom species in culture exposed to different temperatures; they observed that the maximum growth rate occurred at temperature close to that of the environment from which the cells had been isolated. These results suggest that temperature can exert a significant control on species distribution in nature; in fact, seasonal differences in response to temperature and light have been thought to play a part in structuring phytoplankton population composition and succession. Several works for instance, show that different size classes of microalgae respond differently to temperature, (Malone, 1977; Andersson *et al.*, 1994).

Climate changes may lead to indirect effects of temperature on a broader scale. It has been hypothesized that changes in temperature could alter the patterns of upwelling events and consequently modify the occurrence of associated phytoplankton blooms (Hughes *et al.*, 1996). Changes in water temperature also modify vertical stability of the water column and cause a decrease in the upward transfer of nutrients from deep waters to the surface (Goffart *et al.*, 2002). In conclusion, warming of surface waters over the next century could reduce upwelling and decrease primary production of phytoplankton, thus reducing the flux of C from atmosphere to the ocean. Moreover, it may influence the depth of the upper mixed layer, thus altering the supply of PAR in phytoplankton cells, (Beardall & Raven, 2004).

Ultraviolet Radiation Increase. Approximately 9% of the solar radiation is comprised from 100 to 400 nanometers. The Ultraviolet Radiation is arbitrarily divided into UVC (200-280 nm), which are almost totally absorbed by the stratosphere, UVB (280-315 nm) and UVA (315-400 nm). The dominant factor affecting UVB radiation is the Sun's angle rays through the atmosphere; it consists in the angle between the vertical and the center of the solar disc, (SZA, solar zenith angle). For this reason the minimal angle occurs at the tropics at times where the sun is directly overhead and consequently maximal UVB irradiances occurs. A second major factor influencing surface UVB is cloud

cover, which can reduce strongly the UVB reaching the surface. However, UVB radiations are strongly absorbed by ozone in the stratosphere and this absorption depends on the path length as well as concentration of ozone. Any variation in ozone can affect the UVB radiation received at the surface. In the last decades many efforts have been done to understand and measure ozone changes and concentration. The Antarctic ozone hole has remained similar to that during the 1990s and has continued to appear each spring. In the Artic the hole is less severe than in Antarctic, and the ozone depletion is more dependent on year-to-year variability in wind patterns. Outside the Polar Regions, ozone losses are less severe. Relative to 1980, the 1997-2000 losses in total ozone are about 6% at southern mid-latitudes on a year-round basis. At northern mid-latitudes the ozone losses are about 4% in winter/spring and 2% in summer/autumn. In the tropics, there have been no significant changes in column ozone. The averaged global ozone loss is approximately 3%, (McKenzie *et al.,* 2003). Several studies have demonstrated the inverse correlation between ozone and UV, not only in Artic and Antarctic (Hofmann and Deshler,1991; Vincent and Roy, 1993), but also in the Northern Hemisphere such as France and northern Italy (Blumthaler and Ambach, 1990). However the detection of long-term trends in UV is very problematic due to its dependence, other than ozone, to clouds, aerosols and surface albedo, all of which exhibit large variability, (Chubarova *et al.*, 2000; Borkowski 2000; Zerefos *et al.*, 1997). Although the declining in chlorofluorocarbons (CFC) as a consequence of the Montreal Protocol and the predicted future recover of ozone and hence of UVB, the WMO Scientific Assessment Report stated that the ozone layer will remain vulnerable for the next decades or so (McKenzie *et al*., 2003). One current model predicts that increasing depletion of stratospheric ozone may continue until at least 2020, (Salawitch, 1998).

In the next paragraph the effects of UVB radiation on microalgae, its mode of action in determining oxidative stress and reactive oxygen species production will be described in more details.

1.2 UV-B DAMAGE MECHANISMS IN ALGAE AND REPAIR-DEFENCE PROCESSES.

Phytoplankton explicate a very important biological function in the food trophic chain as primary producer and any change in growth, photosynthetic efficiency or community dynamic can have indirect effects on the consumers at higher trophic levels. Because of the requirement for light, the phytoplankton move into the upper layers of the water column and thus is exposed to solar radiation and hence UV radiation. Turbid coastal waters with a substantial amount of suspended materials offer a good filtering (Vosjan and Pauptit, 1992). Although the impact of increased doses of UV-radiation on organisms is not fully understood, many phytobenthic organisms living in intertidal as well as in the upper subtidal zone of coasts are strongly affected (Franklin and Forster, 1997) and changes in macroalgal community structure and decrease in marine productivity are likely (Häder, 1993; Bischof *et al*., 2000). UV radiation at the cellular level can directly express its toxicity either trough primary mechanisms, which are depended on the absorption in the UV region of certain biomolecules (proteins and nucleic acids), or trough secondary mechanisms, such as UV absorption by intermediate compounds, inside or outside the cell, that lead to reactive oxygen species (ROS) production.

Direct mechanisms. Nucleic acids absorb maximally in the UV-C range, with a peak absorbance around 260 nm and exhibit a tail that extends well into the UV-B region. This absorbed energy results in the first excited singlet state, with a lifetime of only a few picoseconds. Most of this energy is dissipated by radiationless processes inside the molecule, but a small fraction is available for a variety of chemical reactions. This can result in photodestruction of nucleotides, with a two to four-fold greater effect on pyrimidines (thymine and cytosine) relative to purines (adenine and guanine). UV-induced reactions cause the production of three principal photoproducts: (a) pyrimidine dimers, (b) photohydrates and (c) (6-4) photoproducts, each of it can be source of different effects.

Pyrimidine dimers can result in mutation, and more importantly in the short term, they can cause the RNA polymerase to stall during transcription. There are evidence that the polymerase remains bound to the dimer, thus

reducing the overall concentration of free RNA polymerase, (Britt, 1996). Photohydrates dehydrate at a time scale of hours and appear to have little toxicological effects. The (6-4) photoproduct is much more damaging than the other two products, it is 300 time more effective at blocking transcription by DNA polymerase, (Mitchell & Nairn, 1989). Moreover it can not be excised and repaired by enzymatic photoreactivation, causing long term effects on transcription and replication, (Brash *et al.*, 1985). DNA damage has been observed in a wide range of aquatic species exposed to UV-B radiation, including microalgae (Buma *et al.*, 1996a), zooplankton (Malloy *et al.*, 1997) and bacterioplankton (Jeffrey *et al.*, 1996). Diatoms exposed to UV-B have shown an increase in cell size, pigment, proteins and carbohydrates content per cell, (Karentz *et al.*, 1991; Buma *et al.*, 1996b). This appears to be associated with an arrested or prolonged cell cycle in which the DNA synthesis phase is extended while the UV-induced dimers are removed by DNA repair mechanisms (Buma *et al.*, 1996a).

Proteins are another target of UV-B due to the presence of chromophores within the protein which absorb in the UV region; this lead to the production of a photosensitiser and the subsequent reaction that cause photo-oxidative break-down or cross-linking of amino acids. This is the sequence hypothesized to be involved in the decrease and damage of RUBISCO enzyme. The primary carbon fixation enzyme seems to be strong affected by UV-B radiation and to a greater extent than other components of photosynthetic apparatus, such as photosystem II reaction center complex (PSII). However, several studies have indicated a variety of sites of damage in the PSII: the primary electron acceptor Qa, the primary charge separation at P680, the primary donor to PSII, Z, and the water oxidizing complex, (Melis *et al.*, 1992; Vass, 1997). *In vivo* conditions, PSII activity in plants is maintained trough a rapid turnover of the protein D1, which explicates a pivotal role within the PSII in binding all primary donors and acceptors active in electron transport. All the sites mentioned above are connected to the D1 protein. Damage to D1 occurs at any irradiance regimes and is efficiently repaired by proteolytic breakdown of damaged D1 and replacement with a newly synthesized protein (Matoo & Edelman, 1987) resulting in turnover of active PSII. This process is known as PSII repair cycle and ensures that there is little net loss of PSII activity under a

wide range of irradiance conditions. Finally, even though net damage to PSII may not be evident during UV exposure, UV damage to PSII could take its toll through the additional metabolic overhead incurred due to faster turnover of D1 (Raven and Samuelsson, 1986).

Direct damage to pigments is well observed under UV exposure in a wide range of biological systems, including the light harvesting apparatus of diatoms (Buma *et al.*, 1996b), cyanobacteria (Quesada and Vincent, 1997), macroalgae (Döhler *et al.*, 1995). Pigment bleaching can result from different mechanisms. Certain protein-based pigments absorb UV energy directly and undergo to photochemical degradation. The light harvesting phycobiliproteins of cyanobacteria appears to be especially sensitive to UVB, in fact phycobiliproteins account for a high percentage of total protein content and they have a high UV absorbance. This suggests that these pigments are an early site of action of UVB radiation and that these UV effects may play a more important role than DNA damage in these organisms (Lao & Glazer, 1996). Many natural pigments such as chlorophylls and phaeophytins, act as a photosensitisers; they absorb radiation and they are exited to a higher energy level, this energy can than be transferred to ground state oxygen ($^3O_2$) and then to singlet oxygen ($^1O_2$) which in turn can have a wide range of destructive effects. Finally, during UV exposure reactive oxygen species (ROS), other than singlet oxygen, are formed and they can cause oxidative degradation of pigments as well as other biomolecules. One class of pigments, the carotenoids, react with ROS and can then be regenerated by natural reduction processes; thus carotenoids explicate a very important function as natural quenching agents of ROS, protecting the cell against UV damage. Many other processes inside the cell are likely to be affected by UVB radiation, such as cell motility, nutrient uptake and nitrogen fixation. Little attention has been given to the physiological effects of UV damage on respiration, even if the few results available indicate considerable variation between species.

Indirect mechanisms. The production and subsequent activity of reactive oxygen species is a key element in UV toxicity. ROS are highly reactive oxidants and are formed by cellular processes under PAR and even in the dark, by a variety of physiological mechanisms. Nevertheless their rate of production

inside and outside the cell is greatly accelerated in the presence of UV radiation. Once a ROS is formed, various fast reactions occur and the resultant photoproducts can be much more reactive and cytotoxic than either their precursors or the direct effect of UV radiation. The nature of these fast reactions is determined by chemical properties of the cell in the vicinity of ROS production, in particular pH, metal concentrations and the presence of lipids.

One of these important ROS is hydrogen peroxide (H_2O_2), produced photochemically both within the cell of aquatic organisms and in the surrounding environment. The main photochemical pathway is by dismutation from superoxide:

$$O_2 + h\nu \longrightarrow O_2^{-\cdot} \longrightarrow H_2O_2$$

Hydrogen peroxide is less reactive then many other ROS and therefore has a relatively long half-life that allows it to diffuse well away from the site of photoproduction. H_2O_2 may exert its toxicity trough direct reaction with biomolecules (proteins, nucleic acids and pigments) or trough Fenton reaction (that will be described more in details in the next chapter), which lead to hydroxyl radicals formation. The latter ROS is a much more reactive oxidant, in fact its half-life is very short, in the range of nanoseconds.

Interaction between UV radiation and oxygen determines the production of the superoxide radicals ($O_2^{-\cdot}$), a ROS which can react with many biomolecules in several ways. It can react directly with pigments, proteins, ascorbate and sugars; in intracellular environments reach in protons, such as the surface of biological membranes, $O_2^{-\cdot}$ undergo a reaction to form hydroperoxyl radical ($HO_2^{\cdot}$), a much stronger oxidant than its precursor, and that can directly attack polyunsaturated fatty acids in membranes; finally, it can react with hydrogen peroxide in the already mentioned Fenton reaction.

Due to the high occurrence of reactive oxygen species inside the cells, which are formed during many of the physiological processes, organisms have evolved a variety of responses to counteract the negative effects of these molecules. A series of enzymes are involved in cell detoxification from superoxide radical and hydrogen peroxide. The first ROS is neutralized trough superoxide dismutase enzyme (SOD) which consists of a group of metalloisoenzymes able to convert $O_2^{\cdot -}$ into oxygen and H_2O_2. Copper, zinc and

manganese are the associated metals. Hydrogen peroxide is then converted into water and oxygen by two other antioxidant enzymes: catalase and ascorbate-peroxidase. Catalase provides a very efficient mechanism to remove H_2O_2 without consuming cellular reducing equivalents and therefore cellular energy. Ascorbate-peroxidase (APX) is a heme-containing protein which catalyzes the reaction between ascorbate and hydrogen peroxide to form water and monodehydroascorbate. It requires a substrate (ascorbate) and it is very efficient in remove H_2O_2 from chloroplasts. Several studies have measured the activity of these key enzymes of cell detoxification, often observing an increased activity under stress conditions.

Finally, UV radiation can indirectly damage membranes trough production of radicals, such as hydroxyl ions, which can then initiate a chain reaction on unsaturated fatty acids leading to formation of lipid peroxides.

In conclusion, the high UV reactivity of many biomolecules (nucleic acids, lipids, proteins), means that all cell types and organisms are susceptible to the toxic effects of UV radiation. The magnitude of damage, however, is highly dependent of many factors: efficiency of protection and repair strategies, intensity of exposure, spectral irradiance, duration of exposure and interaction with other variables.

2. HEAVY METALS IN THE ENVIRONMENT: BIOAVAILABILITY AND EFFECTS ON ALGAE

2.1 SOURCES AND DISPERSION IN THE AQUATIC COMPARTMENT, INTERACTIONS WITH THE BIOTA.

Metals can occur naturally and several of them are essential components of global ecosystems. Depending on their oxidation states metals can be highly toxic to many organisms. Environmental pollution and human activities have lead to increasing concentrations of those elements; the main sources of metals are mining and industrial activities, urban runoff, sewage treatment plants, agricultural runoff, boating activities and others. Many studies have evaluated the toxic effects of certain metals on the biota. Copper pollution in a bay in Massachussetts determined a drastic decline in phytoplankton richness, (Pospelova *et al.*, 2002). Heavy metals such as Hg, Cu, Pb and Cd were observed to inhibit photosynthesis in the green alga *Chlamydomonas*, (Wundram et al., 1996). Oceanic surface waters generally present low concentration of heavy metals which arrive there by atmospheric transport and upwelling. Different is the situation of coastal waters, which receive inputs from rivers runoff and the polluted sewage outlets due to the vicinity to urban centers and industries. Moreover, it seems that nutrient availability, (particularly nitrogen), dramatically increase the ability of algae to accumulate heavy metals (Wang and Dei, 2001a, b), suggesting that agricultural runoff into fresh waters and coastal areas can greatly increase the entry of heavy metals into the food chain.

Trace metals are of environmental interest both as limiting nutrient (Fe, Zn, Mn, Cu, Co, Mo, Ni) and as toxicants; toxic metals include Cd, Hg, Ag, Pb, Sn, Cr, although many nutrient metals can also act as toxicants at elevated concentration (Zn, Cu and Ni). Toxic metals generally enter the cell through the transport systems of nutrient metals and they often displace nutrient metals from their metabolic sites, thus explicating their toxicity. Thus, it is important to consider the interactions between toxic and nutrient metals to be able to understand the mechanisms regulating the uptake of these metals, (Sunda, 1988). Several mechanisms have been proposed to explicate the entry of toxic

metal ions into cells, (Van Ho *et al.*, 2002). One is described as molecular mimicry, whereby metals either compete for binding to multivalent ion carriers (such as Ca^{2+} channels) or, after binding to low molecular weight thiols (such as cysteine), enter the cell by active transport (for example using amino acid transporters), (Pinto *et al.*, 2003). The heavy metals can cause membrane depolarization and acidification of the cytoplasm (Cumming & Schimid, 2003) and in fact membrane injury can lead to disruption of cellular homeostasis. Thus cells have evolved adaptations such as exudation of chelating compounds and active efflux of metal ions by primary ATPase pumps to provide some degree of metal tolerance, (Rosen, 1996).

Algae are the basis of the food web in all aquatic ecosystems, they are the major primary producers and constitute the main food source for bivalve, mollusks, zooplankton and larval stages of some crustaceans and fishes. Any stress which alters the algal cell's biochemical composition will have an impact on its food value. Moreover, algae also bio-accumulate the heavy metals, through the action of chelators which store the metal ions and thus metals may be also accumulated in the food chain.

2.2 HEAVY METALS-INDUCED OXIDATIVE STRESS

As already stated in the first chapter, reactive oxygen species occur transiently in aerobic organisms and can be very harmful at high concentrations. Many environmental factors can induce oxidative stress in the cell by generation of the superoxide anion ($O2^{\cdot-}$) and therefore, modulation of the antioxidant levels constitutes an important adaptative response to face adverse conditions. Indeed, maintenance of a high antioxidant capacity in cells has been linked to increased tolerance against different environmental stress (Thomas *et al.*, 1999). Pollutants metals are involved in several types of ROS-generating mechanisms (Fig.1), (Stohs and Bagchi, 1995). In this paragraph copper and cadmium toxicity will be discussed more in details as their effects were studied in the experiments described in this thesis.

Copper is widely distributed in nature and is an essential element. It is a common co-factor for many enzymes including oxidases and oxigenases. In some algae and higher plants is part of the superoxide dismutase enzyme (Cu-

Zn-SOD), it is part of the mobile electron carriers such as copper-containing plastocyanin (Raven *et al.*, 1999). Similar to iron, copper acts as a catalyst in the formation of ROS and catalyzes peroxidation of membrane lipids. Cu^{2+}, as also Fe^{3+}, participates in the Haber-Weiss cycle, producing $^{\cdot}OH$ from $O_2^{\cdot -}$ and H_2O_2, (Winterbourn, 1982), through these reactions:

$$Cu(II) + O_2^{\cdot -} \longrightarrow Cu(I) + O_2$$

$$Cu(I) + H_2O_2 \longrightarrow Cu(II) + {}^{\cdot}OH + OH^-$$

$$2O_2^{\cdot -} + 2H^+ \longrightarrow H_2O_2 + O_2$$

Copper was shown to significantly accelerate the oxidation of hydroquinone and enhance the formation of DNA strand breaks, (Li *et al.*, 1993b). Glutathione (GSH) was shown to inhibit free radical formations by copper ions due to its ability to stabilize copper in the Cu(I) oxidation state, preventing redox cycling and the generation of free radicals, (Milne *et al.*, 1993). The already discussed role of SOD, catalase and ascorbate peroxidase enzymes is of a great importance even in the dismutation of ROS generated by metals such as copper.

Cadmium is an abundant non essential element that is mainly accumulated in the environment as a result of industrial practices. It is widely used in electroplating and galvanizing, as a color pigment in paints and in batteries. It is a byproduct of zinc and lead mining and smelting. Its toxicity mechanism it is still not clear; cadmium does not appear to generate free radicals, but it does elevate lipid peroxidation soon after exposure, (Muller, 1986). Cadmium and the other metals without redox capacity, such as Pb^{2+} and Hg^{2+}, can enhance the pro-oxidant status by reducing the antioxidant glutathione pool, activating calcium-dependent systems and affecting iron-mediated processes. These metals can also disrupt the photosynthetic electron chain leading to $O_2^{\cdot -}$ and single oxygen ($O_2(^1\Delta_g)$) production (Asada and Takahashi, 1987). Thus, algal tolerance to heavy metals pollution is likely to depend on defense responses that prevent oxidative insult. Algae have evolved a wide range of protective mechanisms to remove ROS such as low molecular weight compounds (GSH, carotenoids, ascorbate and tochopherols) and

enzymatic catalysts of high molecular weight (SOD, CAT, glutathione reductase and others).

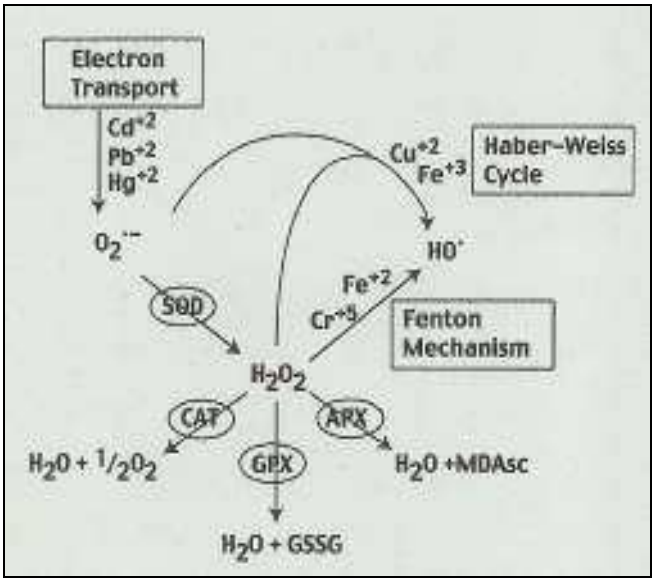

Fig. 1: Heavy metals stress induces cellular generation of ROS, (from Pinto *et al.*, 2003).

GOAL OF THE THESIS

The aim of this research was to understand the phytoplankton behavior and adaptation under environmental changing conditions, in particular we focused on three specific aspects.

The first one was to evaluate which and to what extent physiological changes can occur in the diatom *Cylindrotheca closterium*, (a widespread and abundant species of marine water bodies and sediments), under several stress conditions. Those conditions were chosen considering the main environmental stress factors that the diatom can experience in the field: high and ultraviolet radiation, hypersalinity and metal contamination, alone and in combination. Cellular stress responses was considered from many points of view: cellular growth, photosynthesis, oxidative damage, repair mechanisms and inorganic carbon assimilation capacity. Experiments were conducted on three different isolates: two of them were supplied from laboratories one in the Netherland and one in Australia, while we collected the third strain from the sediments of an italian backwater lagoon, (Pialassa Baiona, Ravenna).

The second goal was to estimate how these cellular responses could affect the phytoplankton community in reaction to global environmental changes (increase UVB, heavy metals etc.).

Third, we wanted to identify and evaluate some cellular response as a marker of environmental stress.

A general introduction is given in chapters 1 and 2. All the methods used are described in chapter 3, while the discussion of the obtained results is offered in chapters 4, 5 and 6.

Chapters 4, 5 and 6, describing different experiments, were organized as single manuscripts, each of them having its own introduction, description of the experimental set up, results and detailed discussion.

In chapter 4, the effects of high photosynthetically active radiation (PAR), ultraviolet radiation and hypersalinity were analyzed both alone and in combination. In chapter 5, the toxicity of sublethal levels of copper and cadmium was evaluated, while chapter 6 focused on the effects of cadmium and ultraviolet radiation and their interactions. In this last experiment a green alga, *Dunaliella tertiolecta*, was also considered for comparison.

MATERIALS AND METHODS

3. Section 1

3.1.1. Growth and photosynthetic parameters measurements (F_v/F_m, Φ'_m, rETR)

Kinetics and parameters of photosystem II (PSII) can be measured by means of pulse-amplitude modulated fluorometry (PAM) (Juneau & Popovic, 1999; Lavorel & Etienne, 1977). Mini-PAM (H. Walz, Effeltrich, Germany) was used to follow the growth of *Cylindrotheca closterium* cultures and to measure the maximum quantum efficiency of PSII charge separation. The minimal fluorescence (F_o) and the maximum fluorescence (F_m) were measured on dark adapted cultures for 15 min. Settings: Light emitted diode gave a measuring light intensity of 0.15 µmol $m^{-2}s^{-1}$ PAR, modulation frequency 0,6 kHz. Halogen lamp gave saturation light pulses of 6000 µmol $m^{-2}s^{-1}$ PAR, with a duration of 0.4 s. F_o values (which are proportional to algal biomass) were used to check culture growth and to ensure that the experiment was carried out with cultures still in their exponential phase. The maximum energy conversion efficiency, or quantum efficiency, of PSII charge separation (F_v/F_m) is calculated as: $F_v/F_m = (F_m - F_o)/F_m$ and was measured both during growth and during the three days exposure to light in mode A, B, C (twice a day, at 08:00 and 18:00h). In the course of the 72 hours treatment, 15 min dark adapted suspensions of *C. closterium* were used to measure relative electron transport rate (rETR) in actinic irradiance (8 steps, one every 30s, from I= 6 to 183 µmol m^{-2} s^{-1}) using the Mini-PAM. Relative linear electron transport rate is $rETR = I * \Delta F/F_m'$, where Φ'_m is steady-state quantum yield read under illuminated conditions (Rijstenbil, 2003). The data obtained from the rETR-curves were fitted with the Jassby and Platt model (Platt *et al*., 1980):

$$rETR = rETR_{max}(1-e^{-\alpha ETR*I/ETRmax}) * e^{-\beta ETR*I/ETRmax}$$

where α and β represent the initial slope of the growth curve and the photoinhibition parameter, respectively.

3.1.2. Lipid hydroperoxides (LPO)

After three days under the three different light conditions (modes A, B, C), 100 ml of algal culture were filtered and, immediately after, cells were scraped off the filter, divided into two parts and transferred into an extraction buffer (0.7 ml cold methanol). Cells were sonicated for 3 min (on/off: 30/40s, to avoid an excessive warming of cells) at an amplitude of 14 μm. The extract was centrifuged (4,500×g) and used for analysis of LPO. Lipid peroxidation was determined based on the formation of a Fe(III) xylenol orange complex measured at 560 nm, (Hermes-Lima, 1995; Boscolo *et al*., 2003). 50 µl of extract was added to 450 µl of reaction mixture (25 ml of 1 mM $Fe(NH_4)_2(SO_4)_2$, 10 ml of 1.1 mM perchloric acid, 10 ml of 1mM xylenol orange). After 1 h dark incubation samples were read at 560 nm (Pharmacia Biotech Novospec II); the amount of lipid peroxides was expressed as nmol LPO (mg lipid)$^{-1}$.

Lipid content (unsaturated, total) was measured with the sulfo-phospho-vanillin method, (Knight *et al*., 1972; Izard & Limberger, 2003). Concentrated sulfuric acid (2 ml H_2SO4) was added to a blank in a tube containing 100 μl of 80% methanol, to tubes with triolein standard (100 μl), and to tubes with 100 μl of sample supernatant. Each tube was incubated for 30 minutes at 100°C, and next cooled down to room temperature in a water bath. After the addition of 5 ml of PV-reagent the tubes were incubated at room temperature for 15 min. Absorbances were read on a spectrophotometer at 530 nm (Pharmacia Biotech Novaspec II).

3.1.3. Determination of protein carbonyl groups

The presence of carbonyl groups in amino acids residues is a hallmark for oxidative protein damage. The used method is based on the reaction between carbonyl groups and 2,4-dinitrophenylhydrazine (DNPH) to form 2,4-dinitrophenylidrazone (max. absorbance at 366 nm) (Levine *et al*., 1990). 150 ml of culture suspension was filtered onto a 0.45 μm cellulose acetate filter and stored at -80° C. Cells were scraped off the filter, divided over three Eppendorf cups and sonicated in 0.7 ml PBS buffer (on/off 30s/40s; 3 min at 18 μm amplitude; energy output 90 W). Procedure: proteins were precipitated by adding HCl-acetone (1:33) and then centrifuged (5 min; 4°C); the pellet was

washed twice with HCl-acetone to remove all chromophores that can interfere with the absorption of the product (DNPH). Samples were washed once with 20% TCA solution and then centrifuged (5 min, 4°C) to remove HCl-acetone. Pellets were divided in two parts, one was used as blank the other as sample; reaction between samples and DNPH (10 mM) was allowed to occur for 1h in the dark. To remove the excess DNPH, pellets were washed with ethanol-etylacetate, (1:1), until the yellow colour in the supernatants vanished. Pellets were evaporated under vacuum (10 min; 45 °C), then dissolved in guanidin-HCl (6 M in 20 mM phosphate buffer at pH 2.3) and kept in a water bath (30 °C; 15 min). Supernatants were transferred into disposable cuvettes to read the absorbance of blanks and samples at 280, 260 (UVIKON 940) and 366 nm (Pharmacia Biotech Novaspec II). The absorption at 280 nm of the blanks was subtracted from the absorption of the samples and then quantified on the basis of a calibration curve with albumin from bovine serum dissolved in guanidin-HCl (0.5-5 mg ml^{-1}), as follows: carbonyl content = ((abs sample- abs blank)/ε)/mg protein, where ε=22000 M^{-1} cm^{-1} is the molar extinction coefficient; carbonyl content was expressed as nmol carbonyl mg^{-1} proteins.

3.1.4. Determination of Superoxide Dismutase activity (SOD)

After three days of exposition to the experimental light conditions (mode A,B,C), algae were collected and 150 ml cell suspensions filtered on a 0.45 μm cellulose acetate filter. Cells were scraped off the filter, divided in two parts and transferred into 0.7 ml of a buffer (50mM KH_2PO_4 with 0.1 mM EDTA, pH 7.0), then sonicated for 3 min on ice at an amplitude of 14 μm. Homogenates were centrifuged for 20 min at 4°C at 7000 g. Supernatant was used for the activity measurements, while subsamples (50 μl, in duplicate) were stored at -20°C for protein analysis with BioRad® reagent (Bradford, 1976), as SOD activity was normalized to protein. Determination of SOD activity was based on the principle that the superoxide radicals (O_2^{*-}) generated in the xanthine - xanthine oxidase reaction will reduce cytocrome c and that SOD will inhibit this reduction (McCord & Fridovich 1969). SOD catalyzes the reaction $O_2^{*-} + 2H^+ \rightarrow O_2 + H_2O_2$. In the assay, O_2^{*-} can react in three ways: (a) reduction of cyt-c: O_2^{*-} + cyt-c-Fe^{3+} ; (b) spontaneous disproportionation: $O_2^{*-} + O_2^{*-} + 2H^+ \rightarrow O_2 + H_2O_2$; (c)

disproportionation catalyzed by SOD. The formation of cyt-c-Fe3+ causes an absorption increase at 550 nm, while SOD inhibits this increase by removing O_2^{*-} radicals. The specific activity of SOD in the samples is expressed as enzyme units (U mg^{-1} protein), where a SOD unit is defined as the amount of extract required to inhibit ferricytocrome c by 50%. Reagents: 0.3 mM xanthine (Sigma) solution (0.25 ml of 6 mM stock solution of xanthine plus 4.75 ml of extraction buffer); 60 μM cytocrome c solution in the extraction buffer; Xanthine oxidase solution of 40 units/8.5 ml diluted five times in the extraction buffer.

Procedure: Blanks were prepared in duplicate, pipetting the following solutions in this order into disposable semi-microcuvettes (total volume 1.5 ml): 0.98 ml of buffer, 0.25 ml of xanthine solution and 0.25 ml of cyt-c solution. To the samples 0.78 ml, 0.25 ml and 0.25 ml of the same solutions as for blanks were added, plus 0.25 ml of algae extract. Blanks and samples were than incubated for 10 min at 25 degrees. After this first step, 0.02 ml xanthine oxidase solution were added both to samples and blanks. The activity was measured for 3 min at 550 nm and 25 ^oC (Pharmacia Biotech 4000 UV/VIS with thermostat). The slope of the blank absorption has to be ± 0.025 AU min^{-1}; the percentage of inhibition (I) is calculated as $I = (1- (\Delta A_{sample}/\Delta A_{blank})) *100$ where ΔA_{sample} and ΔA_{blank} are the absorption change in the sample (containing the extract) and in the control respectively. The volume to be pipetted has to be adjusted in such a way that the inhibition is 50-60% of the control but the summed volume of the buffer and the extract must remain 0.98 ml. The formula used to calculate the volume needed to obtain the 50% inhibition (V_{50}) is: $V_{50} = V_{sample} * 50\% / I$, where V_{sample} is the volume (ml) of the sample with an inhibition of I (%). At last, the specific activity of SOD in the sample is calculated as: $S.A. = 1/ (V_{50} * [protein])$ and is expressed in Unit $(mg\ protein)^{-1}$.

3.1.5. Calculation of cell volume

Lenghts (l) and widths (w) of 50 cells $samples^{-1}$ were measured with a microscope (Olympus A031, 40x objective), a video camera (JVC) attached to a computer with a frame grabber and the image analysis package Qwin (Leica). Cell volumes (μm^3) was calculated as: $l/3 \times \pi \times (w/2)^2$, considering the shape of *C. closterium* as a double cone; this method was used also in Rijstenbil (2003).

3.1.6. Analyses of malondialdehyde (MDA), reduced (GSH) and oxidized glutathione (GSSG)

At the end of the exposition period (72h) replicates (n=2) of cell cultures grown under all light conditions (low, high PAR, high PAR with UVB) and at both salinities (30 and 60) were sampled. 230 ml of cell suspension in each Petri dish were filtered onto a 0.45 μm cellulose acetate filter and then stored at -80°C until analysis. Malondialdehyde (MDA), and reduced and oxidized glutathione (GSH, GSSG) were analyzed in four sub-samples for each condition. GSH and GSSG concentrations in the cell extracts were analyzed with reversed-phase HPLC using the precolumn labeling method with monobromobimane (mBrB) after Meuwly & Rauser (1992). The method is described in detail in Rijstenbil & Wijnholds (1996). GSH and GSSG were calculated as μmol GSH (L cell volume)$^{-1}$. The glutathione redox ratio, defined as GSH/(GSH+0.5*GSSG), was derived from the values of GSH and GSSG in the same subsample (i.e. under the same culture condition). Malondialdehyde (MDA) is a secondary product of the lipid peroxidation. At a physiological pH the anion MDA forms a pink complex with thiobarbituric acid (TBA) that can be quantified spectrophotometrically from its absorbance (E_{max} at 532 nm). The method used here, was described in detail in Rijstenbil (2001). MDA concentrations were derived from the peak areas of the calibration series and expressed as μmol MDA (L cell volume)$^{-1}$.

3.1.7. Statistical analysis

The SNK test was used to determine the significant differences between group means within the ANOVA setting; Cochran's test was used to check homogeneity of variances. Statistical analyses were performed in GMAV5.

3. Section 2

3.2.1 Collection and isolation of *Cylindrotheca closterium*

The diatom was isolated from natural phytoplanktonic associations of sediments of an inner channel of the backwater lagoon, Pialassa Baiona (Ravenna, Italy) on December 2004. Light microscopy pictures are shown in Appendix A. Cultures were maintained axenically in enriched artificial sea water (ESAW medium), (Berges *et al*., 2001), at the salinity of 30 and at the temperature of 19°C. The recipe of ESAW medium is described in the Appendix C. Medium preparation consisted of different steps: at first, all the salts were dissolved in distilled water, then the seawater salts solution was passed trough an ion exchange column (Chelex-100 resin, Bio-Rad Laboratories) to remove all the trace metals impurities present in the salts. Then, the artificial sea water was autoclaved and stabilized for one day at room temperature, before to add all the micro- and macronutrients following the recipe. Impurities introduced from the materials (flasks, etc) have been minimized by soaking all vessels in 1N HCl.

3.2.2. Molecular characterization and phylogenetic analysis of *Cylindrotheca closterium*

DNA extraction, polymerase chain reaction amplifications and sequencing

45 ml of monospecific culture were centrifuged at 6000xg for 10 min, then pellet was resuspended in 420 µl of Nuclease-Free water; the DNA was extracted three times with phenol-chlorophorm using the protocol described by Godhe *et al*., 2001. The quality and amount of genomic DNA was controlled on an agarose TBE gel before polymerase chain reaction (PCR).

The D1 and D2 domains of large sub-unit (LSU) gene was specifically amplified using the D1R and D2C primers (Scholin *et al.*, 1994), applying PCR conditions reported by Daugbjerg *et al*., (2000) and Hansen *et al*., (2003).

The PCR products were purified using the ExoSAP-IT kit (usb) and nucleotide sequences were determined using the BigDye Terminator v1.1 cycle sequencing kit (Applied Biosystems); sequencing reactions were run on an ABI PRISM 310 genetic Analyzer. In order to obtain partial LSU sequences in both

directions, we used two amplification primers. Nucleotide sequences of primers used are shown in table 1.

Sequence alignment and phylogenetic analyses

The partial LSU sequences of *C. closterium* were analysed with ProSeq v2.91 (Filatov, 2002). In order to obtain the divergence between Adriatic strain (specie isolated from the backwater lagoon, Pialassa Baiona, Ravenna) and different geographic strains, our sequences were aligned with those retrieved from the GenBank: AF417666 (strain from Denmark), AF289049 (Belgic strain) for LSU.

A multiple alignment of D1-D2 sequences of *C. closterium* and other species of Heterokontophyta retrieved from GenBank was obtained using the ClustalX 1.83 (Thompson *et al.*, 1997) program. In molecular sistematics and phylogenetic analyses we applied the Kimura2-parameter model and the NJ method of tree reconstruction implemented in Mega 3.1 program (Kumar *et al*., 2004).

Direction / Primer name	**Primer sequence**
Forward	
D1R[a]	5'-ACCCGCTAATTTAAGCATA-3'
Reverse	
D2C[a]	5'-CCTTGGTCCGTGTTTCAAGA-3'

Table 1: Nucleotide sequences of D1 and D2 primers; (a) as reported by Scholin *et al*., 1994.

The phylogenetic tree was realized considering several species of the genus *pseudo-nitzschia*, which were observed in Adriatic sea as reported by Boni *et al*., (2005), and two other species, as reported by Lundholm *et al*., (2001), *Navicula cf. erifuga* and *Phaeodactilum tricornutum*. *Sarcocistis muris* was used as out-group.

3.2.3 Scanning Electron Microscopy (SEM) images of *C. closterium* cells

Cylindrotheca closterium cells were also analyzed by means of scanning electron microscopy, which provides three-dimensional images useful for taxonomic identification. Analyses were done in the laboratory of Marine Botanic, at the Marine Science Institute (Università Polivalente Marche). Cells were pre-treated with hydrogen peroxide (H_2O_2) for 4 hours, in order to remove all organic material and obtained intact frustules, then washed and resuspended in distilled water. SEM images obtained are shown in Appendix B.

3.2.4. EC50 calculations

C. closterium cultures were grown in glass flasks (250 ml) at different metal (copper and cadmium) concentration ranges: 12.5 - 15 - 17.5 and 15 - 18 - 21 - 24 - 27 - 30 µM of copper and cadmium respectively. Two replicates for each metal concentration were done. Cells were counted after 96 hours of metal exposure and the concentration at which growth is inhibited of 50% (EC50) was calculated by means of a non-linear regression estimation (Statistica 6.0) using the logistic equation:

$$V2 = b0 - b0 /[1+(V1/b1)^{b2}]$$

Where V2 is the cell number after 96 hours of exposure; b0 is the initial cell number; V1 is the metal concentration; b1 is expected EC50; b2 is the slope.

EC50 values obtained were 15.14 µM for copper and 17.67 µM for cadmium with standard errors are reported in table 2, while the data plot is shown in Fig. 2.

3.2.5. Copper and cadmium analysis

50 ml of culture were filtered onto cellulose 0.45 µm Millipore filters and then stored at -80°C until analysis. Measurements were done in duplicate. Filters were digested with nitric acid (5 ml) for 4 hours and then analyzed with atomic absorption spectrophotometer (Perkin-Elmer 603). Values are expressed as µg of metal per $(\text{million cell})^{-1}$.

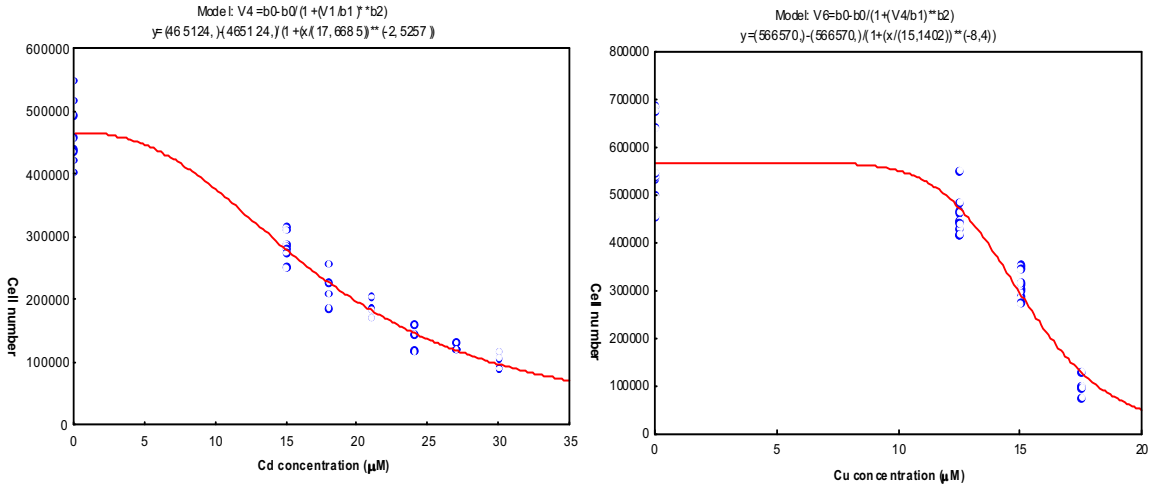

Figure 2: Plot of EC50 estimation, data fitted with logistic equation.

Cd	b0	b1
EC50	465124	17.67
Std.Err.	10517	0.54
p-level	0.0	0.00000
Cu		
EC50	566570	15.14
Std.Err.	20147	0.26
p-level	0.0	0.00000

Table 2: EC50 values (b1, in µM), after 96 hours of metal exposure, standard error and p values obtained with the non-linear regression estimation. Two replicate for each metal concentration.

3.2.6 Polysaccharides analysis

Polysaccharides extraction from culture was realized with the Myklestad method. 2 volumes of ethanol (100%) were added to 80 ml culture and stored at -20°C for 24 hours; then solution was centrifuged 25 minutes at 3000xg at 4°C, supernatant was used to measure extracellular polysaccharides while the pellet was used to measure cellular polysaccharide content.

Polysaccharides were analyzed by the phenol-sulphuric acid method of Dubois (Dubois *et al.*, 1956) using glucose as a standard. In particular, polysaccharides were measured by adding 50 µl of phenol 80% and 5 ml of sulphuric acid to 1 ml culture supplemented with 1 ml distilled water.

3.2.7. Modulated fluorescence measurements

Chlorophyll fluorescence of PSII of the diatom treated with different concentrations of copper and cadmium was evaluated with a pulse-amplitude modulated fluorometer, (PAM). Model used: 101-PAM connected to a PDA-100 data acquisition system, high power LED Lamp Control unit HPL-C and LED-Array–Cone HPL-470 to supply saturating pulses, US-L665 and 102-FR to supply far red light and measuring light respectively, (H. Walz, Effeltrich, Germany). Algal sample analyzed in cuvettes (10x10 mm) mounted on an optical unit ED-101US/M. Measurements were performed at room temperature (25°C) in the dark.

Constant fluorescence of dark-adapted cells (F_o) was measured by using modulated light (ML) of low intensity (1 µmol $m^{-2}s^{-1}$); (F_o) fluorescence level represents the fluorescence yield when all PSII reaction centres are open and consequently Q_A is fully oxidized. Maximum fluorescence yield (F_m) was induced by a short saturating pulse of 6000 µmol $m^{-2}s^{-1}$ for 0.8 s. The change of the fluorescence yield (F) during the following illumination by actinic light (AL) induces the typical Kautsky effect (Kautsky and Hirsch, 1931), a schematic representation is given in Fig. 3. Simultaneously the change of the maximal fluorescence yield (F'_m) is induced by saturating pulses (SP) given periodically (every 40 s). At the steady state of electron transport, AL is turned off and a far-red light (FR) is applied in order to ensure rapid and complete oxidation of Q_A. Under these conditions, the fluorescence level obtained, F'_o, represents the fluorescence yield when all PSII reaction centres are in an open state for light-adapted sample.

Determination of the constant fluorescence level (F_o) and the maximal fluorescence (F_m) permits evaluation of the variable fluorescence (F_v). The maximum quantum efficiency of PSII charge separation, (F_v/F_m), was calculated as, (Bolàr-Nordenkampf *et al*., 1989):

$$F_v/F_m = (F_m - F_o) / F_m$$

At the steady state of electron transport, the operational quantum yield, Φ'_M, was obtained by the ratio, (Genty *et al*., 1989):

$$\Phi'_M = (F'_m - F) / F'_m$$

The photochemical quenching (Q_p), showing the proportion of light excitation energy converted to photochemical act by the active PSII reaction centres, was evaluated as (Schreiber et al., 1986):

$$Q_p = (F'_m - F) / (F'_m - F'_o)$$

The non-photochemical quenching (Q_n), representing all quenching processes of the PSII chlorophyll fluorescence not directly related to photochemistry, was calculated by the ratio (Schreiber *et al*., 1986):

$$Q_n = (F_m - F'_m) / (F_m - F'_o)$$

During measurements, the AL intensity was similar to the one used for the growth of the diatom in order to avoid photoinhibitory effects and to provide optimal conditions for photosynthetic activity.

Other calculated fluorescence parameters included the plastoquinone pool ($F_v/2$, Bolhar-Nordenkampf & Oquist, 1993) and the efficiency of water splitting apparatus (F_o/F_v, Kriedemann *et al*., 1985).

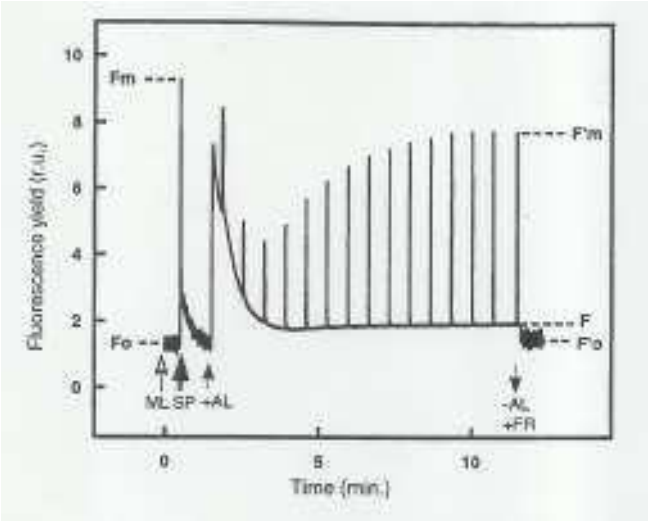

Figure 3: Schematic representation of the fluorescence induction kinetic obtained by using the PAM-fluorometric method. The different types of light used during the measurement are indicated and explained in the text. From Juneau *et al*., 2001.

3.2.8. Ascorbate peroxidase (APX) activity measurements

Ascorbate peroxidase (APX) activity was evaluated following the decrease in absorption of ascorbate. Extracts were made in buffer B: 5mM

potassium phosphate and 0.1 mM EDTA, pH 7. Assay mixtures (final concentrations indicated) were: 100 µl ascorbic acid (5mM), cell extracts (50, 100 µl) and buffer B up to 1 ml. Total assay volume was 1 ml and the incubation time was 10 min at 25°C. Next, 10 µl hydrogen peroxide (0.1 mM) were added and absorption was measured for 3 minutes in a quarzt cuvett at 290 nm. APX activity was calculated from the molecular extinction coeffiecient of ascorbate (2.8 $mM^{-1}cm^{-1}$) and normalized to proteins.

3. Section 3

3.3.1 Inorganic carbon assimilation (P/DIC) and production versus respiration ratio (P/R)

P/DIC curves: Net O_2 evolution and consumption were measured in a Clark-type Hansatech DW1 O_2 electrode and the signal amplified by a Hansatech CB-1 unit, at a saturating light intensity (300 and 250 µmol photons $m^{-2}sec^{-1}$ for *D. tertiolecta* and *C. closterium* respectively) and at 18° C. Cells were washed twice (2500 g for 10 min) in a dissolved inorganic carbon depleted medium (DIC free) and then resuspended in the same medium. Cell density used for the analysis was 4-5 $\times$ 10^6 cells ml^{-1}. Analyses were performed during the exponential phase of cultures.

To obtain a DIC depleted medium, the growth medium (f2) was first acidified and then bubbled with N_2 gas for at least 2 hours; the pH was then readjusted to 8.2 with fresh NaOH solution, (Young *et al*., 2001). Photosynthetic carbon uptake was followed by adding 5 µM of $NaHCO_3$; when oxygen evolution rates had substantially reached a plateau, rates were recorded in response to further $NaHCO_3$ additions. The concentration range used was: 5, 10, 20, 30, 60, 100, 200 and 400 µM; these concentrations were obtained from stock solutions of 5, 20, 50 mM, prepared in distilled water. The results of the P vs DIC curves were fitted to a Michaelis-Menten model using least-squares non linear regression in the programme STATSOFT. In this way it was possible to obtain the maximum rate of oxygen evolution (V_{max}), the DIC concentration at

which oxygen evolution occurs at half of the maximum rate ($K_{m,}$) and the conductance (Γ) from the initial slope of the curve.

P/R ratio: Production was measured as mole of O_2 evolved at saturating light intensity, using the same oxygen electrode described above. Respiration was measured in the dark. The density in the chamber was around 106 cell ml^{-1}. The P/R ratios were calculated from the initial linear part of the slopes.

3.3.2. Maximum quantum yield of Photosystem II and Electron Transport Rate (rETR)

The maximum quantum yield of PSII (F_v/F_m) and the relative electron transport rate were measured using a Phyto-PAM fluorometer. F_v/F_m was measured after a dark adaptation period of 10 minutes, using a sub-sample of the cultures (3 ml).

rETR was calculated by means of rapid light curves, (P/I) which consist of 9 steps of actinic light (4, 16, 32, 120, 240, 295, 350, 405, 460 µmol photons m^{-2} sec^{-1}), each 30 seconds long. The ETR was calculated as:

ETR= 0.84 * 0.5 * photon flux* Yield

Where 0.84 is a standard ETR-factor corresponding to the fraction of incident light absorbed; 0.5 factor takes into account the fact that roughly 50% of all absorbed quanta reach PSII.

The curves were fitted with the equation of Eilers & Peeters (1988) by means of a non-linear regression using Statsoft 6.1:

ETR= PAR/(a*PAR^2 + b*PAR + c)

The calculation of the parameters a, b, c allows estimation of several important parameters of the curve:

α = 1/c

P_{max} = 1/(b+2*SQRT(a/c))

I_k = c/(b+2*SQRT(a*c)

I_{max} = SQRT (c/a)

bpm = b/b+2SQRT(a*c)

where α is the initial slope and is proportional to the effective quantum yield; P_{max} is the maximal production rate; I_k is the characteristic intensity defining the boundary at which oxygen evolution becomes light-saturated; I_{max} is the optimal intensity.

3.3.3. Chlorophyll extraction

Samples were filtered onto a glass fiber filter (GF/C, 25 mm; Whatman) and then kept at -20°C until analysis. Chlorophyll extraction was performed in 10 ml of 90% acetone and kept 24 hours at 4°C. The absorbance of chls *a*, *b* and *c* were read simultaneously at 630, 647 and 665 nm, with a spectrophotometer (Cary 50 Bio). Chlorophyll values were calculated using the equations of Jeffrey and Humphrey (1975):

Chl *a* = $11.85E_{664} – 1.54E_{647} – 0.08E_{630}$

Chl *b* = $-5.43E_{664} + 21.03E_{647} – 2.66E_{630}$

Chl *c* = $-1.67E_{664} – 7.60E_{647} + 24.52E_{630}$

Values were expressed as μg chl $(10^6$ cells$)^{-1}$.

RESULTS

PHOTOSYNTHETIC PERFORMANCE, OXIDATIVE DAMAGE AND ANTIOXIDANTS IN *CYLINDROTHECA CLOSTERIUM* IN RESPONSE TO HIGH IRRADIANCE, UVB RADIATION AND SALINITY

4.1 INTRODUCTION

Intertidal benthic diatom communities are mainly composed of multi-layered biofilms of epipelic species, some of which can reduce the UV exposure time of the uppermost cells by performing vertical migration with an implicit photoprotection by self-shading (Underwood & Kromkamp, 1999). Exposure to ambient UVB does not inhibit the primary production of most benthic diatoms (Peletier *et al.*, 1996). However, the diatom considered for this study, Cylindrotheca closterium (formerly *Nitzschia closterium*), is a semi-planctonic diatom living in the water column, in rockpools and on the sediment; during low tide it is deposited and thereby exposed to an increase in light intensity, UV doses and to changes in osmotic conditions due to evaporation; during high tide it is resuspended in the pelagic zone. Microalgae living in environments characterised by hourly fluctuations, need to be protected against photodamage and dessication.

Exposure to UV radiation and desiccation (drought) stimulate the production of active oxygen species (AOS) that cause oxidative damage, mainly through hydroxyl radicals ($^{\cdot}OH$). Although O_2 (triplet oxygen) itself is a harmless molecule, as a result of chlorophyll excitation during photosynthesis singlet oxygen will be formed that is normally efficiently quenched by accessory pigments (carotenoids), (Krieger-Liszkay, 2004). However, during reduction of oxygen to water it determines a series of stable intermediates which can be very dangerous to the cell, such as $O_2^{-\cdot}$, H_2O_2, $^{\cdot}OH$; these AOS are destructive to proteins and lipids (Mallick & Mohn, 2000; Beardall & Raven, 2004). Photorespiration may be source of H_2O_2 when the glycolate oxidation is brought about by glycollate oxidase, as it happens in many algal groups (Beardall *et al.*, 2003). High photorespiratory flux determines an abundant H_2O_2 production in plants, thus sufficient catalase activity is needed; in stress conditions that impair protein synthesis (e.g. low or high temperature and salt-

stress) a light-dependent decrease in total catalase protein and activity is observed, (Foyer & Noctor, 2000). Previous works indicated that UV and hypersalinity stimulated the antioxidative defence in *Cylindrotheca closterium*, in particular through activation of superoxide dismutase (Rijstenbil, 2003) and that salt stress (salinity value of 60) enhanced active oxygen species production in the same diatom, (Rijstenbil, 2005). Salt stress-induced production of active oxygen species seems to be linked to the activation of NADPH-oxidase, (Al-Mehdi *et al*., 1997); most likely high salinity induces membrane depolarization followed by the activation of the enzyme, which is a major source of superoxide radical ($O_2^{-\cdot}$).

This paper is focused on parallel measurements of oxidative damage, in particular lipid and protein peroxidation (Dix & Aikens, 1993; Ishi *et al.*, 2002), with the antioxidative response of SOD activity and glutathione redox ratio (Rijstenbil, 2002, 2003). In this experimental work, these parallel processes of peroxidation and antioxidative responses were measured by simulating conditions that the semi-planktonic diatom *Cylindrotheca closterium* can experience in the intertidal environment, namely (a) higher irradiance (PAR) and optional extra UV radiation; (b) an increase of (pore water) salinity enhanced by wind-induced evaporation. Cultures grown at salinity value of 30 under low PAR (mode A, 20 μmol photons $m^{-2}s^{-1}$) were considered as controls; cultures grown at salinity value of 60 represent cells exposed to desiccation. Finally, using covers that either cut off or transmit UVB, we also analyzed the physiological damage and defence under intensive solar radiation. Our objective is to investigate whether these two different stressors (irradiance, salt) evoke either independent or complementary responses.

4.2 EXPERIMENTAL SET UP

Cultivation conditions, culture growth and light parameters

Cylindrotheca closterium was cultured at 18°C in artificial medium (salinity values of 30 and 60) (De Brouwer *et al*., 2002; Rijstenbil, 2003). Batch cultures were grown for six days under low artificial light (20 μmol photons m^{-}

$^{2}sec^{-1}$, mode A) in a 12:12h light-dark cycle. Growth was monitored measuring the minimal fluorescence of cells (F_o) every two days using a PAM (pulse amplitude modulated) fluorometer after 15 min dark-adaptation; samples were also taken every two days for cell counting using a Coulter Multisizer II after disrupting the diatom colonies by gentle sonication (30 s; amplitude 7 µm; energy output 35 W) (Rijstenbil, 2003). After six days the value of F_o was still increasing indicating that algae were still in the exponential phase. Each culture suspension (3 l) was divided over six Petri dishes of 500 ml each that were exposed for 72 h to different light conditions: low irradiance (mode A) high irradiance (mode B) and UVB (mode C) within a photoperiod of 12 h. The cultures were illuminated by a set of fluorescent lamps with PAR (400-700nm) and UV radiation (Rijstenbil 2002, 2003). To obtain irradiance in mode B and C, duplicate dishes with medium at both salinities 30 and 60, were covered with perspex and with UVB transparent covers, respectively.

Spectral composition was determined with a MACAM Photometrics SR-9910-PC spectroradiometer. In Fig. 4A the photosynthetically active radiation (PAR, 400-700 nm) is plotted as µmol photons $m^{-2}s^{-1}nm^{-1}$; in mode A, PAR was 20 µmol photons $m^{-2}s^{-1}$; in mode B and mode C, PAR was 250 µmol photons $m^{-2}s^{-1}$. In Fig. 4B, UV dose rates vs wavelength (UVB 280-320 nm; UVA 320-400 nm) are expressed in W m^{-2} nm^{-1}. Daily doses, unweighted and weighted dose rates are shown in Table 3. In mode B, the ratio UVB:UVA:PAR was 0.01:2.1:100 and the daily dose of UVB was 0.3 kJ $m^{-2}d^{-1}$ (12:12h photoperiod) during the three days experiment.

In mode C UVB:UVA:PAR was 0.4:7.4:100 and the daily dose of UVB was 10.2 kJ m^{-2}. After 15 min dark adaptation, the maximum quantum efficiency of PSII charge separation (F_v/F_m) was measured with the PAM fluorometer; measurements were performed twice a day (morning and evening) during the three days of exposition under different light conditions.

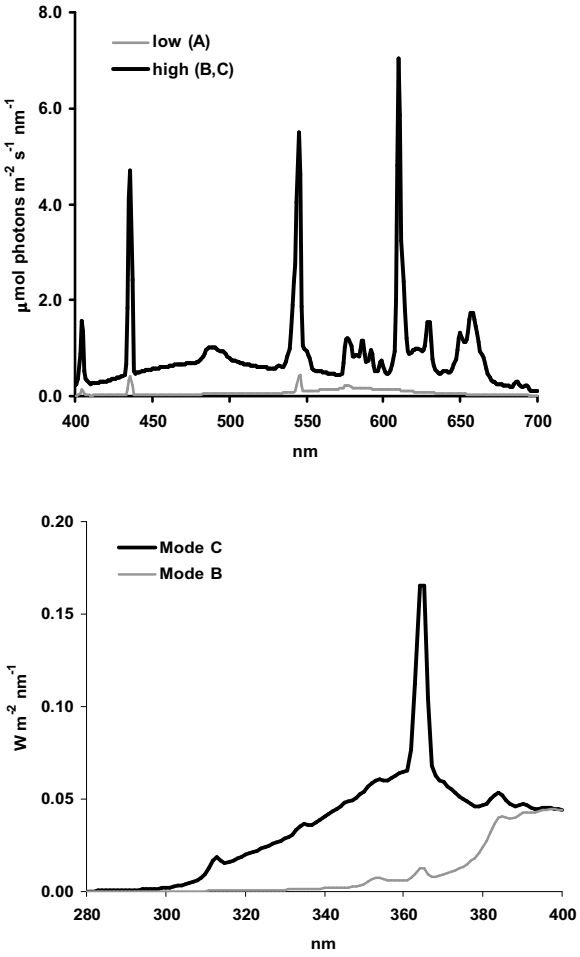

Figure 4: Spectra of artificial light supplied to the diatom *Cylindrotheca closterium* cultures scanned with a MACAM spectroradiometer at 1nm wavelength intervals. (a) PAR (400-700 nm) as µmol m^2 s^{-1} nm^{-1} supplied under low light (mode A) and under high light (mode B, C). (b) UV dose in W m^{-2} nm^{-1} under both conditions.

Unweighted dose rates (W m^{-2})			
Mode	**A**	**B**	**C**
UVB	0.00	0.01	0.24
UVA	0.09	1.17	4.07
UV-total	0.10	1.17	4.30

Daily UV doses (KJ m^{-2} d^{-1}; 08:00-20:00h)			
Mode	**A**	**B**	**C**
UVB	0	0.3	10.2
UVA	4	50	176
UV-total	4	51	186
%UVB:PAR	0.00	0.01	0.43

Table 3: Unweighted dose rates for the three treatments (W m^{-2}) and daily UV doses (KJ m^{-2} d^{-1}). Irradiance was supplied during the day with a photoperiod of 12:12 h.

4.3 RESULTS

Effect of light and salinity on growth and photosynthetic parameters

Minimal fluorescence values (F_o) measured in *C. closterium* cultures indicated an increase in biomass during the six days of growth and these data are in agreement with those obtained by cell counts (salinity value of 30: $y=16.7x-61.8$, $R^2=0.99$, $n=3$, $p<0.02$; salinity value of 60: $y=15.85x-64.32$, $R^2=0.98$, $n=4$ $p<0.035$). Cultures grown at double salinity (60) exhibited a slower growth compared to those at 30 (14%) so that during the first four days, their F_o was below detection. After six days, cultures at both salinities of 30 and 60 were still growing exponentially, and reached 0.65 and 0.60 (million cells ml)$^{-1}$, respectively, (data not shown). In cultures grown under mode A (low light), F_v/F_m (~0.65) did not increase, neither after an 8 h additional low-light treatment nor at the end of the experiment (Fig. 5a); in those under modes B and C, F_v/F_m values were always lower compared to mode A (Anova, $n=2$, $p<0.01$); after 8 h exposure to high irradiance without UVB, (mode B), F_v/F_m had a value of 0.46, but after 72 h exposition to the same light conditions it increased to 0.57 showing a significant recovery; similarly, under mode C (UVB), F_v/F_m showed a recovery from 0.46 to 0.53. At 30 psu the differences in F_v/F_m between the two high irradiance treatments, without (B) or with UVB (C), were significant only after 32, 56 and 72 h ($p<0.01$). Low irradiance (mode A) had no effects on F_v/F_m values of cells grown at salinity value of 60, neither after the first 8 h treatment nor at the end of the experiment, (Fig. 1b). Cells grown at 60 in mode B and C had equal F_v/F_m values after 8 h and 72 h treatment, (Fig. 1b). At salinity value of 60, F_v/F_m values decreased with increasing irradiance ($p<0.05$) with the lowest values under mode C ($p<0.01$).

After 72 h exposition to these light conditions A, B, and C, relative electron transport rates (rETR) were also measured (Fig. 6a-b). Fig. 6a indicates a stimulation of rETR in cells grown at 30, with an increase proportional to irradiance values. rETR of cultures grown at 60 (Fig. 6b) shows a decrease in UVB treated cells, compared to those measured in cultures at salinity value of 30.

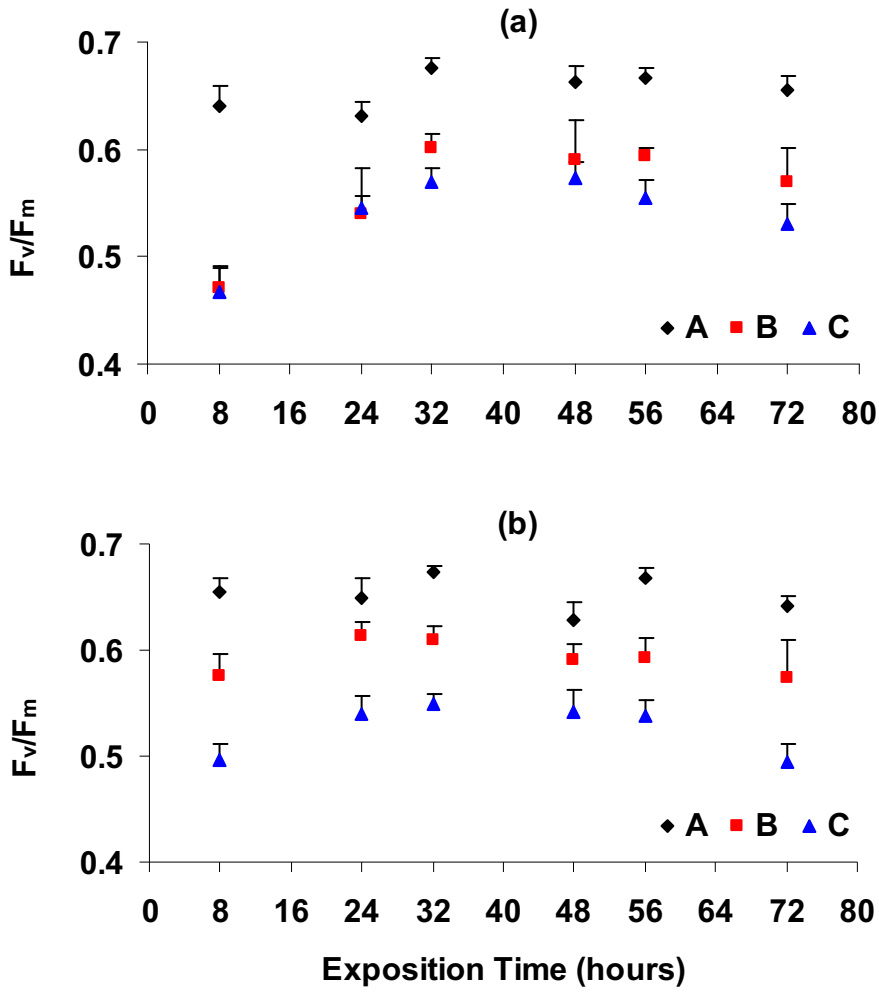

Figure 5: Examples of PSII maximum quantum efficiency charge separation measurements (F_v/F_m) in *C. closterium* cells during 72-h treatments under light conditions A (low light), B (high PAR), C (high PAR plus UVB). Points are averages (n=20) of Fv/Fm in 15-min dark adapted cells; (a) cultures at salinity of 30; (b) cultures at salinity of 60.

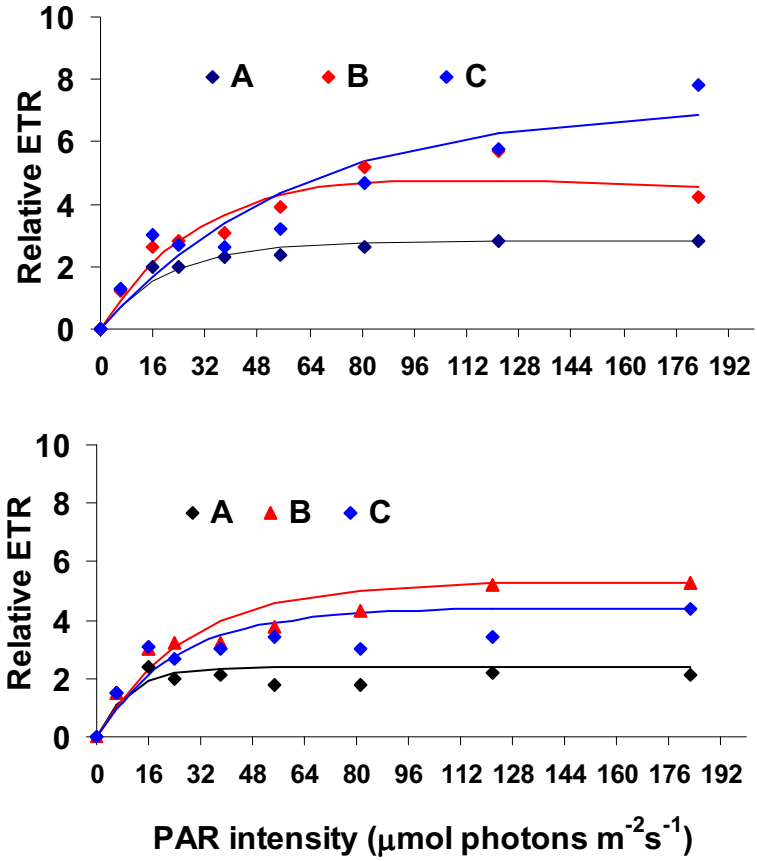

Figure 6: Photosynthesis-light curves as relative electron transport rates (rETR) after 72 h of treatment (A, B, C); the lines represent the different data fitted with Platt's model; (a) cultures grown at salinity value of 30; (b) cultures growm at salinity value of 60.

Antioxidative defences (GSH and SOD activity)

Under hypersaline conditions (S=60) SOD activity was higher compared to that measured in cells exposed to the same light conditions at S=30 ($p<0.001$) (Fig. 7 and Table 4). At S=60 *C. closterium* had a lower SOD activity ($p<0.001$) when grown under the same PAR level, both without (B) and with UVB (C), compared to cells grown under low-irradiance (A).

In cultures grown at S=30, a higher dose of PAR (B), and PAR+UVB (C) did not influence the reduced glutathione pool (GSH) ($p>0.05$; Table 4). In cultures grown at S=60, GSH pools were relatively lower ($p<0.05$) in modes B and C compared to those grown at low irradiance (A) at both salinities. GSSG pools were not influenced by any treatment ($p>0.05$; Table 4). Due to the

relatively lower GSH pools, the redox ratio of glutathione indicated a decreasing trend (at S=30 and S=60, respectively) from low PAR (0.87 and 0.90), to high PAR (0.74 and 0.83), to high PAR plus UVB (0.68 and 0.69); (Table 3). At S=60, GSH pools were relatively higher (A, B), but after UVB exposure (B) the redox ratio (stress index) was similar to the ratio obtained at S=30.

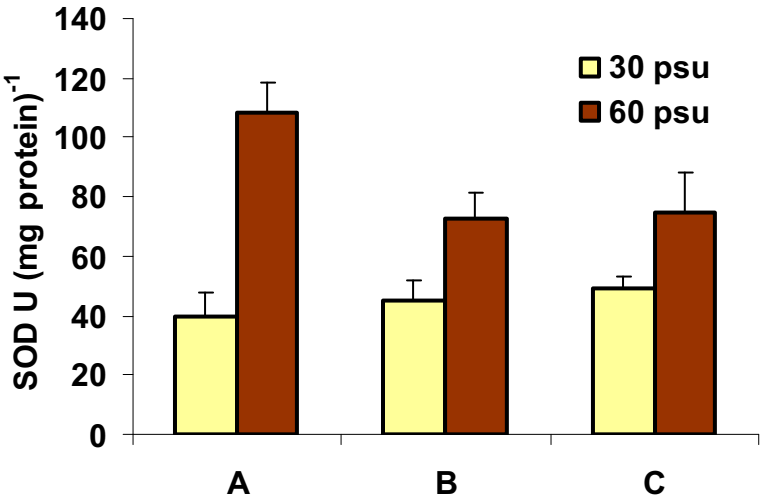

Figure 7: Superoxide dismutase (SOD) activity in *Cylindrotheca closterium* under light conditions (modes) A, B, C, and at the two salinities. SOD was analyzed in cell extracts after 72 h of treatment (12:12 photoperiod) and expressed in enzyme units per mg protein. Data points are averages of duplicate samples; standard deviation is included. (±SD)

Oxidative damage indicators: lipid peroxides, malondialdehyde and protein carbonyl groups contents

Peroxidation processes were quantified through analyses in cell extracts of (a) lipid peroxide (LPO); (b) the lipid-peroxidation by-product malondialdehyde (MDA); (c) carbonyl groups in protein, (all data in Table 4).

Total unsaturated lipid contents were almost twice as high at S=60 than at S=30 ($p<0.001$), however differences were not due to light conditions, apart from a decrease under mode B at S=60 ($p<0.05$).

LPO concentrations normalized to lipid content did not differ between the different irradiance treatments at S=30. Under hypersaline conditions (S=60) lipid peroxides were significantly higher than under normal salinity, ($p<0.01$),

(Fig. 9); the highest increase was observed under modes A and C, ($p<0.05$ and $p<0.01$, respectively). At S=60 cells exposed to high irradiance without UVB, (mode B), had lower LPO content than cells in mode A and C ($p<0.05$).

In cells grown at S=30 the high-irradiance treatment without UVB (mode B) caused a significant increase in MDA content compared to the low-irradiance treatment (mode A) and PAR+UVB (mode C) ($p<0.05$). MDA content of cells exposed to low irradiance under hypersalinity conditions (S=60) was higher than that of cells grown at S=30 ($p<0.05$). The largest MDA contents were found in UVB-exposed cultures (mode C) grown at a S=60, with values that were higher than those in UVB-treated cells grown at S=30 ($p<0.01$).

Cells grown at S=60 proteins had lower carbonyl contents compared with those grown at S=30 ($p<0.001$), (Fig. 8). In cells grown at S=60 no differences were observed ($n= 4$, $p>0.05$) between irradiance conditions A, B and C. At S=30 carbonyl contents were higher only in UVB-treated cells ($n= 4$, $p<0.01$), (Table 4).

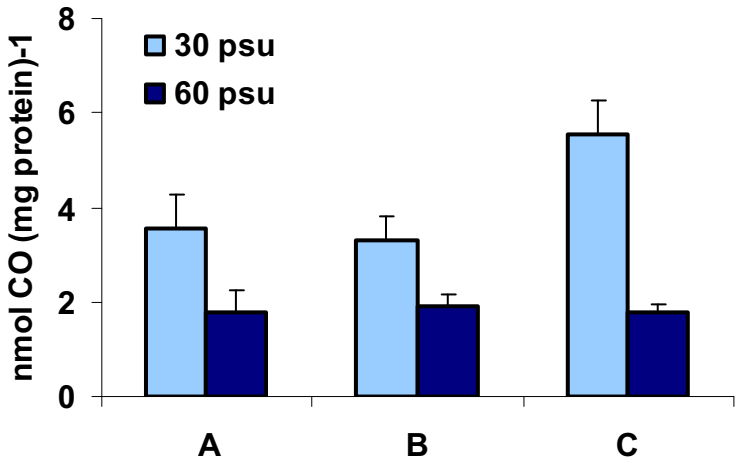

Figure 8: Peroxidation of proteins of *C. closterium* under the conditions (treatments) as in Figure 7; carbonyl groups in cell extracts normalized to protein content and expressed as nmol CO (mg protein)$^{-1}$.

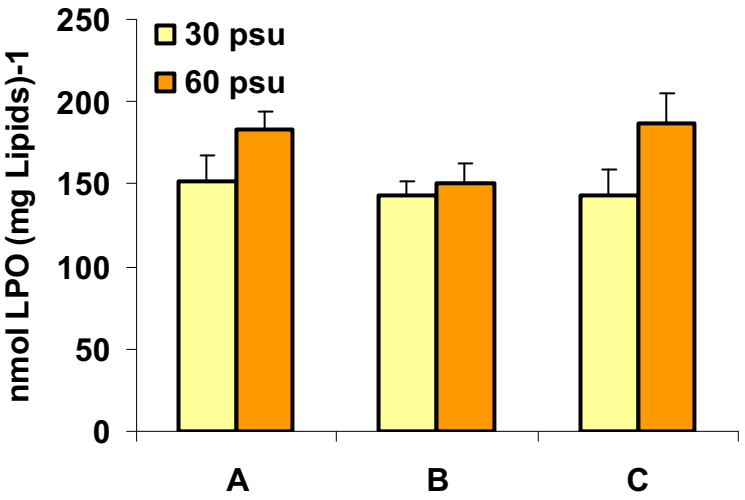

Figure 9: Lipid hydroperoxides in cell extracts under conditions (treatments) as in Figure 7; values are expressed as nmol LPO (mg lipids) $^{-1}$

Salinity	30 psu			60 psu		
Light Conditions	Mode A	Mode B	Mode C	Mode A	Mode B	Mode C
Defence Parameters	Mean ± Dev.st	Mean ± Dev.st	Mean ± Dev.st	Mean ± Dev.st	Mean ± Dev.st	Mean ± Dev.st
SOD	39.5 ± 8.5	45.2 ± 6.6	42.8 ± 4.4	108.3 ± 10	72.4± 0.02	74.4± 13.5
GSH	6.29 ± 2.9	3.52 ± 2.5	2.52 ± 1.5	9.02 ± 2.8	6.04 ± 0.94	3.75 ± 1.01
GSSG	1.99 ± 1.61	1.50 ± 1.41	1.85 ± 0.83	1.86 ± 0.59	2.50 ± 1.01	2.57 ± 0.25
GSH/(GSH+0.5*GSSG)	0.87	0.74	0.69	0.90	0.83	0.69
Damage Parameters						
MDA	48.6 ± 2.21	66.9 ± 4.61	56.1 ± 6.01	57.1 ± 3.31	61 ± 2	71.2 ± 4.49
CO	3.57 ± 0.69	3.32 ± 0.51	5.53 ± 0.74	1.78 ± 0.45	1.89 ± 0.26	1.77 ± 0.19
LPO	151.9 ± 16.04	142.8 ± 9.1	143.1 ± 16.5	183.2 ± 10.6	150 ± 12.2	187.1 ± 17.5
Lipid content	0.0041 ±0.0006	0.0037 ±0.0005	0.0035 ±0.0003	0.009 ±0.001	0.007 ±0.0003	0.008 ±0.0005

Table 4: Values of all the parameters analyzed. Oxidative stress and defence parameters in *C. closterium* cells during 72-h treatments under different light conditions. Data are expressed as means ± standard deviation. SOD activity is expressed as Units (mg protein)$^{-1}$; GSH, GSSG and total MDA as µM (L cell volume)$^{-1}$; Carbonyl content as nmol (mg protein)$^{-1}$; Lipid peroxide as nmol (mg lipid)$^{-1}$ while lipids content as mg (mln cells)$^{-1}$.

4.4 DISCUSSION

Our experimental study addressed the effect of UVB and high salinity, both alone and in combination, on *Cylindrotheca closterium* a semi-planktonic diatom species which at low tides can be exposed to strong fluctuations in light intensity and UV radiation, as well as to dessiccation. The unweighted UVB doses, supplied under mode C (10.2 KJ m^{-2} d^{-1}), equaled maximum values attained on sunny days (Peletier *et al.*, 1996). In mode C the UVB:PAR ratio was 0.43:100 which is similar to the solar ratio on a sunny day in temperate areas (solar UVB:UVA:PAR measured on sunny day was 0.4:7.7:100). PAR supplied under mode A (20 µmol photons m^{-2} s^{-1}) allowed a high photosynthetic efficiency also at increased salinity (60); the high F_v/F_m values measured during the 3 days exposure also suggested that cells were not nutrient limited (Kromkamp & Peene, 1999). However, at salinity value of 30 a daily dose of UVA and UVB of 50 and 0.3 KJ m^{-2} d^{-1}, respectively (mode B), supplied with 250 µmol photons m^{-2} s^{-1} PAR, caused a strong inhibition of PSII (decrease of F_v/F_m) already after the first 8h exposure, but Fv/Fm recovered to higher values after ending UV treatment; doubled salinity did not show to put an additional pressure on PSII (Fig. 5-a). A reduction of quantum yield under high light is not always a result of photoinhibitory damage but indicates rapid activation of mechanisms to dissipate excess excitation energy (Smirnoff, 1993). In cells under mode C (Table 3) a combined effect of the factors, high light plus UVB radiation and salinity increase, caused a stronger decrease of the photosynthetic efficiency of PSII. A similar decrease in *C. closterium* cells, exposed to the same condition for 4 hours, was observed; under this condition a decrease was observed in the de-epoxidation status of the diatom xanthophylls that take part in the xanthophyll cycle diadinoxanthin and diatoxanthin (Rijstenbil, 2005), thus, highlighting the activation of mechanisms acting in dissipation of excess excitation energy. A stronger PSII inhibition by UVB compared to UVA was also found in *Thalassiosira pseudonana* (Rijstenbil, 2002) and, similarly to what observed in *C. closterium* (Rijstenbil, 2003), the lack of reciprocity between UV dose rate and duration of exposure indicated that UV-inhibition is UV-dose rate-, rather than UV-dose duration dependent

(Neale, 2000). Our results show that during the 72h treatment, *C. closterium* did not exhibit a steady decrease in F_v/F_m; results shown in Fig. 5(a,b) indicate that the balance between photodamage and repair was established after every 12:12h light:dark cycle. Relative electron transport rates (rETR) at the end of the treatment were enhanced under high light at salinity value of 30, (Fig. 6 a), whereas under hypersaline conditions (60) the UVB treated cells exhibited the moderation of rETR, (Fig. 6 b); maximum rETR decreased from 7.8 to 4.4, and the saturation light intensity decreased from 40 to 23 μmol photons m^{-2} s^{-1}. These results can be taken as representative of the culture photosynthetic capacity in that rates of photosynthesis estimated from PAM fluorometry, oxygen evolution or carbon fixation, were shown to have parallel behaviour in a number of phytoplankton species (Barranguet & Kromkamp, 2000; Masojidek *et al.*, 2001).

Salinity plays an important role in structuring biological community along estuarine salinity gradients; sharp spatial salinity gradients and seasonal variations of pore water salinity at a single location is likely to be physiologically stressfull to benthic organisms (Little, 2000). Salinity values on wind-tide flats may range from (S=) 10 to 55 depending on sites, while pore water salinity (10 cm deep), in wet and damp microhabitats of blue-green algal flat of an estuary, has been estimated to range from (S=) 0 to 160, (Withers & Tunnel, 1998). For NW-European tidal flats on sunny and windy days S=60 seems more realistic and at that salinity value production rates of active oxygen species (AOS) in *C. closterium*, exposed for 4 h to irradiance conditions similar to those used here, were higher than at S=30 (Rijstenbil, 2005). Desiccation as it may occur on tidal flats may therefore stimulate AOS production, which agrees with our observations of a strong stimulation of the superoxide dismutase (SOD) activity at doubled seawater salinity (60). Until now observations of protein carbonyl contents in micro-algae were lacking and we found (for the first time) that at S=60 the oxidative damage to proteins (carbonyl content) was significantly lower than at S=30 (Fig. 8). This result suggest that enhanced SOD activity may allow cells to eliminate superoxide and hydrogen peroxide efficiently, thus reducing the risk of hydroxyl radicals production according to the Haber-Weiss reaction, hence, reducing protein damage. We observed a minor stimulation of SOD activity at S=30 under UV exposure, possibly as a response to an

increased AOS production; UV-induced AOS production is well documented (e.g., Rijstenbil, 2001, 2005). At S=70 SOD activity in *C. closterium* was much higher compared to SOD activity at S=35 (Rijstenbil, 2003). Water stress, as that simulated by hypersaline conditions, is known to enhance $O_2^{\bullet-}$ production in chloroplasts (Asada & Takahashi, 1987); for example, AOS production in *C. closterium*, measured as green-fluorescent 2',7'-dichlorofluorescein (DCF), was higher at S=60 than at S=30 (Rijstenbil, 2005). Salt-induced AOS production may be related to NADPH-oxidase activation (Al-Medhi *et al.*, 1997; Rijstenbil, 2003) which catalyses the single electron reduction of molecular O_2 to superoxide ($O_2^{\bullet-}$) (Lyndsay & Giembyzc, 1997). Severe water deficit in pea plants caused a decrease in total ascorbate content and APX activity, and a shortage of photosynthetic NADPH, which is necessary to glutathione reductase (GR) activity (Iturbe-Ormaetxe *et al.*, 1998).

Reduced glutathione (GSH), the major non-protein thiol, is an effective antioxidant; in mode A its pool was higher under hypersaline conditions (S=60) compared to normal salinity (S=30) and a stronger decrease was observed in cells exposed to the concomitant effects of hypersalinity and UVB (mode C). The redox ratios decreased with increasing irradiance under both salinities. Under mode B the redox ratio was higher at S=60 than at S=30, suggesting the occurrence of moderate oxidative stress, however, the calculated ratios were in the range of 0.88-0.68, which are characteristic of non-stressed planktonic diatoms (Rijstenbil, 2001, 2002). After a 4h light treatment (Rijstenbil, 2005) comparable to our modes B and C, GSH redox ratios were 0.40 and 0.34, respectively, which were far lower than the ratios measured after 3 days treatment with 12h light per day (this work). The temporary decrease of this oxidative stress index highlights the fact that the cells are able to adapt to the light conditions supplied through the activation of a defence mechanism (enhanced SOD activity; steady GSH synthesis rates). Glutathione peroxidase (GPX) may also be involved in cell detoxification via a reduction of lipid peroxides into inert alcohols, using GSH as a substrate (Girotti, 1998 and reference therein). At S=60 and under high light intensity plus UV, the depletion of GSH was not associated to an increase in GSSG, which might be due to consumption of glutathione in S-glutathiolation processes (Klatt & Lamas,

2000), i.e., formation of mixed disulfides between protein-SH and GSH to protect proteins from more extensive irreversible oxidative stress. This was observed also during senescence of the dinoflagellate *Lingulodinium polyedrum*, (Sigaud-Kutner *et al*., 2005).

Oxidative damage to lipids measured as increase in malondialdehyde (MDA) and lipid peroxides (LPO) contents showed that LPO contents at S=30 were not significantly different between treatments, while at S=60 its values increased significantly showing the highest increase in mode A and C ($p<0.01$). Under hypersaline conditions (S=60) the unsaturation lipid degree and the lipide peroxides content were strongly enhanced ($p<0.001$), compared to normal salinity (S=30).

MDA content increased in mode B (S=30) and C (both salinities). In *Thalassiosira pseudonana* MDA contents were higher after UVB- than after UVA exposure, suggesting that lipid peroxidation was related to weighted UV-dose rates (Rijstenbil, 2002). Our results also highlight the increase in UVB-induced lipid peroxidation production when in combination with hypersaline conditions. Our method for LPO analysis (Hermes-Lima, 1995) was, for the first time, adapted to micro-algae. Hence, no literature phycological data were available for comparison. LPO content was referred to the total unsaturated lipids contents as membranes are prime targets of degradation processes induced by drought and under water stress lipid contents may decrease, as peroxidation activities may be enhanced (Monteiro de Paula *et al.*, 1990). At increasing drought stress fatty acid unsaturation increased in *Arabidopsis thaliana* (Gigon *et al.*, 2004). In *C. closterium* total unsaturated lipid content increased strongly at double salinity compared to normal salinity (ANOVA $p<0.001$), supporting the idea that the unsaturation lipid degree responds to the degree of desiccation, even though the underlying mechanisms are not yet clarified.

In conclusion, our results confirm that high ambient (but realistic) UVB radiation and hypersalinity are able to induce oxidative stress in this diatom species, especially when applied in combination. First of all, the antioxidative defence system was strongly activated, mainly through the action of SOD, resulting in an efficient prevention of protein damage at salinity value of 60. This

represents a positive balance between damages and defences in *C. closterium* which enable it to survive under emersion conditions. Therefore *C. closterium* showed to be quite resistant to high PAR and UV radiation, as was also observed in other diatoms and phytoplanktonic species (Peletier *et al*., 1996). Light- and salt-induced oxidative responses can have important ecological consequences, such as the change in community dynamics in response to fluctuating conditions.

CADMIUM AND COPPER SUBLETHAL EFFECTS ON *C. CLOSTERIUM*: GROWTH, PHOTOSYNTHESIS AND OXIDATIVE DAMAGE.

5.1 INTRODUCTION

Heavy metals pollution is a common threat of many environments and water bodies. The backwater lagoon from which this species was collected is in fact contaminated by many industrial activities; background levels on the sediments of copper ranged from 11 to 79 ppm respectively (Miserocchi *et al*., 1990), while cadmium levels in the waters are below detection limits.

Our goal was to understand the physiological responses of the diatom *Cylindrotheca closterium*, an important and abundant specie of the phytobenthos of that lagoon, to copper and cadmium contamination. In general, diatoms are sensitive to phytoplankters with respect to trace metals and other toxicants (Fisher & Frood, 1980); Perez and colleagues (2006) found that total abundance of diatoms decreased linearly with respect to increasing copper concentrations. Moreover, community size structure may be affected by metals; Sanders & Cibik (1988), observed a replacement of large centric diatom by smaller diatoms as a consequence of arsenic inputs.

Several analyses were performed on our experiments to obtain a more complete picture of the toxicity effects of copper and cadmium; in fact growth, metal uptake, oxidative damage to lipids, polysaccharides production, and antioxidant enzyme activities (SOD and APX) were measured after long-term copper and cadmium exposure (96 hours) and photosynthetic capacity (F_v/F_m, F_o/F_v, $F_v/2$, Q_p, Q_n, Φ'_m) was measured after both short- and long-term exposure (24 and 96 hours). The sublethal concentrations of copper and cadmium tested here are higher than the levels of dissolved metals which algae can experience, but not so unrealistic, if we consider that acute contaminations (due to high metals discharge) and metal regeneration from sediments may occur, mainly in coastal and/or polluted areas.

Algae are recommended as biological monitors for heavy metals pollution (Whitton *et al*., 1989) and hence it is very important to design experiments which analyze metal toxicity from an overall point of view and this can be

achieved by concomitant measurements of growth, oxidative damage, antioxidative responses and photosynthesis.

5.2 EXPERIMENTAL SET UP

The diatom *Cylindrotheca closterium* was isolated from the sediments of an inner channel of a backwater italian lagoon, (Pialassa Baiona, Ravenna). The taxonomic identification at the specie level was carried out by means of molecular techniques (see paragraph 3.2.2) and electron microscopy (SEM) pictures (see paragraph 3.2.3). The diatom was cultured in ESAW medium (Berges *et al*., 2001), (recipe in appendix C), at the salinity of 30 and at the temperature of 18°C.

Experiments were carried out on cultures exposed to sublethal concentrations (< EC50), of copper and cadmium for 96 hours; EC50 is the concentration at which growth is reduced of 50%. In order to calculate the EC50 after 96 hours of metals exposure, cultures (250 ml) were exposed to different metal concentration ranges. Growth was measured as fluorescence emission on a first range of concentrations: 10 - 20 - 40 - 60 - 80 and 12.5 - 14 - 25 µM of copper and cadmium respectively. Then, a fine tuning was done: 12.5 - 15 - 17.5 and 15 - 18 - 21 - 24 - 27 - 30 µM of copper and cadmium respectively, (Fig. 10). EC50 values obtained after 96 hours of exposure to the metals were 15.14 µM for copper and 17.67 µM for cadmium, (see paragraph 3.2.4); Fig. 11 shows cell survival expressed as percentage of controls.

Batch cultures of the diatom in exponential growth phase, (9 liters), were divided over six flasks of 1500 ml each. Copper toxicity was studied adding the metal as $CuCl_2 2H_2O$ to obtain a concentration of 13.5 and 15 µM (total bioavailable concentration of 0.94 and 0.97 µM respectively). Cadmium was added as $CdCl_2$ to obtain a dissolved concentration of 13 and 16 µM (total bioavailable concentration of 5.41 and 7.41 µM). Cultures to which metals were not added were used as controls and metal exposure lengthen 96 hours. Computational simulations of chemical equilibrium were performed with the speciation computer program Visual MINTEQ in order to calculate both the

bioavailable metal concentration (free and labile) and the complexed concentration, (mainly EDTA-complexes). The calculations were based on the pH of the medium, at the moment of metals addition and after 96 hours, and on the initial chemical composition of the medium. The labile fraction is due to the Cu, Cd – inorganic ligands, (OH^-, CO_3^{2-}, Cl^-, NH_3).

Several determinations were performed on cultures: growth and photosynthesis (F_v/F_m, F_o/F_v, $F_v/2$, Q_p, Q_n, Φ'_m) were measured during the exposure time (at 24, 48 and 96 hours), while metal uptake, oxidative damage to lipids and proteins and antioxidative enzymes activities (SOD and APX), were measured after cells were collected.

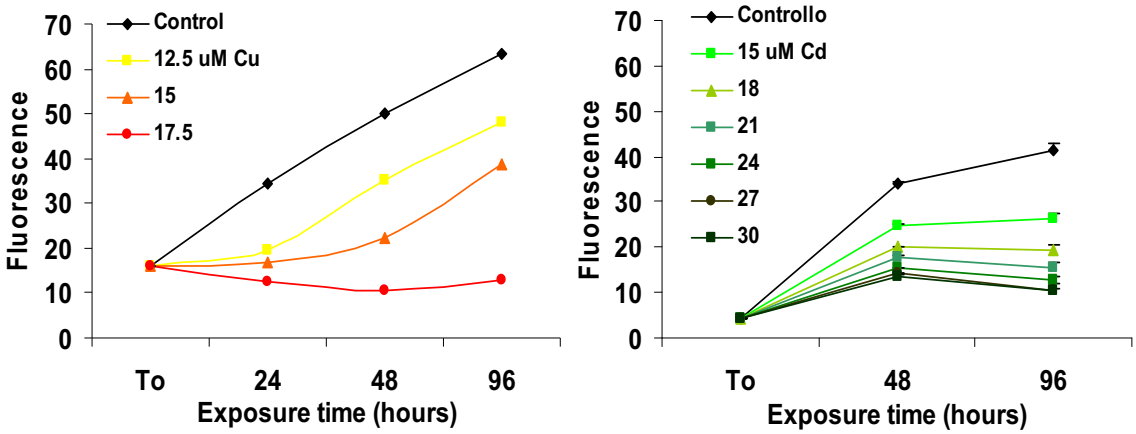

Figure 10: Growth of *C. closterium* express as fluorescence emission; fluorescence was measured when the metals were added to the cultures (To) and after 24, 48 and 96 hours. After 96 h cells were collected for analysis. Numbers are average of two replicates ± standard deviations. Graph on the left: different copper concentrations expressed in µM. Graph on the right: different cadmium concentrations expressed in µM.

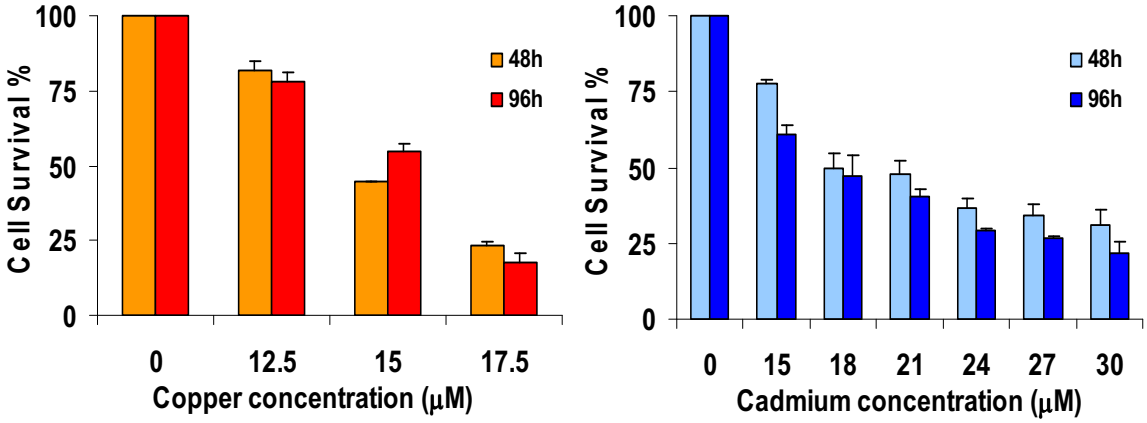

Figure 11: Cell survival expressed as percentage of controls.

5.3 RESULTS

Molecular analysis

As shown in Fig. 12 the band size relative to PCR products are of the expected size (around 700bp). The partial LSU rDNA genes from our Adriatic isolate of *C. closterium* were sequenced and results from BLAST searches into GenBank database confirmed that the obtained sequences were homologous to ribosomal genes of diatoms in particular to 28S rDNA gene.

The LSU rDNA sequence (D1 and D2 domain) of the Adriatic isolate of *C. closterium* was 566pb long (soon available in public database GenBank). This sequence differed from the other available on GenBank, which were: a strain form Denmark (AF417666) and a strain from Belgium (AF289049). The sequence divergence between the strains gave 49 and 1 variable nucleotide positions respectively, with a variation of 8.7% and 0.2%.

The phylogenetic tree (Fig. 13) shows a high similarity between our *C. closterium* strain and the one from Denmark (same cluster), both of them are in the same cluster as the others *Cylindrotheca* species. All the pseudo-nitzschia species are grouped in another cluster; this phylogenetic analysis confirmed what found in the phylogeny of the Bacillariaceae by Lundholm *et al*., (2002).

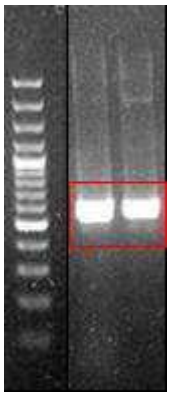

Figure 12: PCR products, on the left is represented the molecular size marker while on the right inside the red box are shown the DNA bands amplified with PCR; bands are of around 700bp as expected.

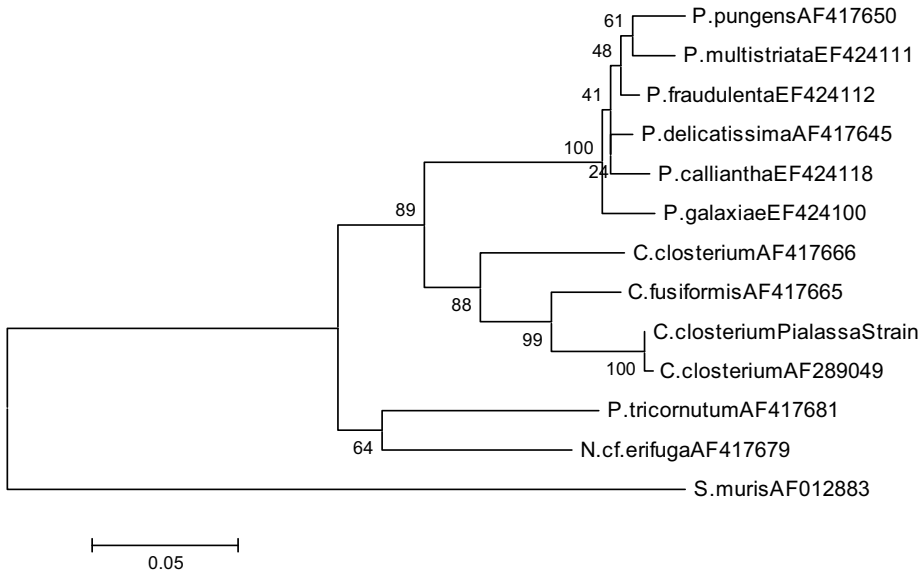

Figure 13: Phylogenetic tree based on the 28S rDNA gene. *Sarcocistis muris* is used as out-group.

Metal speciation

Computational simulations results of chemical equilibrium are shown in table 5. Total bioavailable (free and labile) copper and cadmium concentrations were far lower then the ppm added; labile fraction increased with increasing

metal concentrations, but it decreased with increasing exposure time. Copper resulted to be much more complexed to EDTA than cadmium.

	µM	pH after addition	FREE	LABILE	Total Bioavailable	EDTA complexes	pH after 96h	FREE	LABILE	Total Bioavailable	EDTA complexes
Copper	13.5	8.6	0.025	0.92	0.94	12.55	9.5	0.001	0.439	0.44	13.06
	15	8.9	0.015	0.95	0.97	14.02	9.4	0.003	0.640	0.64	14.35
Cadmium	13	8.5	0.238	5.17	5.41	7.53	9.5	0.080	1.768	1.85	11.13
	16	8.6	0.326	7.09	7.41	8.51	9.0	0.000	5.433	5.43	10.26

Table 5: Computational simulations results. Free, Labile and Total Bioavailable metal concentrations and EDTA- complexes are express in µM.

Copper and cadmium affected growth in a different way, as shown in Fig. 14. Growth, expressed as cell numbers, decreased with increasing concentrations of both metals, but while cadmium reduced cells number with increasing exposure time, copper determined the strongest reduction after 24 hours, then cultures recovered to higher densities. Growth rate, expressed as percentage of control (Fig. 15), decreased with increasing time of exposure; copper showed the strongest decrease after 24 hours.

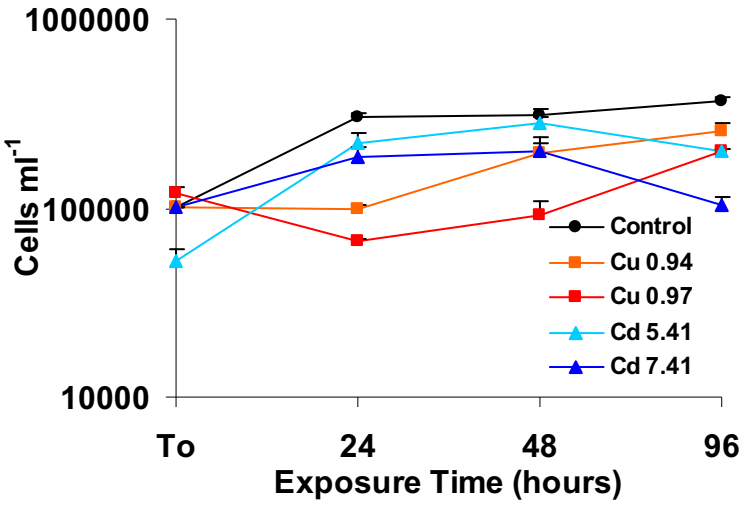

Figure 13: Growth curves of control and metal treated cultures. Concentrations are expressed in µM and values correspond to the total bioavailable concentration after addition. Growth is followed after 24, 48 and 96 hours of exposure to the metals.

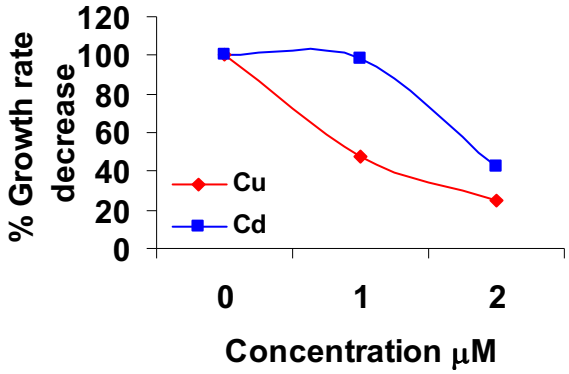

Figure 14: Growth rate (d^{-1}) decrease expressed as percentage of control. X- axis represents metals concentrations: 0 is equivalent to control, 1 corresponds to 0.94 and 5.41 μM of copper and cadmium, 2 corresponds to 0.97 and 7.41 μM of copper and cadmium.

The total intracellular (internal plus externally bounded) copper decreased with increasing Cu concentrations, as shown in Fig. 16. The percentage of copper absorbed was 41 and 16 % at 0.94 and 0.97 μM respectively. Interestingly, the copper intracellular content, (expressed as μg of Cu per million cells), significantly decrease from 24 to 96 hours of exposure; copper values in fact were 1.8 after 24 hours while 0.82 after 96 hours ($p<0.001$), (data not shown). On the contrary, total intracellular cadmium content increased at increasing Cd concentration supplied; the percentage of cadmium absorbed was only 2.5 and 1.9 % at 5.41 and 7.41 μM.

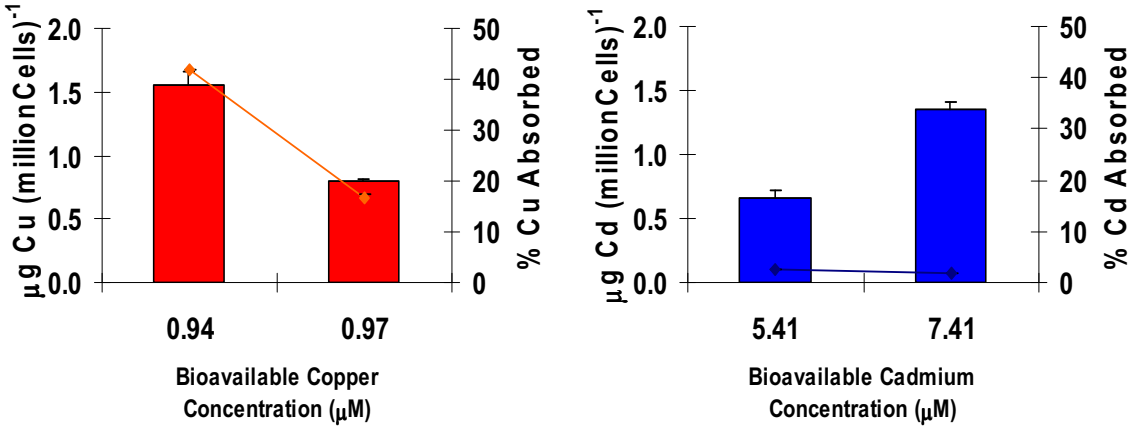

Figure 16: Intracellular copper (on the left) and cadmium (on the right) content as μg of metal per cell. Uptake was also expressed as percentage of the metal added on the secondary y- axis. Intracellular metals content was evaluated after 96 hours of exposure.

Exposure to copper and cadmium at concentrations of 0.94 and 7.41 μM respectively during 96 hours determined a significant increase in both the intracellular ($p < 0.05$) and extracellular ($p < 0.01$) polysaccharide production, (Fig.17).

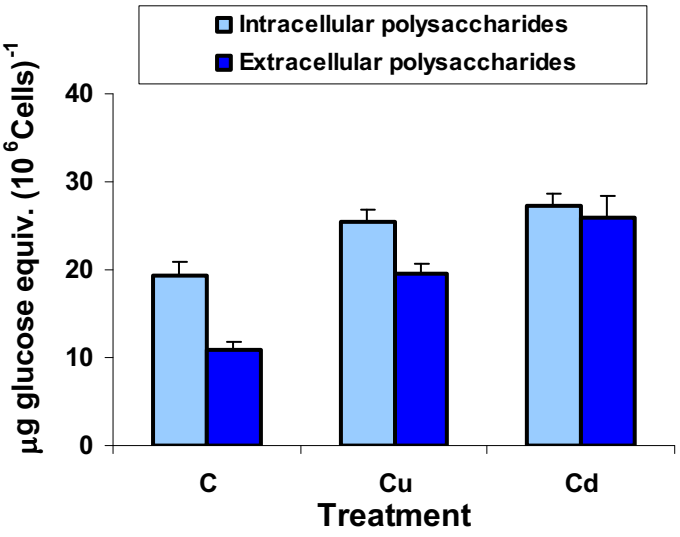

Figure 17: Measurement of intra- and extracellular polysaccharides production expressed as μg of glucose equivalent per million cells, obtained after 96 hours of exposure to 0.94 and 7.41 μM of copper and cadmium respectively.

Oxidative damage to lipids to due metals exposure was measured as lipid peroxide (LPO) content and expressed as nmol LPO per mg of unsaturated lipids, (see paragraph 3.1.2). The highest copper concentration determined a significant increase in lipid peroxide content ($p < 0.01$) compared to control; exposure to 7.41 μM cadmium determined a lipid damage higher than both controls and cultures exposed to 0.94 μM of copper ($p < 0.05$), (Fig. 18). Lipid content decreased significantly only under the higher copper concentration ($p < 0.01$). Malondialdehyde (MDA) content, a secondary product of lipids peroxidation, was observed to increase already after 24 hours of exposure to both the highest Cu and Cd concentrations, (data not shown).

Enzymatic activities of two key enzymes of the antioxidative cell system, superoxide dismutase (SOD) and ascorbate peroxidase (APX), were evaluated after 96 hours of exposure to copper and cadmium and results are reported in

Fig. 19. Cadmium exposure determined a strong increase in both enzymes activity; the highest Cd concentration supplied significantly increase SOD activity ($p<0.05$) and under both Cd concentrations APX was significantly stimulated ($p<0.001$). Copper treatment caused a reduction of APX enzyme under both concentrations supplied ($p<0.05$), while SOD activity was not significantly affected ($p>0.05$). Protein content was not affected by the exposure to both metals, ($p>0.05$).

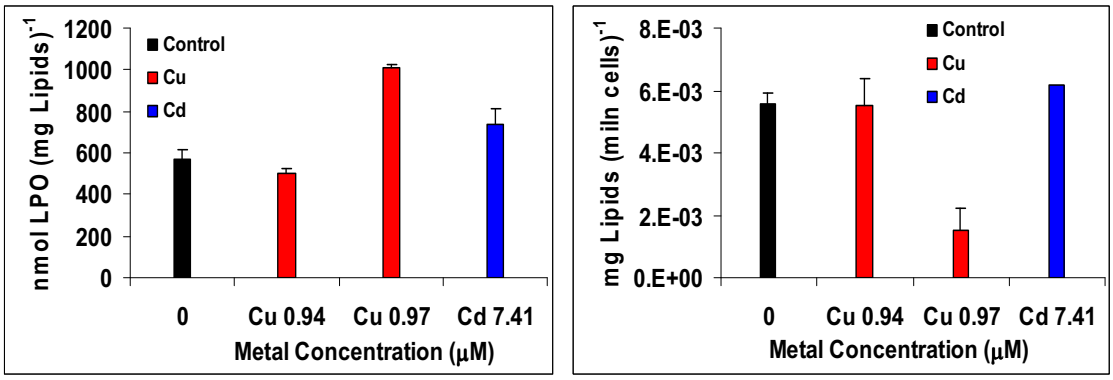

Figure 18: Graph on the left: nmol of lipids peroxide expressed on the basis of mg of lipids. Cells were analyzed after 96 hours of exposure to the metals. Graph on the right: Content of lipids expressed as mg of lipids on the basis of million cells. Values are average of two replicates.

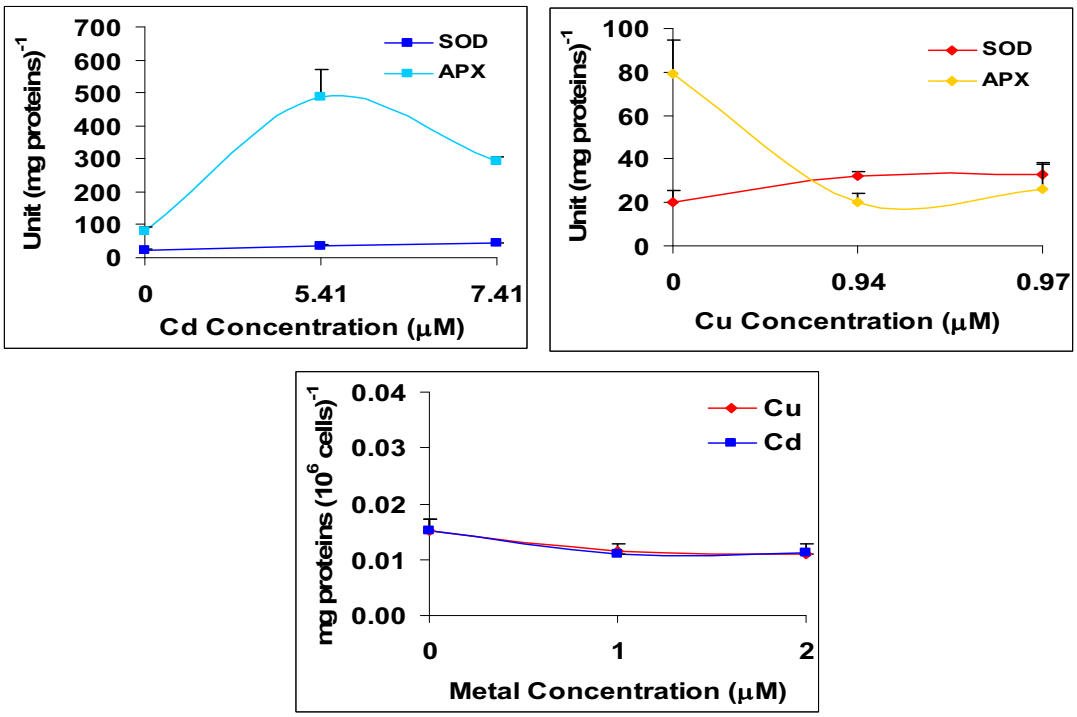

Figure 19: Upper graphs: SOD and APX activity of control, copper treated cells (0.94 and 0.97 µM) and cadmium treated cells (5.41 and 7.41 µM). Bottom graph: protein content. 0, 1, 2 represent copper and cadmium concentrations: 0, 0.94, 0.97 µM and 0, 5.41 and 7.41 respectively.

Maximum quantum efficiency of photosystem II (F_v/F_m) was measured following metals exposure after 24, 48 and 96 hours; results are reported in Fig. 20. Copper and cadmium, at both concentrations tested, significantly reduced the F_v/F_m with respect to control cultures after 24 hours ($p < 0.01$). After 48 hours, copper treatment at both concentrations did not further inhibit PSII efficiency, ($p > 0.05$), showing higher values of PSII efficiency with respect to control and cadmium treated cells ($p < 0.01$), at the end of the experiment (96 hours). On the contrary, F_v/F_m values of cadmium exposed cultures decreased significantly with increasing time of exposure and with increasing Cd concentrations ($p<0.01$).

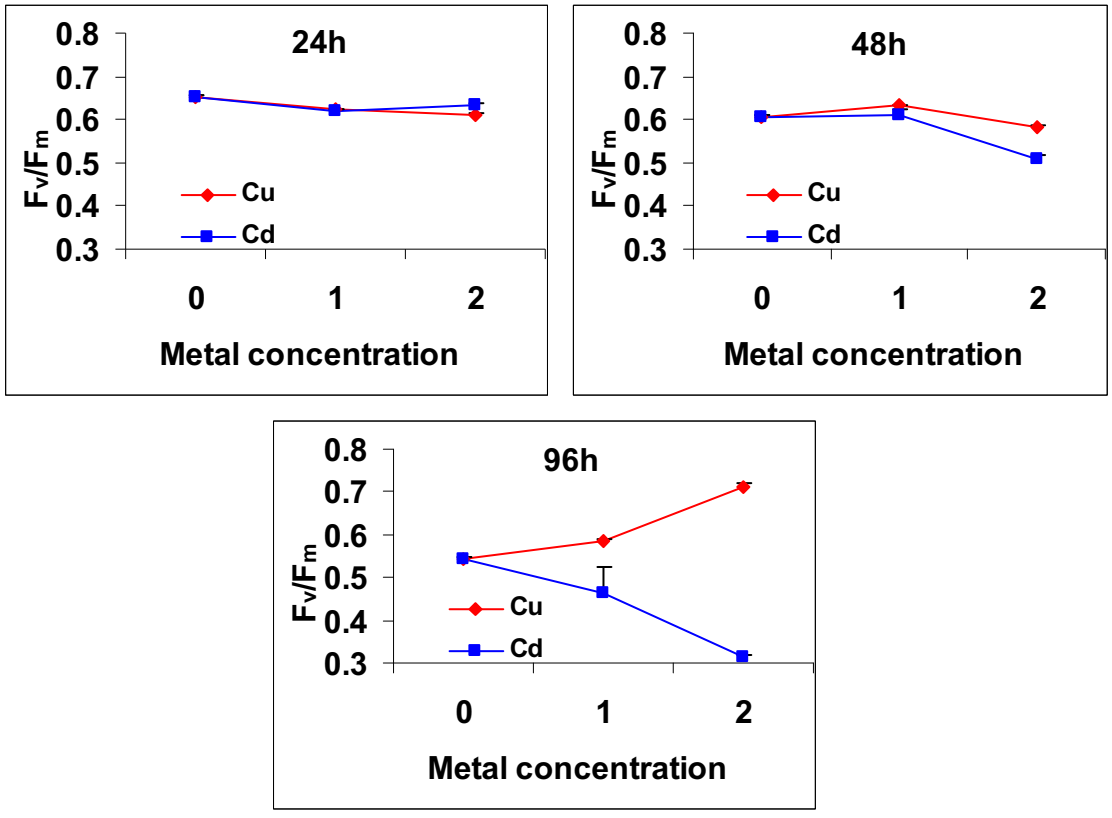

Figure 20: Maximum efficiency of photosystem II (Fv/Fm) measured after 24, 48 and 96 hours of exposure to copper and cadmium. Metal concentration are expressed in μM. On the X- axis: 0= control, 1= 0.94 μM of copper and 5.41 μM of cadmium, 2= 0.97 and 7.41 μM of copper and cadmium respectively. Measures are average of two replicates ± St. Dev.

Fig. 21 represents the impact of tested metals on maximal fluorescence (F_m), plastoquinone pool ($F_v/2$) and efficiency of water splitting apparatus (F_o/F_v). Cadmium reduced the maximal fluorescence yield of 20% after 96 hours of exposure, while copper had a negative effect only after 24 hours and then F_m resulted to be even higher than control. Cadmium was found to exert a severe toxic effect on plastoquinone pool ($F_v/2$); this toxic effect was found to be higher at higher Cd concentrations and with increasing exposure time. At Cd concentration of 7.41 μM only 40 % of the plastoquinone pool was active after 96 hours of treatment.

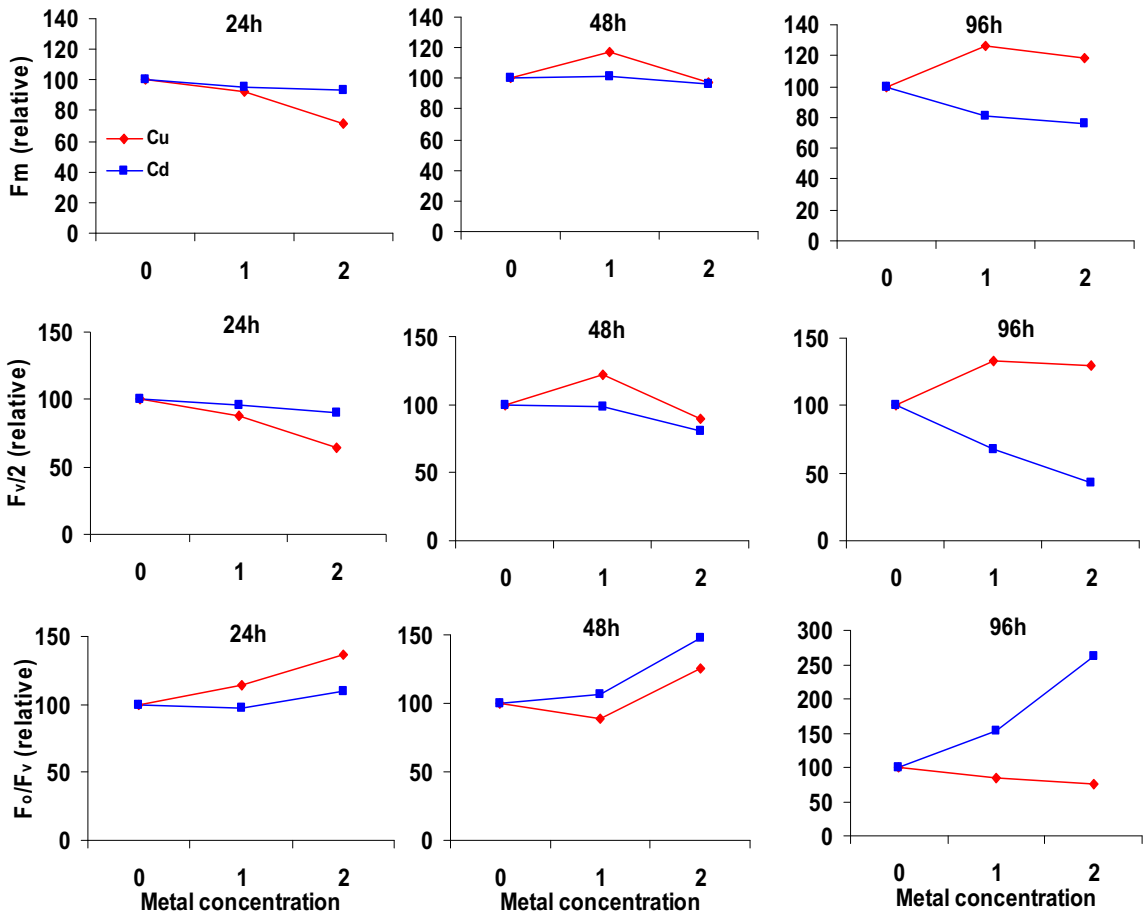

Figure 21: Measurements of maximum fluorescence yield (Fm), plastoquinone pool (Fv/2) and efficiency of water splitting apparatus (Fo/Fv) taken after 24, 48 and 96 hours of metal exposure. On the X- axis: 0= control, 1= 0.94 μM of copper and 5.41 μM of cadmium, 2= 0.97 and 7.41 μM of copper and cadmium respectively. Values are all expressed as percentage of the control.

Copper, at the two concentrations tested, inhibited the plastoquinone pool function of 15 and 35% respectively, after 24 hours, but after 96 hours $F_v/2$ values where higher then the control. The efficiency of water splitting apparatus, represented by the ratio F_o/F_v, was affected by cadmium treatment as appeared from the severe rise of that ratio; this rise was higher at higher Cd concentrations and with increasing exposure time (up to 300-fold rise after 96 hours). F_o/F_v ratio increased due to copper treatment only after 24 and 48 hours of exposure while at the end of the experiment was lower than the control. In Fig. 22 results of the effective yield, photochemical quenching and non-photochemical quenching measured after 24, 48 and 96 hours are reported. Cadmium concentration of 5.41 μM slightly affected the Φ'_m compared to control after 24 and 48 hours but further exposure to 96 hours caused the effective yield to drop from 0.5 to 0.2; a similar behavior was observed for the Q_p while the non-photochemical quenching increased strongly after 96 hours. Higher Cd concentration, (7.41 μM), enhanced these negative effects, which were more intense even after 24 hours. On the contrary, exposure to 0.94 μM of copper only slightly affect the effective yield and the photochemical quenching, showing values close to controls; higher copper concentration, (0.97 μM) determined the highest inhibition of Φ'_m and Q_p after 24 hours, but then the photosynthetic capacity was restored.

Finally, fluorescence induction kinetics were measured on cultures after 24 and 96 hours of exposure to copper and cadmium and graphs are reported in Fig. 23. The photosynthetic activity was inhibited by exposure to 7.41 μM of Cadmium already after 24 hours, since the maximum fluorescence (F_m and F'_m) were decreased by 9% and 36% compared to control; treatment prolonged to 96 hours gave an inhibition of 39% and 44% respectively. Copper exposure to 0.94 μM during 24 hours caused an inhibition of Fm and Fm' of 7% and 10% respectively and no enhanced inhibitory effect was seen after 96 hours.

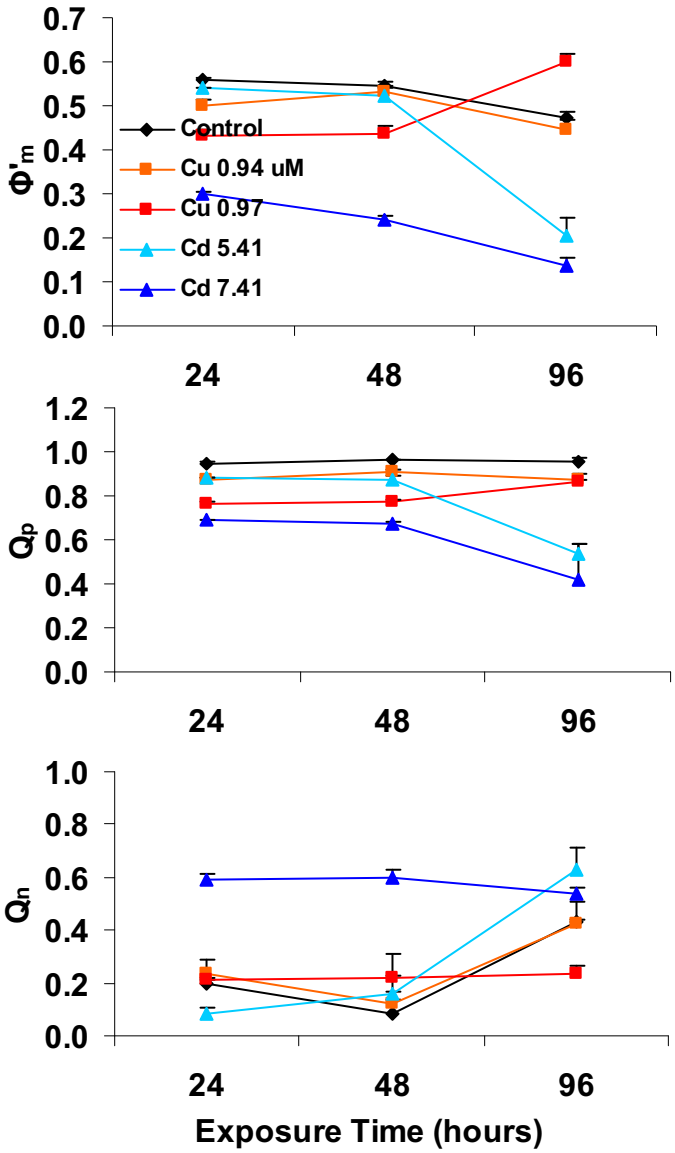

Figure 22: Effective yield (Φ'_m), photochemical quenching (Q_p) and non-photochemical quenching (Q_n), measured after 24, 48 and 96 hours exposure to all metal concentrations tested.

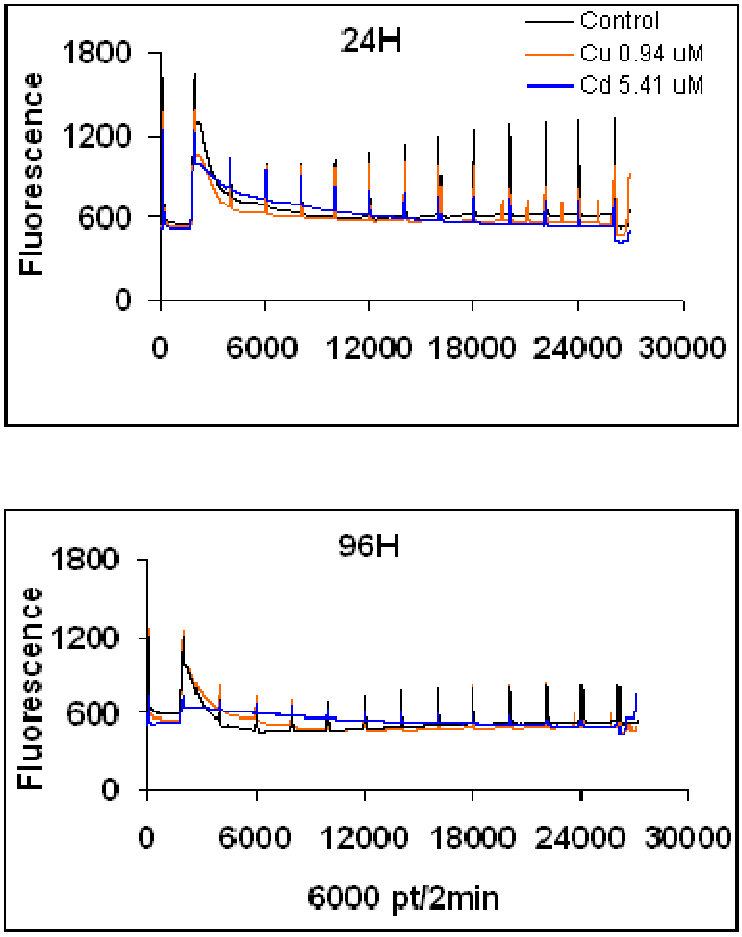

Figure 23: Fluorescence induction kinetics obtained with PAM-fluorometry. Curves are average of two replicates.

5.4 DISCUSSION

Toxic metals typically are taken up into cells by nutrient metal transport systems. Cells regulate the uptake rate of nutrient metals to maintain their intracellular concentrations at optimal levels needed for growth and metabolism. During exponential growth, the external concentration of labile inorganic species, the cellular metal uptake rate, the cellular metal concentration and the specific growth rate are all related to each other by a set of interconnecting relationships.

Our results showed that the total bioavailable Cu and Cd fractions are much lower than the total metals in solution, as was also observed by Lage *et al*. (1994), in cultures of the dinoflagellates *Amphidinium carterae* and *Prorocentrum micans* exposed to copper. Gerringa and colleagues (1995) found that ionic Cu decreased in cultures of *Ditylum brightwellii*, due to a substantial increase in ligand concentrations. In our experiments free metal ions and labile inorganic complexes increased with increasing Cu and Cd concentrations but strongly decreased with increasing exposure time (from 24 to 96 hours). Copper determined the strongest decrease of cultures cell number after 24 hours of exposure. Growth rate inhibition of phytoplanktonic organisms in the presence of metals has been related to the binding of the metals to sulphydryl groups of enzymes, which are important in the regulation of cellular division, (Fisher *et al*., 1981).

The main difference observed here between copper and cadmium treatment was that, while sublethal copper levels showed higher toxicity after 24 hours of exposure and then cultures recovered their growth and photosynthetic capacity, sublethal cadmium levels led to more gradual but irreversible effects. The decrease in cell density over the first 24 hours of exposure to copper (apparent lag-phase), did not lengthen beyond one day as copper concentrations increased. This was also observed in the green alga *Selenastrum capricornutum* exposed to different copper concentrations, (West *et al*., 2003). If induction of defense mechanisms was important, we might have expected to observe a lag-phase in the cell concentration vs. time response, proportional to the degree of stress, (Rijstenbil & Poortvliet, 1992). Algae have

adopted several strategies to survive and reproduce in metal-polluted environments. The main goal of these strategies is to prevent exposure of sensitive targets (e. g., DNA, proteins) to reactive metals. Control of metal uptake, through increase production of extracellular copper chelators or through binding of metals at the cell surface or to mucilage (Gerringa *et al*., 1995), excretion of accumulated metals and intracellular immobilization of accumulated metals are the main mechanisms to protect algae from toxic effects. We observed a significant increase of intra- and extracellular polysaccharides production in response of exposure to 0.94 uM of copper and 7.41 uM of cadmium during 96 hours; these biomolecules could have helped to reduce metals toxicity. Increased production of polysaccharides were observed also in C. fusiformis, (Pistocchi *et al*., 1997).

Speciation calculations clearly showed that copper is much more complexed to EDTA than cadmium and that these Cu-EDTA complexes increase with increasing exposure time. At the beginning of the experiment all the EDTA present in the medium may have been complexed with alkaline earth and other heavy metals, but after that, due to the fact that Cu-EDTA complexes are thermodynamically more stable than the other main metal-complexes (Anderson & Morel, 1978), a significant fraction of the copper was then bound by the EDTA. These chemical kinetics may account for the different effects of copper observed after 24 and 96 hours of exposure; a fast response to copper stress, in terms of growth and cell motility, was observed in dinoflagellates batch cultures after only 3 hours of copper exposure (Lage *et al*., 1994). It is also possible that, as a consequence of the initial copper impact (after 24 hours), some cells died and released various substances in the medium which could have bound the metal and therefore contributed to the decreased in the labile copper fraction. In fact, growth and photosynthetic capacity recovered after 96 hours of copper exposure.

The optimal ionic Cu concentration for marine algae is assumed to be between 10^{-11} and 10^{-13} mol/L, (Sunda & Guillard, 1976). A complete study conducted by Brand *et al*., (1986) showed that reproduction rates of phytoplankton species were inhibited of 50% at ionic copper concentrations of 10^{-10} and 10^{-11} M and that diatoms were the least sensitive to Cu.

Concentrations of ionic copper supplied in our experiments were a bit higher (around 10^{-9} M), but *Cylindrotheca closterium* cells were still able to divide despite some oxidative burst occur. In fact, at the highest Cu concentration supplied here to *C. closterium* cells a significant increase in lipid peroxidation, measured as LPO content increase, was observed; a similar effect of copper was observed also in *Scenedesmus* sp. treated with 2.5 and 10 μM for 6 hours and 7 days (Tripathi *et al*., 2006). It is fairly known that binding of copper to thiols disrupts redox status of the cell thereby enhancing the production of reactive oxygen species (ROS) (Dietz *et al*., 1999). Due to the redox-active nature of Cu^{2+} it catalyses the formation of extremely reactive hydroxyl radicals, (Pinto *et al*., 2003). Mallick (2004), also found an increased lipid peroxidation at increasing copper concentrations in *Chlorella vulgaris*.

Superoxide dismutase (SOD) enzyme activity was not significantly increased after 96 hours of copper exposure, but it is possible that the time course of SOD induction could have been much higher few hours after copper addition. Response of SOD activity of *Gonyaulax polyedra* exposed to sublethal concentrations of copper was markedly fast, with maximal values observed after 2 hours of exposure (Okamoto & Colepicolo, 1998).

Copper treatment inhibited APX activity at both concentrations tested and this behavior was observed also in *Chlorella vulgaris* exposed to copper (Mallick, 2004). On the contrary, a stimulation of both these enzymes was observed in *Scenedesmus* sp. cells treated with 2,5 μM of copper (Tripathi *et al.*, 2006); at higher copper concentration (10 μM) instead, APX activity was highly inhibited in both short- (6 hours) and long- term (7 days) exposure. APX enzyme destroys the toxic H_2O_2 using ascorbate as substrate; the dehydroascorbate formed in this process can be reduced to ascorbate again by GSH, the latter being regenerated by gluthathione reductase (GR) in the presence of NADPH. Thus GR and APX are believed to act in conjunction to metabolize H_2O_2 to water, through the cycle known as Halliwell-Asada pathway. Therefore, in view of high NADPH requirement of GR and the depletion of GSH pool as observed in *Chlorella vulgaris* (Mallik, 2004), a possible inactivation of APX under oxidative stress is quite possible. Moreover, in spite of the failure of the APX enzyme in scavenging H_2O_2, *C. closterium* survived even at 0.97 μM of

copper showing a recover of all photosynthetic parameters; this behavour suggests the occurrence of some other protective mechanisms, such as proline production, which is observed to increase during Cu exposure in algae (Wu *et al*., 1998).

Cadmium, in contrast to other heavy metals such as copper, does not seem to act directly on the production of oxygen reactive species (via Fenton and/or Haber Weiss reactions) but can inhibit the activity of several antioxidative enzymes (SOD, APX, CAT, GR) and enhance lipid peroxidation (Gallego *et al*., 1996). Cd was found to produce oxidative stress on *C. closterium*: at 7.41 μM of Cd, lipid peroxide content increased and the activity of SOD and APX enzymes was enhanced. Similar results were found in the marine alga *Nannochloropsis oculata:* both lipid peroxidation and the levels of APX and GR increased as a consequence of exposure to 10 μM of Cd (Lee & Shin, 2003).

Copper may inhibit photosynthesis and respiration thus reducing protein content (Lage *et al*., 1994), nevertheless we did not observe a decrease in protein content neither due to Cu or Cd.

The maximum quantum efficiency of PSII was resulted to be a good indicator of metals treatment; it showed a very good relationship with diatom growth and it requires few minutes to be done. F_v/F_m illustrated the direct effect of copper and cadmium on the photochemistry; it resulted to be inversely correlated to both Cu and Cd metal concentrations after 24 hours exposure. Copper is known to decrease the electron transfer rate in chloroplast; sublethal concentrations of copper (0.16 μM) provoked photoinhibition of PSII under light in *Chlorella pyrenoidosa*; in fact, F_v/F_m decreased at increasing photon flux intensity mainly due to a gradual and essential decrease of F_m and to a rapid but minor increase of F_o fluorescence yield (Vavilin *et al*., 1995). Algae are generally exposed to elevated concentrations of heavy metals in polluted water bodies for a long period of time; sometime short-term exposure also occurs due to accidental discharge of metals into a water body. Hence, there is a need to evaluate toxicity and oxidative stress during both short- and long- term exposure to heavy metals. In the light of the above, the present experiment analyzed the response of the photosynthetic apparatus of *C. closterium* after 24 hours (short term exposure) and after 96 hours (long term exposure) following

metals (copper and cadmium) addition. Further experiments will be necessary to evaluate also the induced short term oxidative stress in terms of enzymes activity (SOD, APX, GR), lipids and proteins damage. Results of photosynthetic efficiency measurements (F_v/F_m, Q_p, Q_n, $F_v/2$, F_o/F_v) on copper treated cells, showed the highest effect after 24 hours of exposure, while after 96 hours cells had completely recovered their photosynthetic capacity. Hence, copper caused a stronger oxidative stress in short-term than in long-term exposure, as occurred also in *Scenedesmus* sp. (Tripathi *et al*., 2006). This behavior can be explained with an acquired tolerance against metal-induced oxidative stress in the long term, perhaps due to enhanced scavenging of ROS or sequestration of metals into intracellular compartments. Metabolism-mediated efflux of metal ions may also confer metal tolerance to some organisms (Gaur & Rai, 2001); this agree with our results, which showed a decrease in copper intracellular content after 96 hours compared to short-term exposure (24 hours). Exposure to sublethal copper concentrations did not inhibit the photosynthetic electron transport of that diatom, after 96 hours; however copper could become more toxic if present in combination with others contaminants. Synergistic effects between Cu and 1,2-dihydroxyanthraquinone (1,2-dhATQ, a photoproduct of the polycyclic aromatic hydrocarbon anthracene) have indeed been demonstrated by Babu and colleagues (2001) in *Lemna gibba*, there, authors showed that 1,2dhATQ blocks electron transport at the Cytocrome b_6/f complex causing a net reduction of the plastoquinone pool to PQH_2: copper accepts electrons from the reduced species (e. g. PQH_2) and pass them to available electrons acceptors (e. g. O_2) leading to ROS production. Thus, non toxic concentrations of copper can become extremely toxic when the redox balance of a biological system is previously altered.

As already stated above, cadmium showed to be highly toxic to the diatom investigated even if the EC50 was higher than the one measured for copper. Photosynthetic parameters decreased as Cd concentrations increased as observed also in the green microalga *Scenedesmus* exposed to several metals (Mallick & Mohn, 2003). Here, the F_o/F_v ratio abruptly increased, up to 300% at 7.41 μM of Cd, suggesting that the metal has a severe impact on the water-splitting apparatus, most probably by replacing manganese (Mn) from the

water-splitting apparatus of the oxidizing side. Competing metals such as copper and cadmium inhibit uptake of Mn by its cellular transport system, as seen in several diatoms (Sunda & Huntsman, 1983). Increasing Cd concentrations inhibited growth rate of *Thalassiosira pseudonana* only at low Mn concentrations, this effect is due to Cd inhibition of Mn uptake rate leading to Mn-deficiency, (Sunda & Huntsman, 2001).

In conclusion, our experiments underlined the induced copper and cadmium oxidative stress in the diatom *C. closterium*. Copper resulted to be more toxic due to its lower EC50 compared to Cd; nevertheless copper effects on growth and photosynthesis were severe only following metal addition (24 hours) while exhibiting a complete recover after 96 hours. Thus, copper toxicity caused cells to die just after copper addition and then cell breakage may have increased organic Cu-complexing ligands which compete with cells to stabilize and reduce ionic copper concentration in spite of a further copper increase.

On the contrary cadmium treatment showed a gradual but irreversible damage to cells, both in terms of growth reduction, oxidative damage and photosynthesis inhibition. The stress degree resulted to be proportional to the Cd concentration supplied.

Fluorescence measurements realized by means of PAM fluorometry demonstrated to be a very useful non invasive tool which gives many information rapidly; the maximum efficiency of photosystem II (F_v/F_m) and the efficiency of the water-splitting apparatus (F_o/F_v) were found to be good indexes of the cells photosynthetic apparatus state.

CADMIUM AND UV RADIATION INTERACTIONS: EFFECTS ON GROWTH, PHOTOSYNTHESIS AND CARBON ASSIMILATION IN *Dunaliella tertiolecta* AND *Cylindrotheca closterium*.

6.1 INTRODUCTION

Cadmium (Cd) is a widespread heavy metal released into the environment by heating systems, metal industries, waste incinerators, urban traffic, cement factories and agricultural fertilizers. Cd damages the photosynthetic apparatus, lowers chlorophyll and carotenoid content, affects the activity of several enzymes through replacement of other metal ions and produces oxidative stress, (Sanità di Toppi et al., 1999). As already stated in the general introduction of this thesis, cadmium effects can be counteracted in algae by exudation of complexing agents, immobilization in the cell wall and synthesis of phytochelatines. Cadmium can also be accumulated in algae and plants and thus be dangerous to human health because it enters the food chains.

Ultraviolet radiation (UV) has many harmful effects in all living organisms including humans. Due to the decrease in the ozone layer, which absorbs the short wavelengths (UVB), an increase in the UVB radiation has been observed in recent decades, and predictions show that the ozone layer will remain vulnerable to further depletion in the near future, (McKenzie et al., 2003). In photosynthetic organisms the UVB leads to inhibition of photosynthesis and growth, (Vassiliev et al. 1994), inhibition of nutrient uptake, (Beherenfield et al., 1995) and DNA damage (Buma et al., 2000, 2001).

The aim of this study was to investigate the effects of cadmium and UVB alone and in combination, on two different microalgae, (a green alga and a diatom). Photosynthetic organisms from both terrestrial and aquatic environments may be exposed simultaneously to Cd and UVB and this could cause severe stress, since both factors affect basic metabolic processes. Our goal was to understand to what extent Cd and UVB radiation alone would affect growth, inorganic carbon assimilation, oxygen evolution and photosynthetic

performance and if synergistic effects can occur. Few studies have been conducted on the interactions between Cd and UVB and those have been carried out mainly on plants, cyanobacteria and an aquatic bryophyte.

The chlorophyte *Dunaliella tertiolecta*, used for this study, is known to possess active mechanisms for dissolved inorganic carbon (DIC) acquisition, (as both HCO_3^- and CO_2), and CO_2 accumulation (Amoroso *et al*., 1998); on the contrary, nothing is known about the diatom *Cylindrotheca closterium*. A second objective of this work was thus to investigate the importance for cells to possess CO_2 concentrating mechanisms (CCMs) or not, when exposed to Cd and UVB. CCMs increase the CO_2 concentration at the active site of 1,5-bisphosphate carboxylase-oxygenase (RUBISCO), both in cyanobacteria and algae, and they are responsible for one third of the 100 Pg of organic carbon produced in net primary productivity on earth each year (Raven, 1997b,c).

6.2 EXPERIMENTAL SET UP

Experiments were conducted on two different species, a green alga *Dunaliella tertiolecta* (strain CS 175, from the CSIRO Marine Sciences Algal Culture Collection, Hobart) and a diatom *Cylindrotheca closterium* (CSIRO strain CS-5). Both species were cultured in f2 medium. The water used for medium preparation was collected from the ocean at Queenscliff (Melbourne) and stored at 4 ^oC, the salinity was 37. The water was then enriched with nutrients and vitamins and the pH adjusted to 8.2. The medium was filtered through a 0.2 µm sterile filter and decanted into pre-autoclaved bottles. Cultures were maintained in a thermostatic chamber (18° C) with a 12:12h light – dark cycle, under a photosynthetically active radiation (PAR) of 100 µmol photons m^{-2} sec^{-1}, (measured with a LICOR 1000 Data logger). During growth, cells were counted using a haemocytometer (Neubauer)

A first series of cultures (grown in 30 ml polyethylene bottles) was exposed to different cadmium concentrations and the growth was followed with a fluorescence spectrophotometer (Hitachi F-2000) twice a day. For *D. tertiolecta* the excitation wavelength was 435 nm and the emission wavelength was 680 nm, while for *C. closterium* they were 440 and 680 nm respectively.

The metal was supplied as $CdCl_2$. These first tests were done on both species, in order to understand what was the concentration of the metal causing a significant reduction of growth; the experiments were then repeated with that Cd concentration, supplied alone and in combination with ultraviolet radiation.

D. tertiolecta was first grown with 1, 3, 5, 10, 15 ppm of Cd and then a fine tuning was done using 3, 4, 5, 6, ppm of Cd. In the end we decided to study the effects of 3 ppm and 3.7 ppm of cadmium under only PAR light, while we chose 3.7 ppm of Cd to study the interactions with UV radiation. *C. closterium* was grown with 1, 3, 5, 10, 15 ppm of Cd and then the range was restricted to 0.4, 0.8, 1, 1.5 ppm of Cd. The effects of the metal were measured by growing the diatom with 0.5, 0.75, 0.95 ppm of Cd under PAR light, while the interactions with UV were studied growing *C. closterium* with 0.95 ppm of Cd. The UV-B dose supplied was 0.7 Wm^2, while the UV-A dose was 8 Wm^2 supplied for 12 hours a day, (lamp UVA-340, Q panel CO. USA; Crompton 4100K/33 cool white). Cultures (250 ml) for studies of interactions between Cd and UVB were grown in glass and quartz flasks for exposure to PAR and UVB respectively.

Several analyses were performed on the cultures to test the effects of metal toxicity itself and in combination with UV radiation. During the exponential phase, photosynthetic efficiency (F_m/F_v) and relative electron transport (rETR) were measured using a Phyto-Pam fluorometer, (see Chapter2-Section3 for methods).

During the exponential phase we also measured the ratio between production and respiration rate, P/R, and photosynthesis as a function of dissolved inorganic carbon (P/DIC curves), both estimated using an oxygraph. The chlorophyll content was also evaluated, (for methods see chapter3-section3).

6.3 RESULTS

Experiments with *Cylindrotheca closterium* .

Effects on Growth. Cultures of *C. closterium* grown with Cd concentrations ranging from 1 to 15 ppm gave a growth reduction of more than 50% with respect to the control, for concentrations above 1 ppm (Tab.1). For this reason we decided to do a fine tuning, growing the diatom within the range of 0.4-1.5 ppm of Cd. In this case we obtained a growth reduction of 40, 63 and 69% with 0.4, 0.8 and 1 ppm respectively (Fig.24 and Tab.6).

Experiments were then carried out to test the effects of Cd with 0.5, 0.75 and 0.95 ppm under PAR, while only the last concentration was used to evaluate the interactions between Cd and UV. Growing the diatom with 0.5 ppm of Cd did not seem to alter the growth rate with respect to control, in fact μ was 1.12 day^{-1}(st dev. 0.210) for the control and 1.16 d^{-1} (st dev. 0.120) for Cd treated cells, (data not shown).

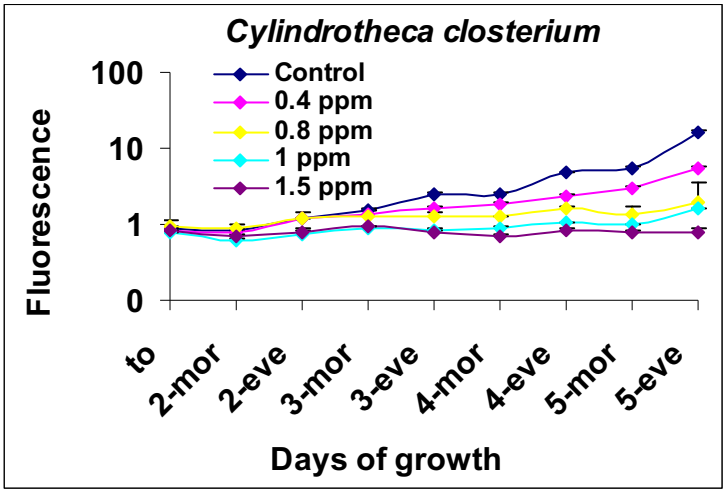

Fig.24: Growth curves, under different Cd concentrations, measured by following fluorescence emission. Measures were done twice a day (in the morning and in the evening). T_o corresponds to a density of 10000 cell ml-1.

Test1 Cd (ppm)	μ (h^{-1})	St. dev.	% Growth Reduction vs control	Test 2 Cd (ppm)	μ (h^{-1})	St.dev.	% Growth Reduction vs control
control	0.061	0.004	/	control	0.035	0	/
1	0.021	0.004	66	0.4	0.021	0.001	40
3	0.009	0.002	85	0.8	0.013	0.007	63
5	0.012	0.003	81	1	0.011	0.002	69
10	0.006	0.003	91	1.5	0.002	0.003	95
15	-0.002	0.001	104				

Tab. 6: *Cylindrotheca closterium* grown with different Cd concentrations and relative growth rates (μ) and standard deviations (3 replicates); the yellow columns represent the decrease in growth with respect to control.

In figure 25-A and 25-B the growth curves of cultures grown with 0.75 and 0.95 ppm of Cd under PAR light and with 0.95 ppm Cd under PAR and UV, are reported.Even if there is a decrease in growth rate values, (Tab. 7), at the highest Cd concentration, differences are not statistically significant. Presence of UV led to a longer lag phase- in fact both control and Cd treated cells required a couple of days more to reach the same cell number as in the experiment with only Cd and PAR light.

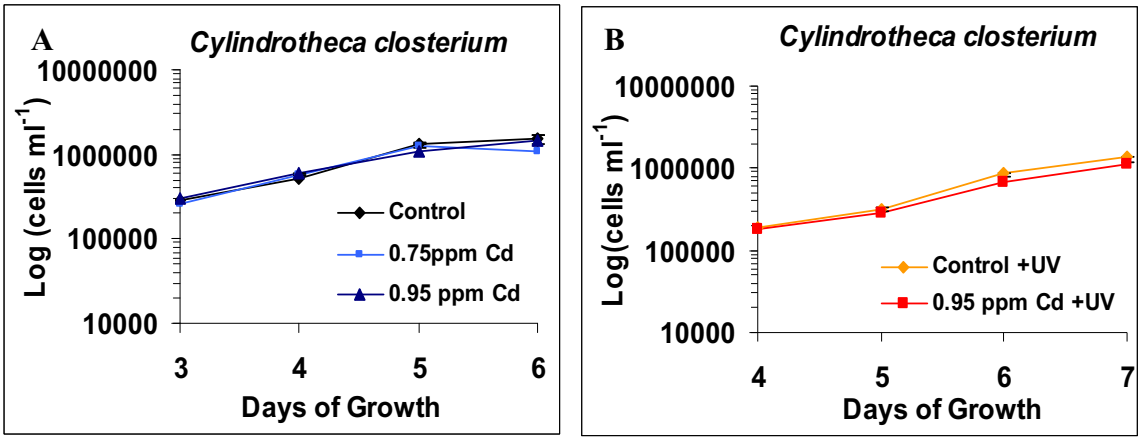

Fig.25: A-B) Growth curves of cultures exposed to Cd and PAR light. C) Growth curves of *C. closterium* exposed to Cd and UV treatment. The starting density is 10000 cells ml^{-1} in all cultures.

Cd (ppm) PAR	μ (h^{-1})	St. dev.
control	0.77	0.016
0.75	0.79	0.074
0.95	0.61	0.145
PAR+UV		
control	0.75	0.011
0.95	0.68	0.05

Tab. 7: *Cylindrotheca closterium* grown with different Cd concentrations and different regime light; relative growth rates (μ) and standard deviations (2 replicates) are reported.

The cellular chlorophyll content was also evaluated; measurements of absorbance of chl *a*, *b*, and *c* were performed and the main pigments were chl *a* and *c*, as expected for a diatom, (Fig. 26). Cultures grown with Cd and PAR light did not exhibit any significant difference between the three Cd concentrations tested (Anova, $p>0.5$). The addition of UV radiation determined a decrease in both chl *a* and *c* content of control cells (ANOVA, $p<0.01$).

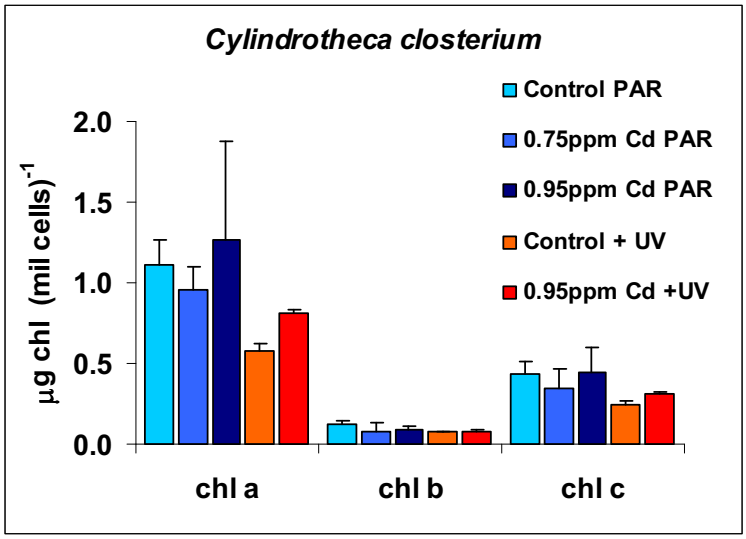

Figure 26: Chlorophyll content in *C. closterium* expressed as μg of chl per milion cells.

Effects on carbon assimilation, production and respiration. During the exponential phase of cultures measurements of oxygen evolution vs DIC concentrations were performed; the relative kinetic parameters (Vmax, Km, Γ) obtained in cultures exposed to increasing Cd concentrations and PAR or PAR + UV light are shown in figure 27.

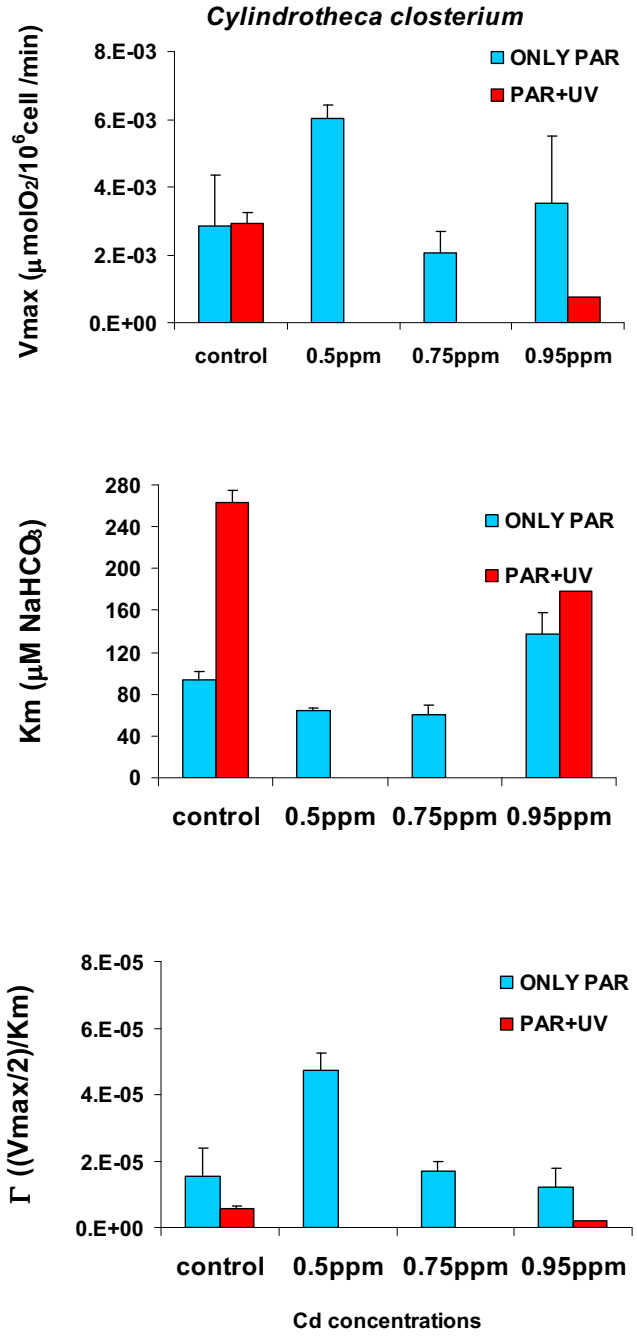

Figure 27: kinetics parameters obtained from oxygen evolution vs [DIC] plots. Values are an average of two replicates and Vmax and Γ are normalized to cell number. Data from experiments with Cd under PAR light and Cd under PAR + UV are presented.

The maximum rate of oxygen evolution (V_{max}) of *C. closterium* grown under PAR light did not seem to change with respect to Cd concentrations; the DIC concentration at which oxygen evolution occurred at half of the maximum rate (K_m) is slightly lower at 0.5 and 0.75 ppm of Cd, while it is higher at 0.95 ppm. The conductance values (Γ), obtained from the initial slope, are higher only at 0.5 ppm of Cd with respect to control. Control cells of *C. closterium* exposed to UV radiation exhibited a strong increase in K_m and a strong reduction in conductance with respect to control cells grown only under PAR light. The interaction between UV and Cd (0.95 ppm) led to a strong reduction in all the parameters with respect to control cells exposed to UV without cadmium.

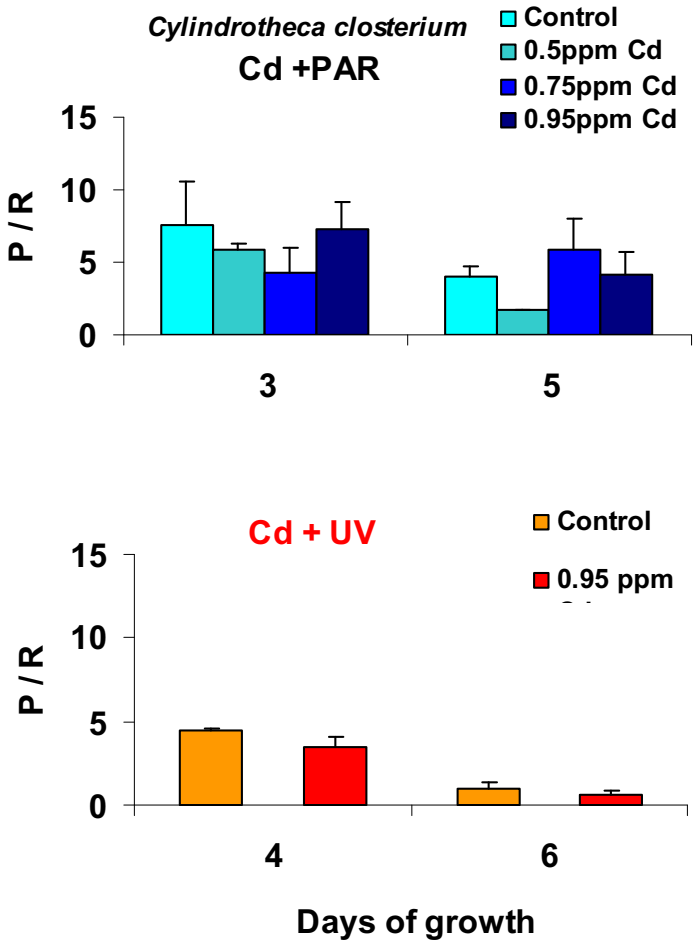

Figure 28: Ratio of production and consumption of oxygen measured with the oxyghraph. Values are all normalised to cell number and averaged from two replicates. Oxygen production was measured at a saturating light intensity of 250 µmol photons m^{-2} sec^{-1}. Respiration was measured in the dark.

In figure 28 the ratios between production and respiration for all the conditions tested are reported. Cells grown under different Cd concentrations and PAR light did not show differences in P/R ratios, (upper graph), while the values decreased with increasing age of the cultures (from day 3 to 5), which is mainly due to an increase in respiration processes. A much stronger effect is evident when cells are exposed to ultraviolet radiation, in fact control and Cd treated cells have lower P/R values with respect to cultures grown only under PAR. Even in this case the ratios decreased with increasing age of the cultures, from day 4 to 6, as a consequence of higher respiration processes. The synergy between Cd (0.95 ppm) and UV led to a decrease in P/R values with respect to control cells exposed to UV.

Effects on photosynthesis. The maximum efficiency of photosystem II, $((F_m-F_t)/F_m)$, was measured in sub-samples of cultures dark adapted for ten minutes. The addition of 0.5 ppm of Cd did not inhibit the PSII activity. In fact values were similar to those of control cultures and around 0.65 (data not shown; ANOVA, $p>0.5$). Similarly, higher Cd concentrations (0.75 and 0.95 ppm) did not show any effect on PSII, (Figure 29-A); the values were always around 0.65 during the exponential phase, as in controls, (Factorial ANOVA, $p>0.5$).

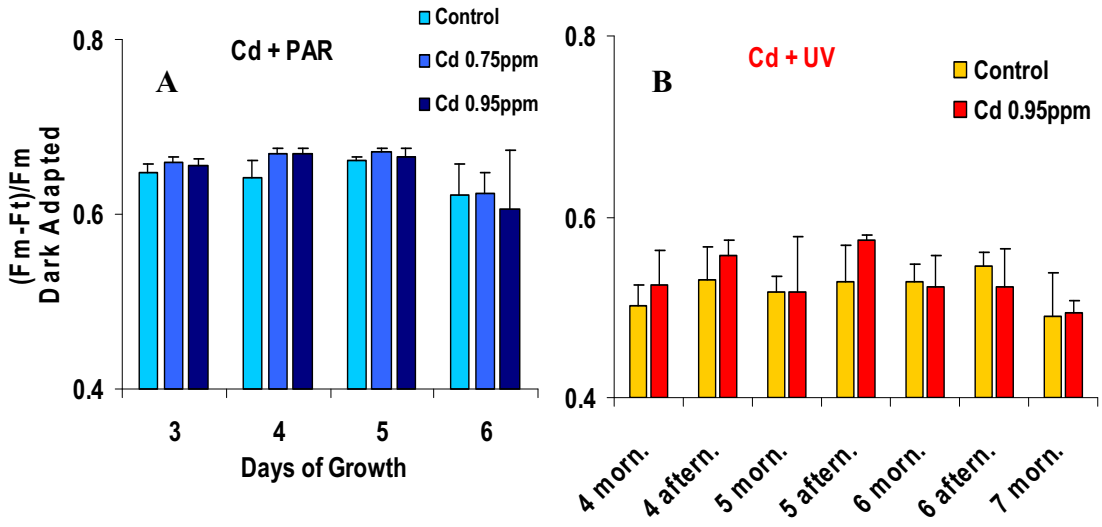

Figure 29: A) Maximum dark adapted yield of cultures exposed to two Cd concentrations (0.75 and 0.95 ppm) and PAR light (12:12h). Measurements were taken every day during the exponential phase. Two replicates. Differences tested with factorial ANOVA. B) maximum dark adapted yield of control and Cd treated (0.95 ppm) cultures exposed to UV, (12:12h). Measurements were taken twice a day: in the morning after 12 hours of UV light ON, and in the late afternoon after 8-10 hours of dark. Two replicate cultures (N=6), differences analyzed with factorial ANOVA.

In figure 29-B the values of the maximum dark adapted yield of cultures exposed to UV radiation are reported. The values were measured twice a day, in the morning, after 12 hours of UV lamps on, and in the afternoon, after 8-10 hours of dark. There are no significant differences between control and Cd treated cells, ($p>0.5$); values are slightly higher in the afternoon. The main result was that PSII was inhibited due to the presence of UV radiation; in fact values were far lower than in the cultures exposed only to PAR light, ($p<0.01$). In figure 29-B values were around 0.5-0.55, while in PAR grown cultures they were higher than 0.6.

The relative electron transport rate (rETR) was calculated from the rapid light curves obtained every day with a Phyto-PAM. In figure 30 results from the cultures grown with 0.75 and 0.95 ppm under PAR light are reported. There are no differences in the maximum rETR of control and Cd treated cells, values are between 20 and 25, without any difference even during the growth period.

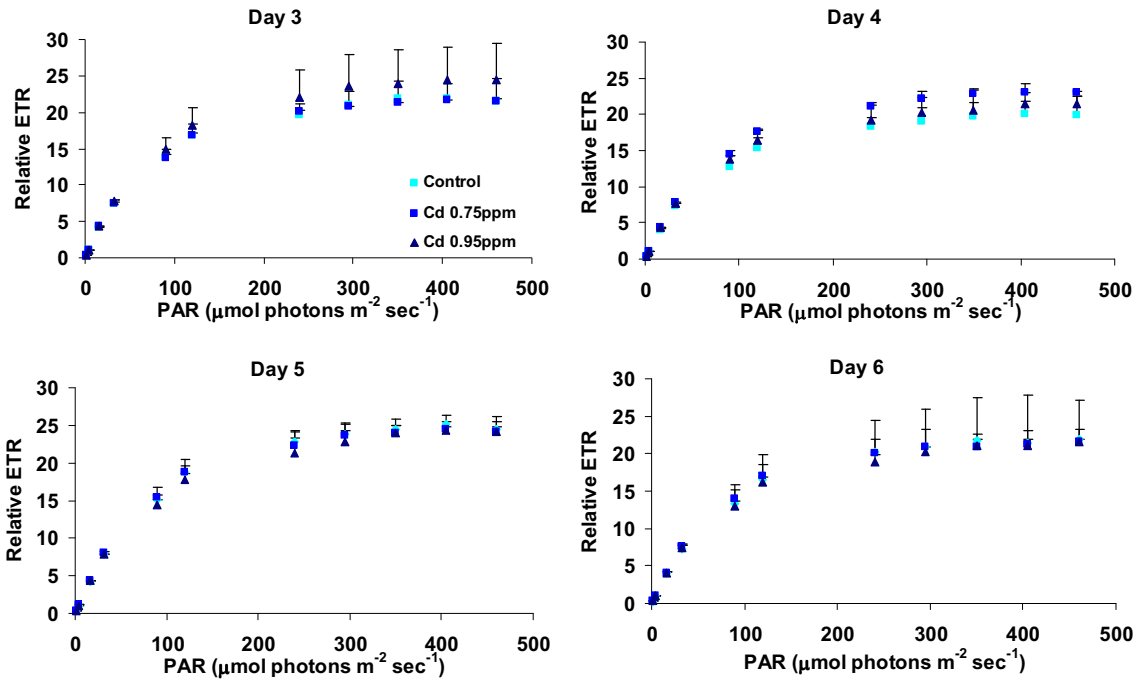

Figure 30: Rapid light curves obtained with a Phyto-PAM and measured every day during the exponential growth. PAR intensity was increased every 30 seconds. On the y-axis is represented the relative electron transport, (rETR= 0.84*0.5*photon flux*Yield). Two replicates; means ± dev.st.

In Figure 31 rapid light curves of cultures grown under UV lights are represented. At day 4 the maximum rETR measured just after 12 hours of UV lights on, was 25 in both control and Cd treated cells; from day 5 to 7 this values decreased to 15. The $rETR_{max}$ values, measured every day after a dark period of 8-10 hours, were always around 15. There are no differences between control and Cd exposed cells.

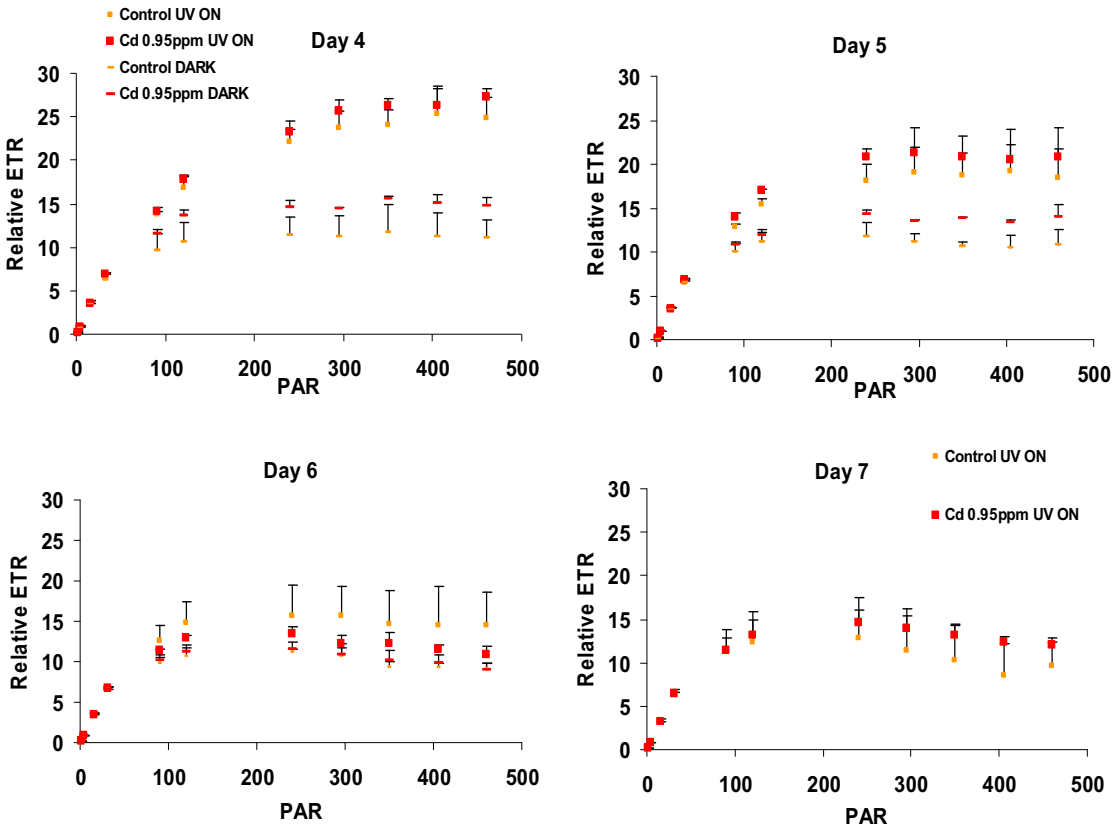

Figure 31: Rapid light curves of cultures grown with UV radiation (12:12h). Two replicates, rETR are expressed as means ± St.dev.

Several parameters were estimated from these rapid light curves. Cultures treated with different Cd concentrations (0.5, 0.75 and 0.95 ppm) grown under PAR light, did not exhibit differences in α_{ETR}, I_k, P_{max}, I_{max}, (data not shown). When cells were exposed to UV radiation, (Fig.32), α_{ETR} did not change during growth, while I_k, P_{max}, I_{max} decreased, showing the lowest values after 8-10 hours of dark. There are no differences between control and Cd treated cells.

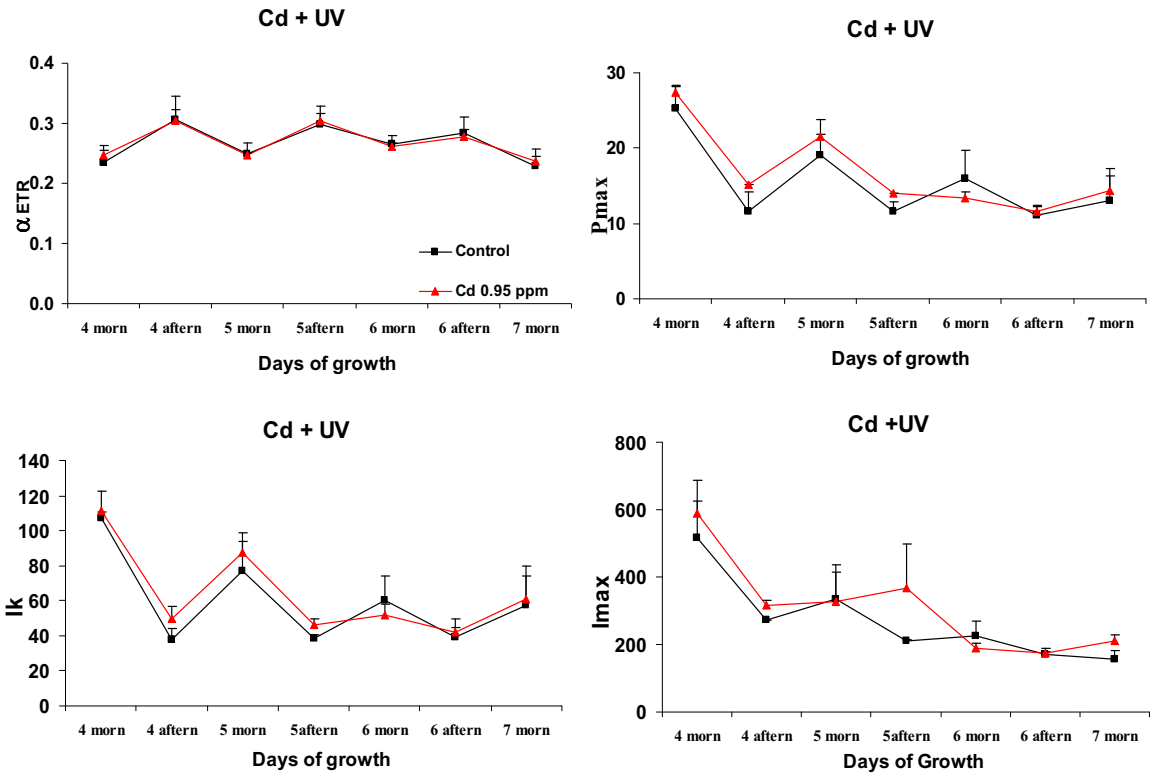

Figure 32: Kinetic parameters calculated from the rapid light curves on cultures grown with UV radiation (12:12h).Measurements were done in the Morning, after 12 hours of UV lamps on and in the Afternoon after 8-10 hours of dark.

Experiments with *Dunaliella tertiolecta*.

Effects on Growth. Cells of *D. tertiolecta* were grown with different Cd concentrations (Tab.8, test 1) ranging from 1 to 15 ppm. Values of the relative growth rates are shown in the table 3; above 3 ppm the percentage of growth reduction compared to control was always around 50 %, thus we decided to do a fine tuning between 3 and 6 ppm of Cd, (test 2).

Test1 Cd (ppm)	μ (h^{-1})	St dev.	% Growth Reduction vs control	Test 2 Cd (ppm)	μ (h^{-1})	St dev.	% Growth Reduction vs control
control	0.028	0.004	/	control	0.024	0.005	/
1	0.034	0.002	-20	3	0.015	0.001	37.7
3	0.017	0.001	41.6	4	0.005	0.003	78.2
5	0.012	0.006	56.1	5	0.007	0.001	72.2
10	0.016	0.001	42.8	6	0.008	0.001	67.2
15	0.013	0.005	53.6				

Tab. 8: Changes in growth rates (μ) of *Dunaliella tertiolecta* grown with different Cd concentrations (n= 3 replicates); the yellow columns represent the decrease in growth as a percentage of control.

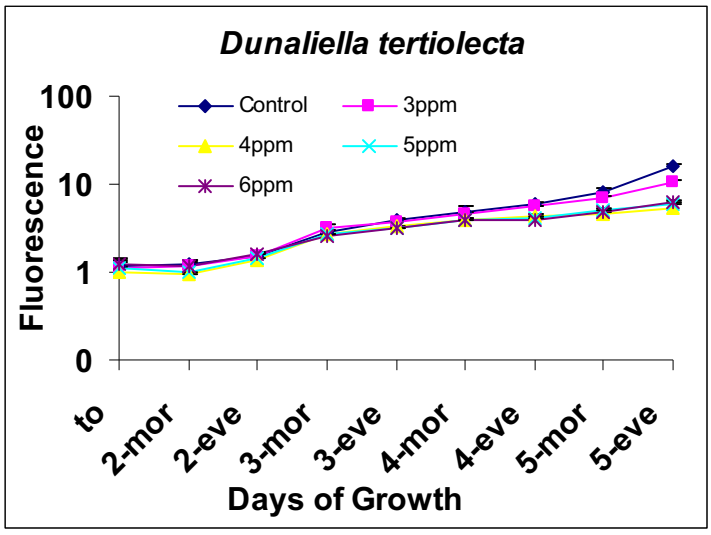

Fig.33: Growth curves, under different Cd concentrations, measured by following fluorescence emission. Fluorescence is expressed on a logarithmic scale. Measurements were done twice a day. The initial density corresponds to of 10000 cell ml^{-1}.

The growth curve is shown in figure 33, while the growth rates are reported in table 8; above 4 ppm the percentage of growth reduction is around 70% while at 3 ppm is of 38%, thus we decided to choose 3 and 3.7 ppm as the concentrations for all the experiments with PAR lights, and 3.7 ppm for all the experiments with UV. In figure 34 (A, B, C) all the relative growth curves are reported. Cells grown with 3 ppm of Cd had a growth rate of 0.17 (μ (d^{-1}), St.dev. 0.06) while that of the control was 0.43 ± 0.04; the percentage of growth reduction is 61% in Cd treated cells, even if at day 11th they reached the same cells number than the control, (Fig. 34-A).

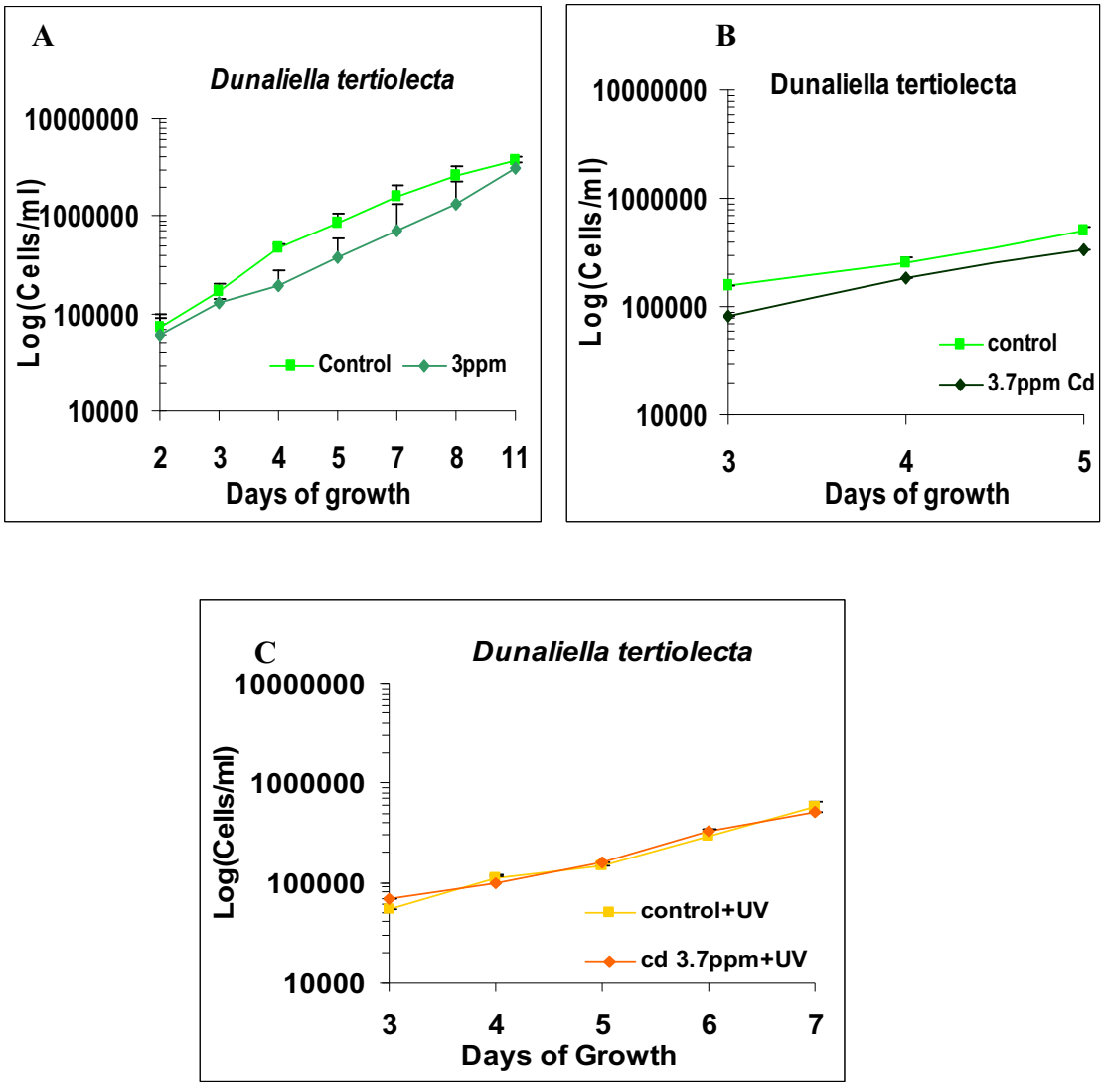

Fig.34: A-B) Growth curves of cultures exposed to Cd and PAR light. In A the culture was followed for 11 days, while in B only for 5 days. C) Growth curves of *D. tertiolecta* exposed to Cd and UV treatment. The starting density is 10000 cells ml^{-1} in all cultures.

Cultures exposed to PAR light and grown with 3.7 ppm Cd exhibited a higher μ with respect of the control, 0.69 d^{-1} ± 0.10 and 0.59 d^{-1} ± 0.009 respectively, (Fig. 34-B). Nevertheless, Cd treated cultures after 5 days of growth had a lower cell number with respect to the control. Finally, when cultures were exposed to UV radiation for 12 hours a day, (Fig.34-C), the growth rates of control and Cd treated cells were 0.71 ± 0.13 and 0.60 ± 0.01 respectively, (15% of growth reduction, but not statistically different), even if with no differences in the final cell number. As observed also with *C. closterium*, cultures grown under UV, required 1-2 days more to reach the same cell density of cultures grown only under PAR light.

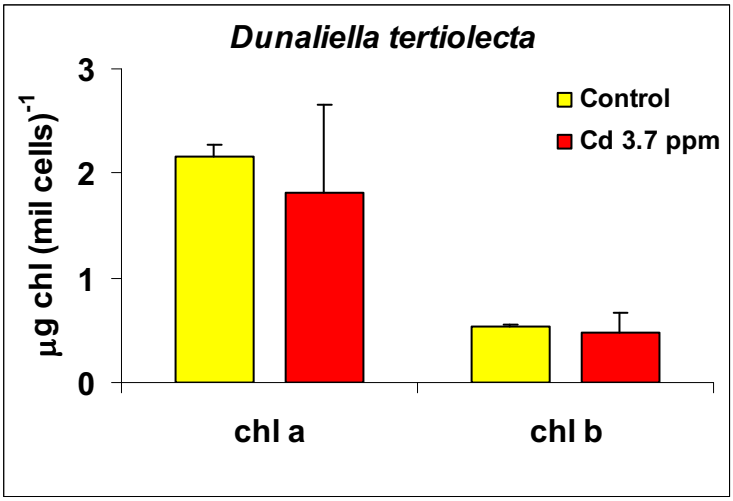

Figure 35: Chlorophyll content, expressed in μg per million of cells, of control and Cd treated cultures (3.7 ppm), both grown under UV radiations. Two replicates for each condition, data analyzed with Statsoft (One way ANOVA).

The chlorophyll content of cultures grown under UV was measured, (Fig. 35). There are no significant differences between control and Cd treated cells (3.7 ppm), (One way ANOVA, $p>0.5$).

Effects on carbon assimilation, production and respiration. Kinetics parameters obtained from oxygen evolution vs DIC concentrations for cultures exposed to increasing Cd concentrations under PAR and UV lights are shown in figure 36.

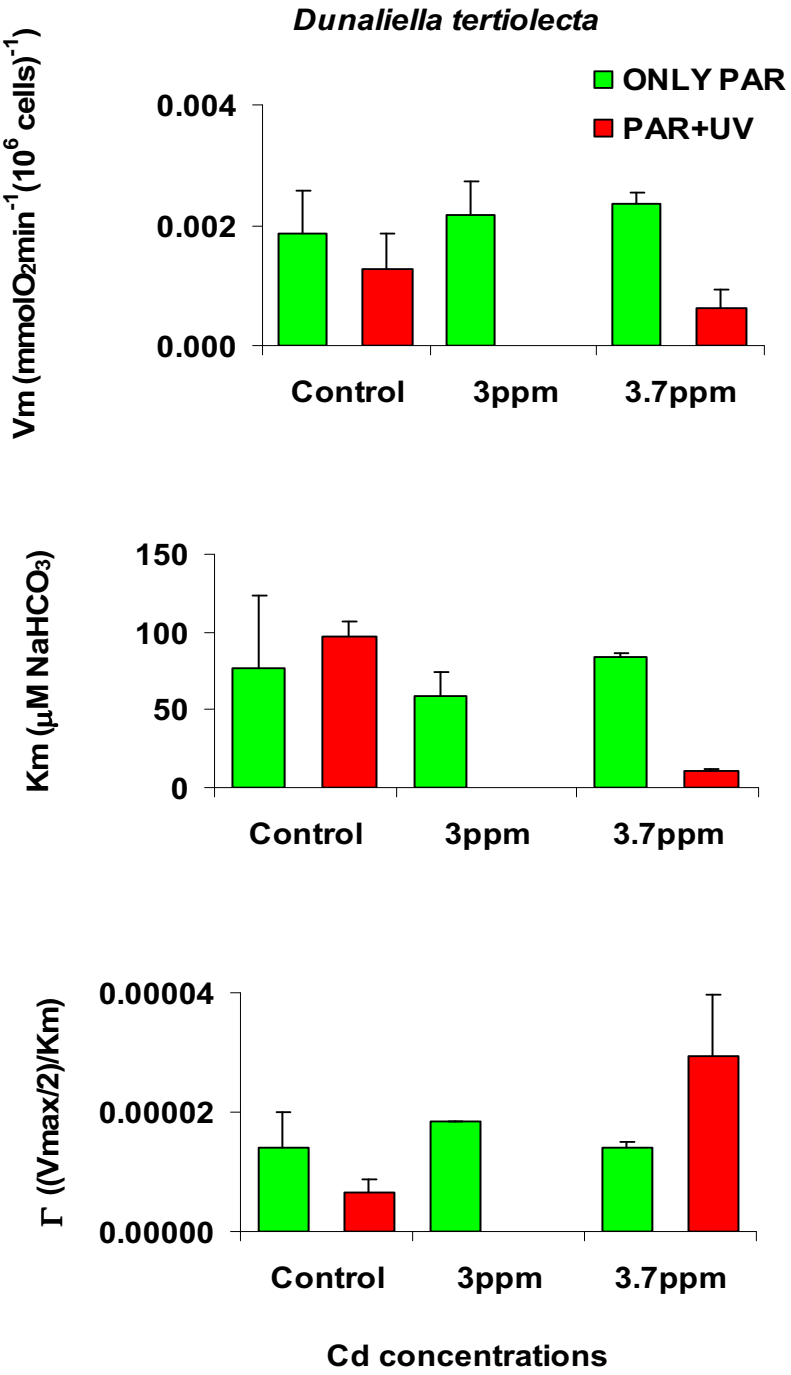

Figure 36: Kinetic parameters obtained from oxygen evolution vs [DIC] plots. Values are an average of two replicates. Data obtained from experiments with Cd (3 and 3.7 ppm) under PAR light and Cd (3.7 ppm) under UV are presented.

Under PAR light, the maximum rate of oxygen evolution (V_m), the DIC concentration at which oxygen evolution occurred at half of the maximum rate (K_m) and the conductance values (Γ), did not change with increasing Cd concentrations. On the other hand, when algae were grown under UV radiation both control and Cd (3.7 ppm) treated cells were affected. In fact, control cultures exhibited a lower V_m and Γ and a slightly higher K_m. The effect on Cd treated cells was even stronger if compared to the control; V_m and K_m are much lower, while Γ is far higher.

In figure 37, the ratios between production and respiration for all the conditions tested are reported. The two Cd concentrations tested on cultures grown under PAR light (upper graph), did not produce any effects on P/R ratios.

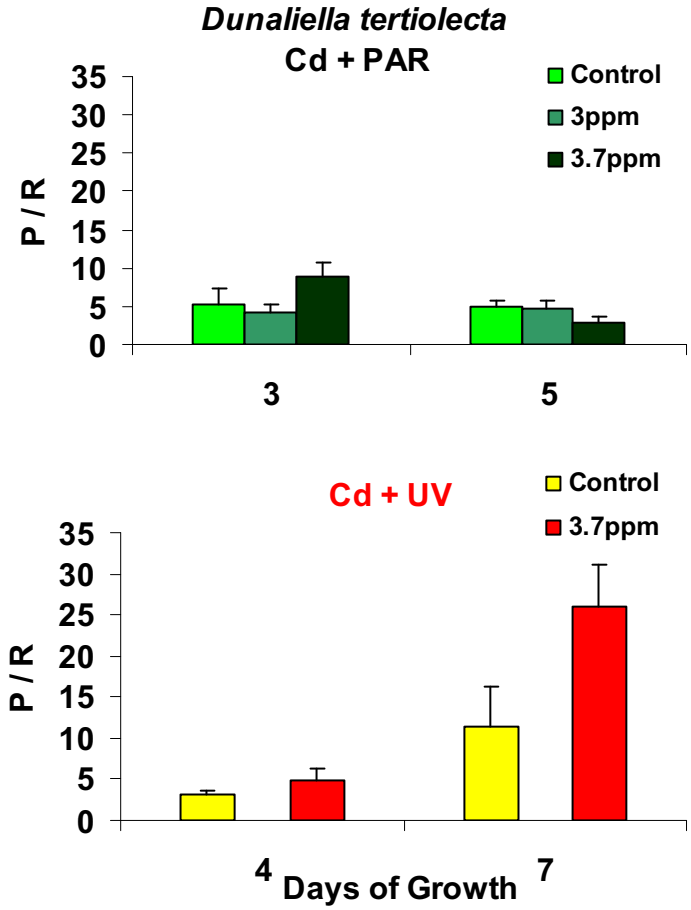

Figure 37: Ratios of production and consumption of oxygen measured with the oxygraph. Values are all divided by cell number and averaged from two replicates. Saturating light intensity used during measurements of oxygen production was 300 µmol photons m^{-2} sec^{-1}.

Only at the higher Cd concentration (3.7 ppm) there was a decrease of the ratio with increasing age of the culture (from day 3 to 5), which was mainly due to an increase in respiration processes. A stronger effect was observed on cultures grown under UV lights (Fig. 37, lower graph). Control cultures had lower P/R ratio at day 4 than those grown under PAR, but it increased at day 7. The same behaviour was observed in cultures grown with Cd and UV and the P/R ratios were even higher than that of control cultures.

Effects on photosynthesis. The maximum quantum yield of PSII was measured as an expression of PSII capacity in sub-samples of cultures dark adapted for ten minutes. Algae grown with 3 ppm of Cd did not show differences with respect to control cultures, (data not shown, factorial ANOVA, $p>0.05$). Similar results were found when cells were grown with 3.7 ppm of Cd under PAR light, (Fig. 38-A). The addition of UV radiation led to a decrease in the maximum yield both in control and Cd treated cells, (Fig.38-B). The maximum yield of PSII in control algae dropped to 0.422 after the first 12 hours of UV (day 3 morning), and then recovered to 0.517 after 12 hours of dark. This trend was observed every day, but the difference due to the succession of UV lights and dark was less severe after 7 days.

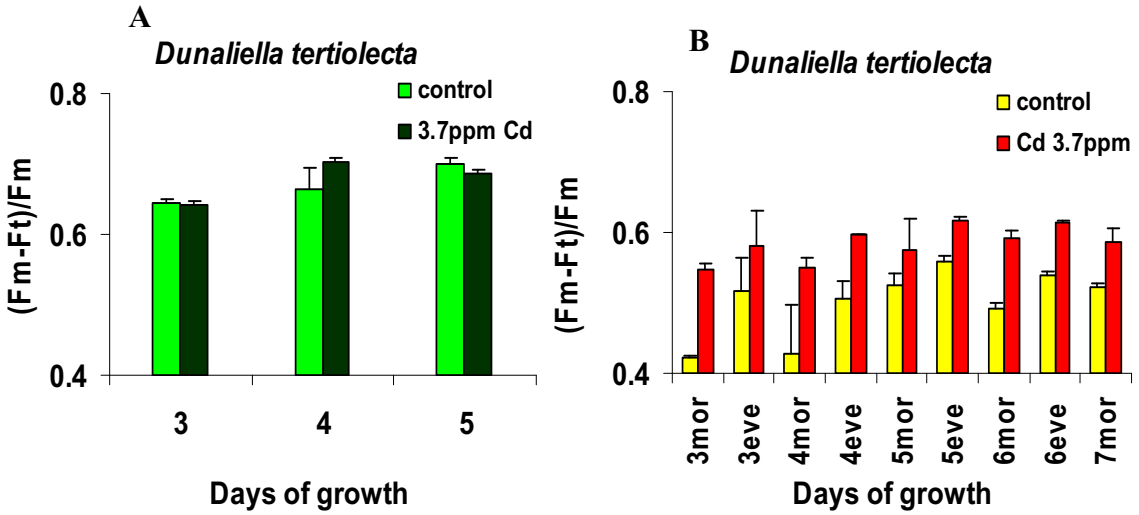

Figure 38: A) Maximum dark adapted yield of cultures exposed to Cd (3.7 ppm) and PAR light (12:12h). Measures taken every day during the exponential phase, two replicates. B) Maximum dark adapted yield of control and Cd treated (3.7 ppm) cultures exposed to UV, (12:12h). Measures were taken twice a day: in the morning after 12 hours of UV light ON, and in the late afternoon after 8-10 hours of dark. Two replicates.

Cultures treated with 3.7 ppm of Cd and UV lights had a maximum yield of PSII of 0.548 after the first 12 hours of exposure to UV radiation and then recovered to 0.582 after 12 hours of dark. After 3 days of exposure to UV, Cd treated cells had a higher maximum quantum yield of PSII compared to control cells, this difference was less marked during the growth of the culture.

As described also for *C. closterium*, the relative electron transport rate (rETR) was calculated from the rapid light curves measured with the Phyto-PAM every day.

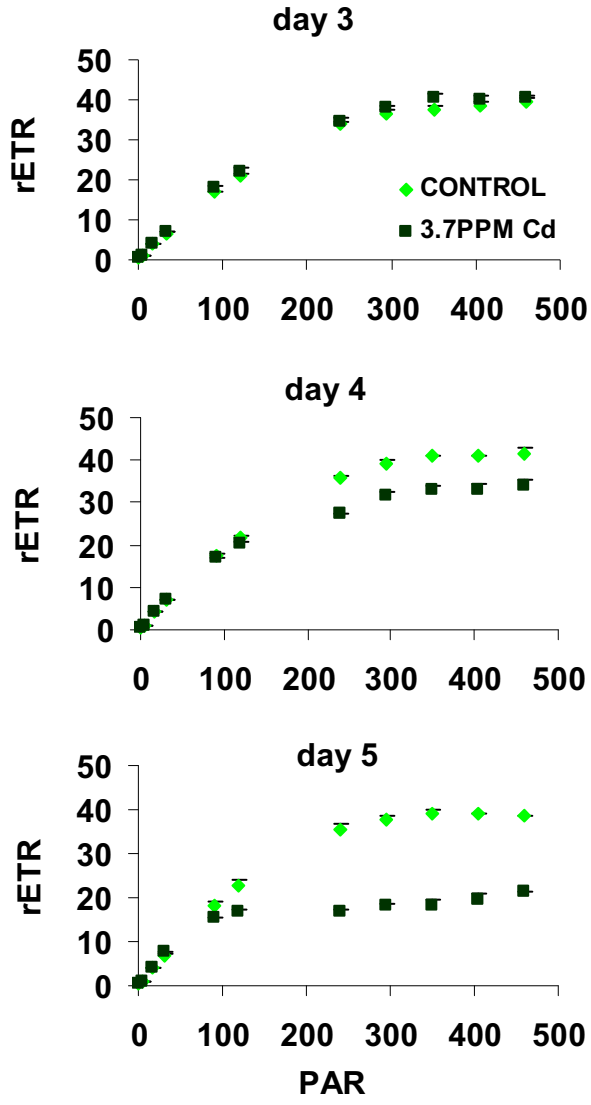

Figure 39: Rapid light curves obtained with a Phyto-PAM and measured every day during the exponential growth phase. PAR intensity was increased every 30 seconds. On the y-axis is represented the relative electron transport, (rETR= 0.84*0.5*photon flux*Yield). Two replicates; means ± St dev.

The maximum rETR of control and Cd treated cells (3 ppm) grown under PAR light was 40 in the first 5 days of growth and then decreased to 20-30 at day 9, (data not shown). In figure 39 the rETR of cultures grown with 3.7 ppm of Cd are reported. Control cells had a stable rETR during the 5 days of growth, with maximum values around 40, while Cd treated cells exhibited a decrease in the $rETR_{max}$ from 40 to 20. Due to the cadmium effect, P_{max} and I_k decreased during the 5 days of growth while alpha and I_{max} increased, (Fig. 40).

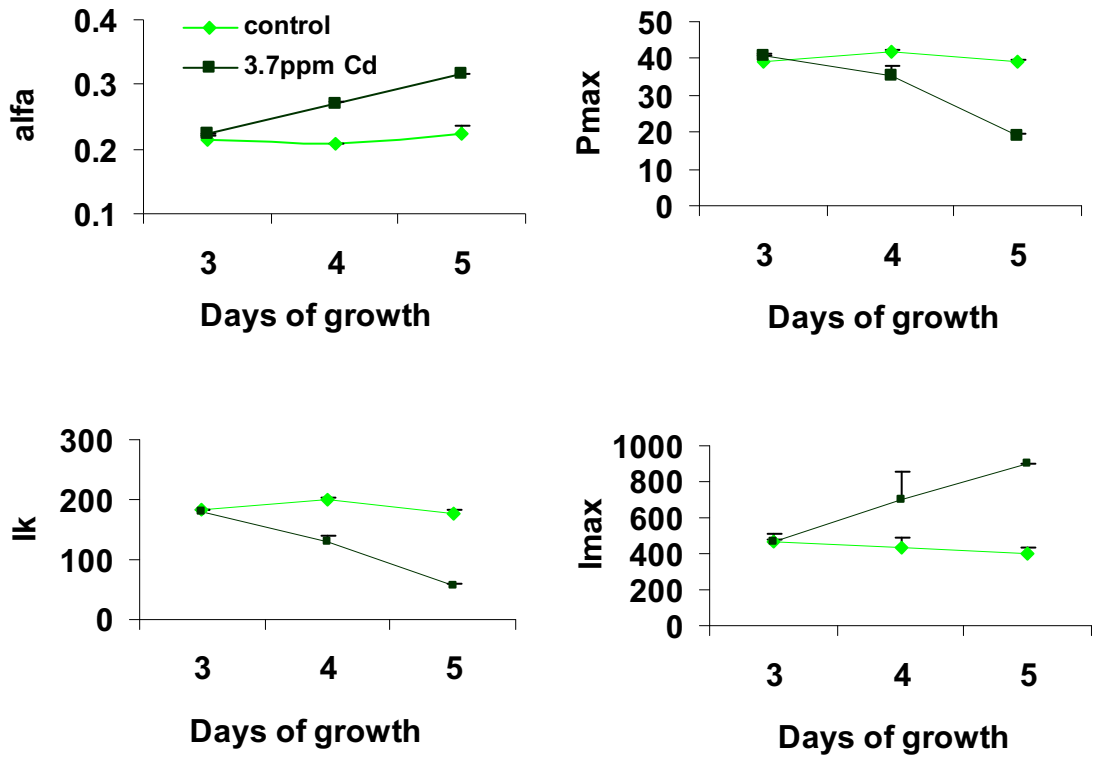

Figure 40: Kinetic parameters calculated from the rapid light curves on cultures grown with UV radiation (12:12h).

When algae where grown with UV radiation the $rETR_{max}$ of both control and Cd treated cells were 20 and 25 respectively and they did not change during the 7 days of growth, (Fig.41). When the relative electron transport was measured after 8-10 hours of dark it was always higher than after 12 hours of exposure to UV.

Furthermore, the rETRmax of cells grown with 3.7 ppm of Cd and UV was always slightly higher than that of control cells.

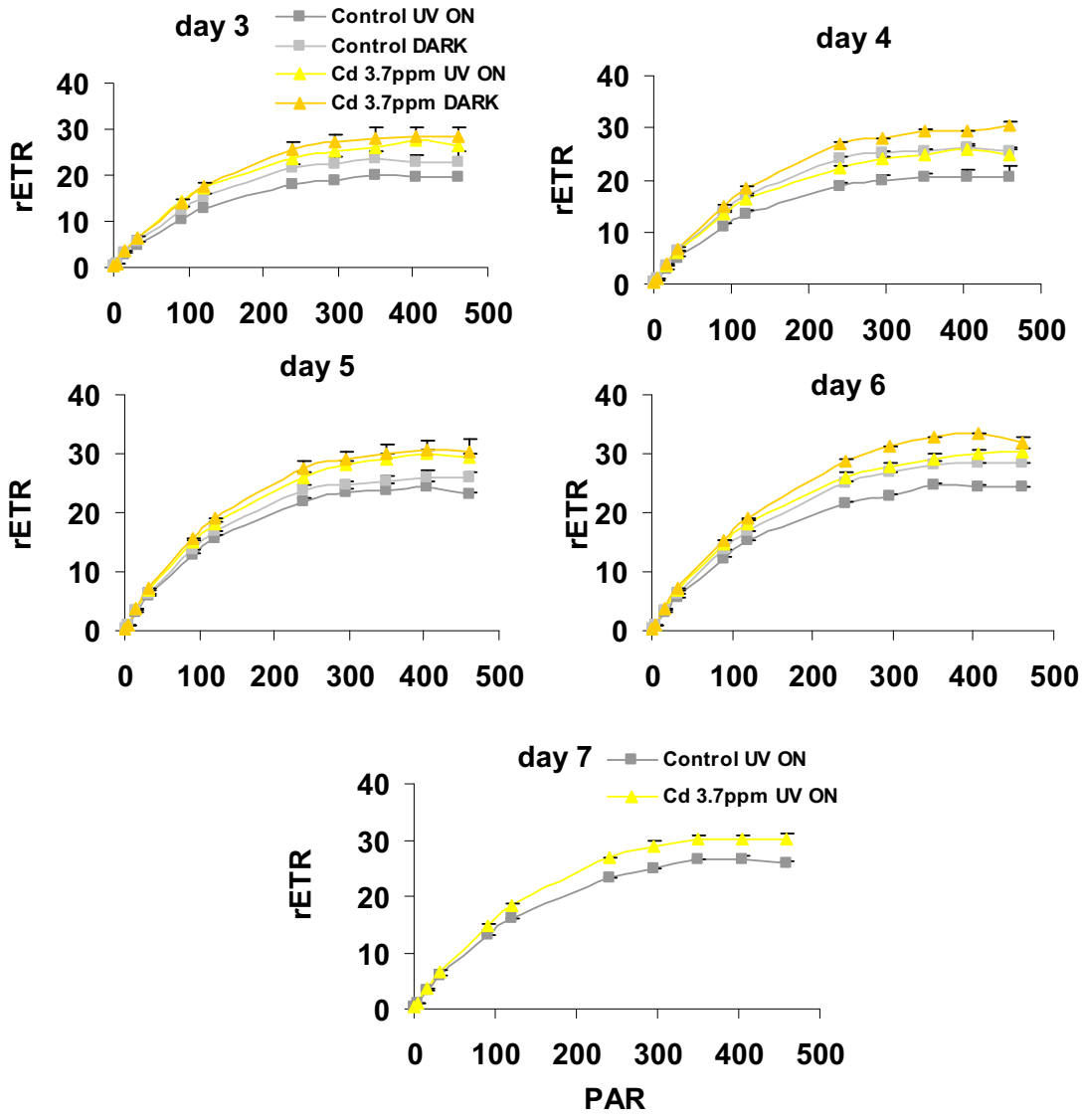

Figure 41: Rapid light curves of cultures grown with UV radiation (12:12h). Two replicates,. rETR are expressed as means ± st. dev.

The kinetic parameters obtained did not show variations during growth, and the values of all parameters were somewhat higher in Cd treated cells than in control cells, (Fig.42).

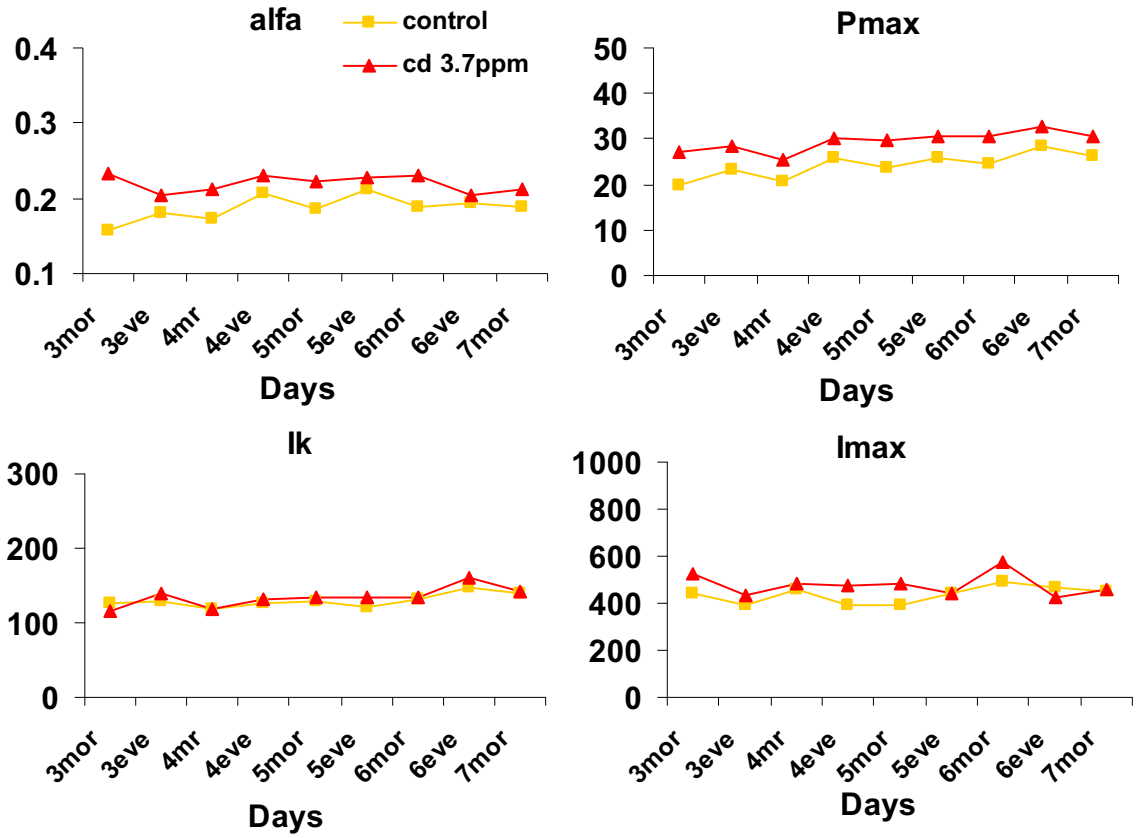

Figure 42: Kinetic parameters calculated from the rapid light curves on cultures grown with UV radiation (12:12h). RLC were measured every morning after 12 h of UV lights on and in the afternoon after 8-10 hours of dark.

6.4 DISCUSSION

The experiments described above were designed to test the effects of a heavy metal (cadmium) alone and in combination with ultraviolet radiation, on two different species of microalgae, *D. tertiolecta* and *C. closterium*. The green alga *D. tertiolecta* was more Cd-resistant than the diatom; in fact *C. closterium* showed a reduction in the growth rate of 50 % with 1 ppm of Cd, while *D. tertiolecta* required exposure to 4-5 ppm to obtain the same percentage of growth reduction. This is consistent with the fact that the sensitivity to heavy metals is species-dependent (Blanck *et al*., 1984; Blanck & Wangberg, 1988). Results suggest that the lower cadmium concentrations, tested under PAR lights on *D. tertiolecta*, were not able to inhibit carbon assimilation and oxygen production; photosynthesis was impaired only with 3.7 ppm of Cd, which resulted in a 50% reduction of the $rETR_{max}$. This lack of effect may be due to protective mechanisms activated by the cells, such as extracellular ligands or phytochelatin production, which may reduce cadmium toxicity (Rauser, 1995; Cobbett and Goldsbrough, 2002).

The diatom *C. closterium* grown with 0.5, 0.75 and 0.95 ppm of Cd under PAR lights also exhibited a good resistance, with no variations on chlorophyll content, photosynthesis or P/R ratio. However, results also suggest that the DIC acquisition was increased when cells were grown with 0.5 ppm of Cd, (higher conductance and lower Km). At the higher Cd concentrations tested here, (0.75 and 0.95 ppm), the DIC affinity decreased. Even though we did not measure external carbonic anhydrase nor directly measure CCM activity, in this species, we may hypothesize a different role for cadmium, at 0.5 ppm, other than a toxic one. In fact, cadmium has been suggested to play a role as a nutrient for the diatom *Thalassiosira weissflogii*, (Lee *et al*., 1995) and it was found to be the co-factor in the metallo-enzyme carbonic anhydrase (CA) in the same microalga (Cullen *et al*., 1999).

The presence of UV during growth had negative effects on both species. Inhibition of oxygen evolution and inorganic carbon assimilation by UVBR is well documented in both macroalgae (Häder *et al*., 1996) and phytoplankton (Lesser *et al*., 1994). The diatom *C. closterium* grown here with UVBR (12:12h) exhibited a decrease in inorganic carbon affinity (higher Km and lower

conductance), oxygen evolution, PSII activity and relative electron transport. This was also observed in *Dunaliella tertiolecta*, even if the effects on carbon assimilation and oxygen evolution were less pronounced than in *C. closterium*. In contrast, the inhibition of PSII activity observed in *D. tertiolecta* was more severe.

The uptake of CO_2 and HCO_3^- by CCM involves cyclic photophosphorylation associated with electron transport around PSI, while the assimilation of inorganic carbon requires noncyclic electron transport and the concerted action of PSI and PSII, (Palmqvist *et al*., 1990; Bendall and Manasse, 1995). Beardall and colleagues (2002) reported that a short time exposure of *D. tertiolecta* to UVBR (2.8 Wm^{-2}) seriously impaired PSII but only slightly damaged PSI activity, thus, the capacity of cells to actively transport inorganic carbon was not affected. Our results suggested that a long time exposure of *D. tertiolecta* to a lower dose of UVBR strongly damaged the PSII activity, but did allow recovery processes, and only slightly inhibited carbon uptake and oxygen production. This is consistent with the results found by Heraud & Beardall (2000). The same exposure to UVBR of the diatom *C. closterium* did affect the activity of PSII and strongly inhibited inorganic carbon assimilation. In any case the UVBR fluence rates used in this study allowed some recovery processes to occur.

The maximum photosynthetic capacity ($rETR_{max}$) measured under PAR light in *C. closterium* is far lower than that of *D. tertiolecta*, but in both species, UV treatment caused a 50% reduction of this parameter. Our results underline the different sensitivity to UVB radiation of the two species. It is thus very important to study these effects on many species to be able to predict effects on a community scale. Moreover, due to the predicted rises of global atmospheric CO_2, which would down-regulate the CCM activity (Miller *et al*., 1984; Shirawa & Miyachi, 1985), it would be also important to analyze the effects of UVBR under different CO_2 concentrations, to understand the complex interactions between the components of the global climate change and the physiological performance of different species of phytoplankton.

Interactions between cadmium and UVB were measured here in those cultures grown under the concomitant action of the two stress factors. Only few

studies that analyze these interactions are available in the literature and most of those have been carried out on plants and cyanobacteria. Rai *et al*., (1998) have suggested that UVB may affect heavy metal uptake by altering membrane permeability, as a result of peroxidation of membrane lipids in UVB exposed cells. Synergistic effects of UVB (0.4 Wm^{-2}) and different Cd concentrations were evaluated in wheat seedlings, (Shukla *et al*., 2002); these authors found that at Cd concentrations higher than 1 ppm, growth retardation and chlorosis were significant and these effects were enhanced in the presence of UVB. In fact, cadmium may damage different photosynthetic targets such as Chlorophyll, photosystems II and I, oxygen evolving complex, Rubisco and others enzymes of the Calvin cycle, (Sanità di Toppi *et al*., 1999; Popovic *et al*., 2003).

In our study we observed a decrease in Chl *a* and *b* content of cells exposed to UVB, both in *D. tertiolecta* and *C. closterium*; these results are congruent, since chlorophyll and the photosynthetic machinery are recognized targets of UVB, (Jansen *et al*., 1998). The bryophyte *Jungermannia exsertifolia* exposed to 0.56 ppm of Cd showed a decrease of Fv/Fm, ETRmax, Chl a/b ratio and carotenoids and a sharper inhibition of all these parameters when exposed to Cd and UVB together, (Otero *et al*., 2006). Nevertheless, the concomitant presence of Cd did not cause a further decrease of chl content in the two species studied.

Physiological damage is usually enhanced by the combination of Cd and UV radiation, (Shukla *et al*., 2002; Shukla & Kakkar, 2002; Prasad *et al*., 2005), although this intensification may depend on the variable considered. In our study, in fact, significant synergistic effects of Cd and UVB showed themselves in inhibiting carbon assimilation and decreasing production-respiration rates in *Cylindrotheca closterium*, while not altering the photosynthetic apparatus. On the contrary , the green alga *Dunaliella tertiolecta* exhibited a higher activity of CCM, an increase in P/R ratio and a higher $rETR_{max}$. These different effects of Cd in the presence of UVB on the two species considered, may be due to several reasons. Firstly, there are some inter-specific differences, as control cultures of *D. tertiolecta* exposed only to PAR lights are more Cd-resistant, they have an higher content of Chl *a* and *b* and a rETRmax twice that of the diatom

C. closterium. Moreover, heavy metals can be chelated by organic ligands exuded by cells during growth; polysaccharide production in algae is well documented. The degree to which these substances are produced is dependent on many factors and may be also species-dependent. Natural DOC is a major agent of UV attenuation in most waters, and is believed to provide protection against UV to aquatic organisms, (Scully & Lean, 1994; West *et al*., 1999). Interactions between natural DOC and UV radiation may be complex and there is some evidence that copper bioavailability can be increased, (West *et al*., 2003). It is thus possible that some kind of interactions occurred, under the conditions tested here, which benefited an increased Cd bioavailability for the diatom or a decrease for the green alga. Finally, we can also hypothesize some more active protective mechanisms in *D. tertiolecta*.

APPENDIX

Appendix A

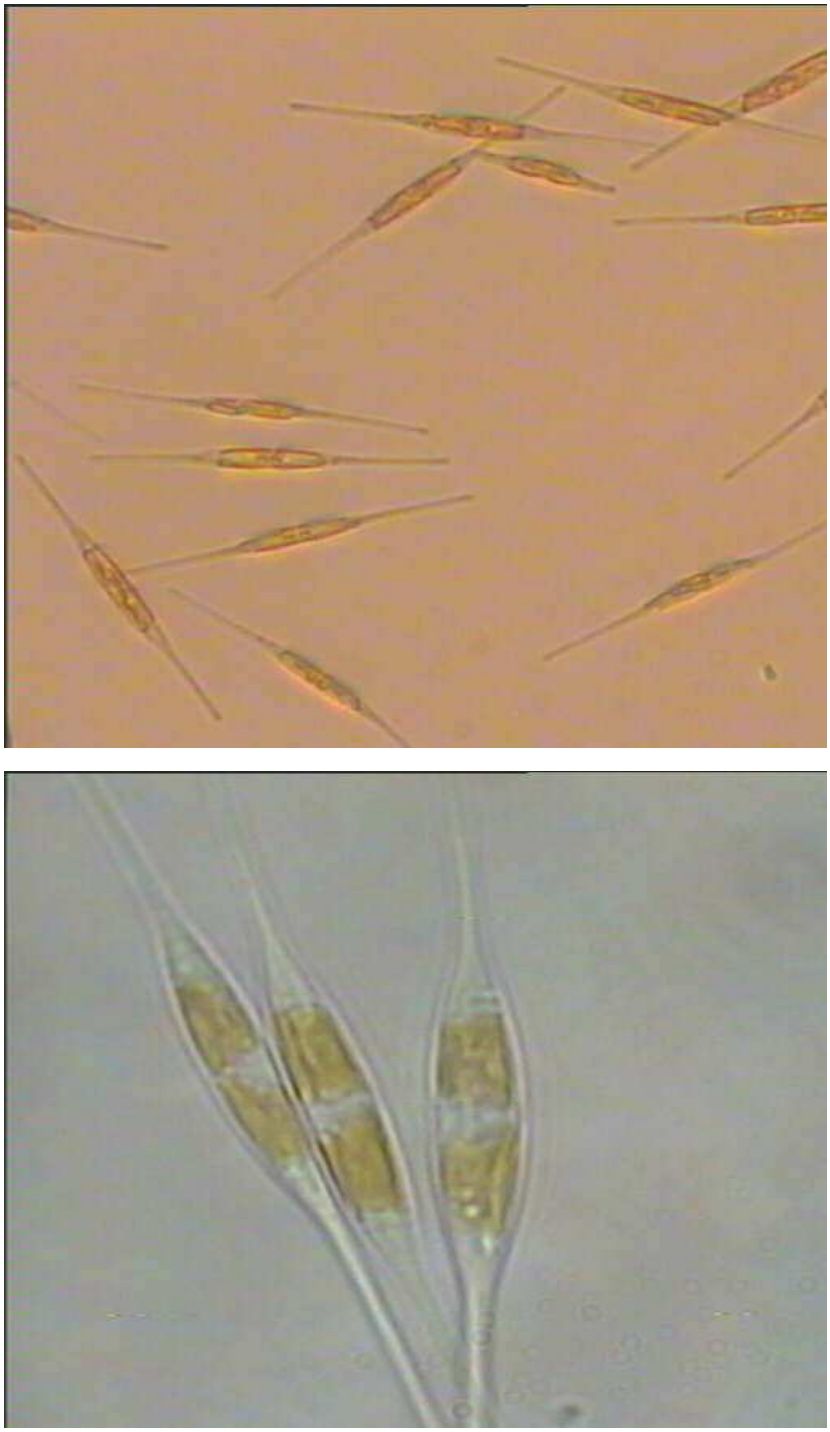

Light microscopy pictures of *Cylindrotheca closterium* (Pialassa strain).

Appendix B

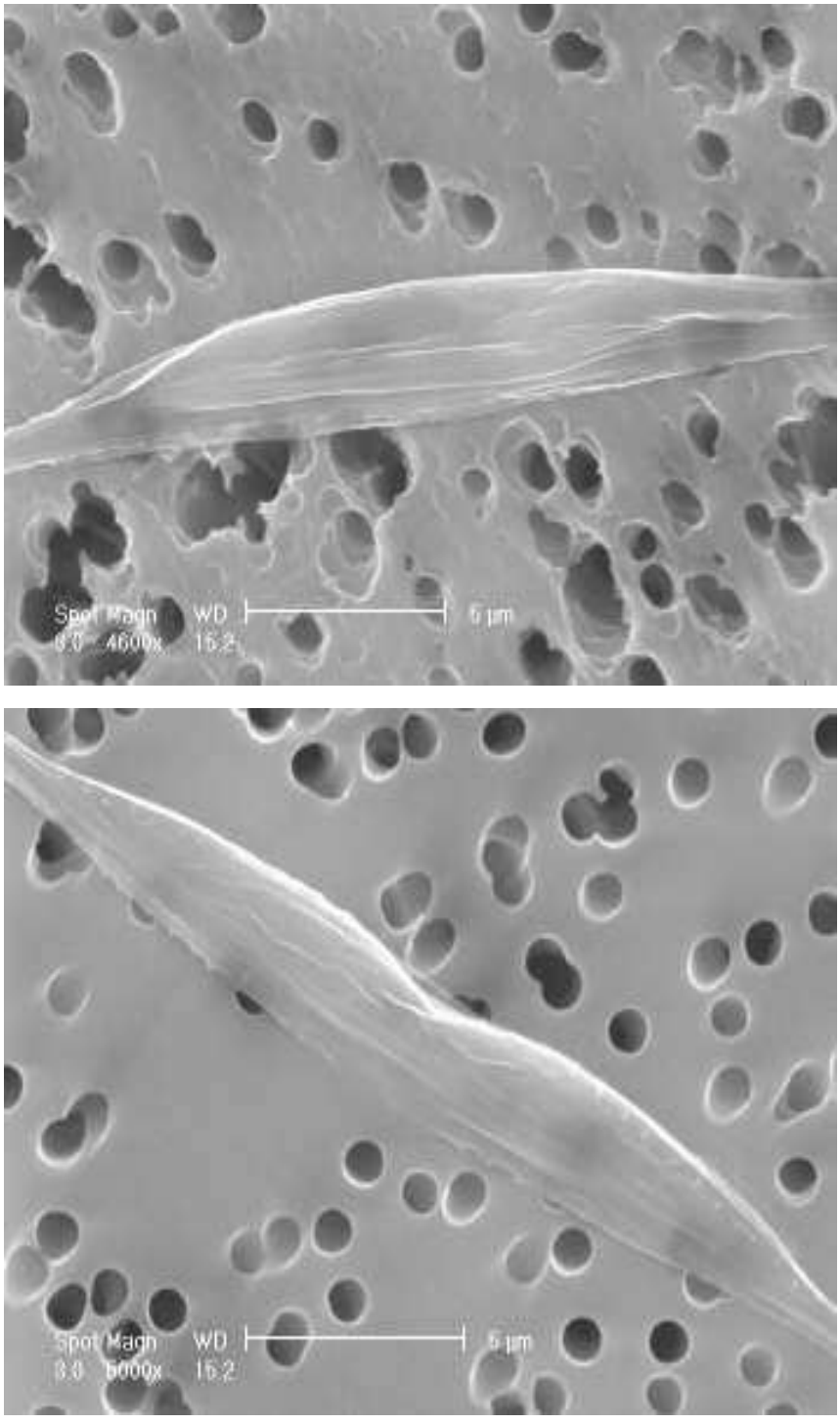

Electron microscopy images (SEM); zoom on valves of *C. closterium*.

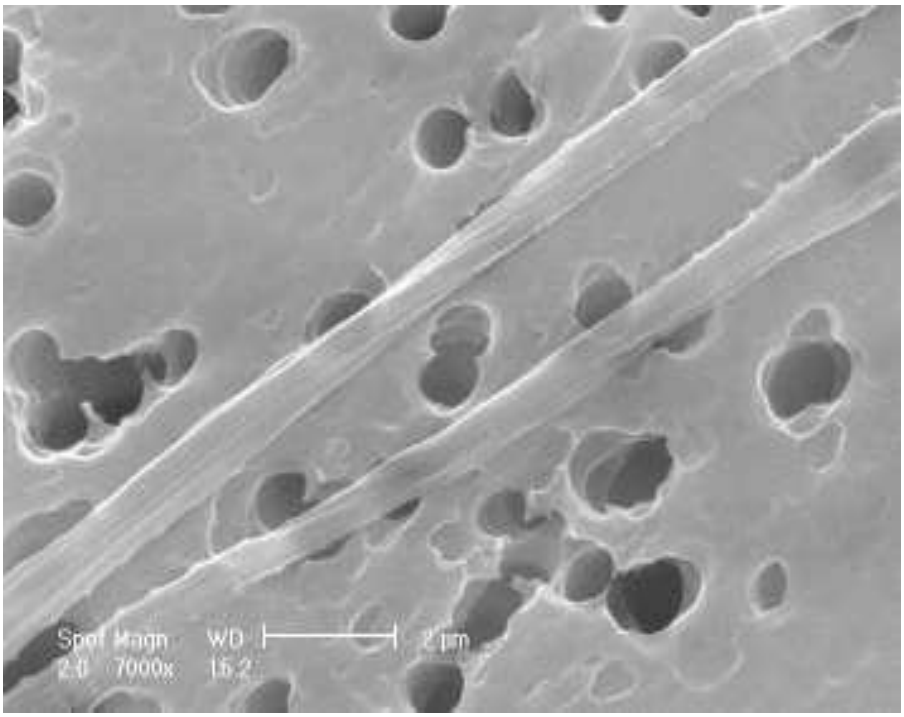

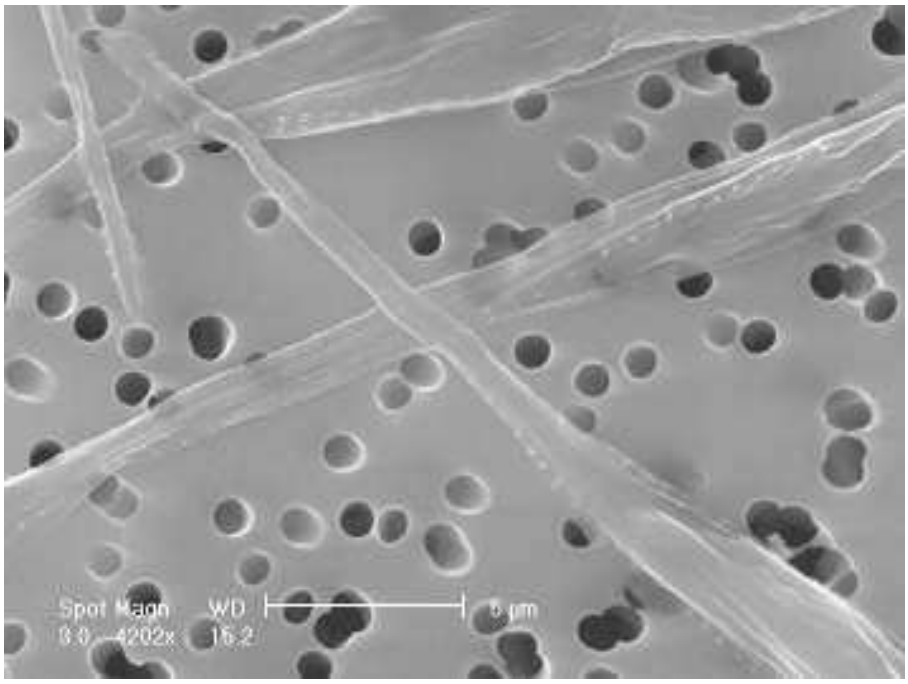

Electron microscopy micrographs, frustule details.

Appendix C

	g L^{-1} stock solution	Final concentration in media
Salt solution I -anhydrous salts		
NaCl	21.19	363 mM
Na_2SO_4	3.55	25 mM
KCl	0.599	8.04 mM
$NaHCO_3$	0.174	2.07 mM
KBr	0.0863	725 µM
H_3BO_3	0.0230	372 µM
NaF	0.0028	65.7 µM
Salt solution II –hydrated salts		
$MgCl_2 \cdot 6H_2O$	9.59	41.2 mM
$CaCl_2 \cdot 2H_2O$	1.344	9.14 mM
$SrCl_2 \cdot 6H_2O$	0.0218	82 µM
Major nutrients I-nitrate		
$NaNO_3$	46.7	549 µM
Major nutrients II -phosphate		
$NaH_2PO_4 \cdot H_2O$	3.09	21 µM
Major nutrients III -silicate		
$Na_2SiO_3 \cdot 9H_2O$	15	105 µM
Metals stock I –iron		
$FeCl_3 \cdot 6H_2O$	1.77	6.56 µM
$Na_2EDTA \cdot 2H_2O$	3.09	6.56 µM
Metals stock II –trace metals		
$ZnSO_4 \cdot 7H_2O$	0.073	254 nM
$CoSO_4 \cdot 7H_2O$	0.016	5.69 nM

$MnSO_4 \cdot 4H_2O$	0.54	2.42 µM
$Na_2MoO_4 \cdot 2H_2O$	1.48×10^{-3}	6.1 nM
Na_2SeO_3	1.73×10^{-4}	1 nM
$NiCl_2 \cdot 6H_2O$	1.49×10^{-3}	6.3 nM
$Na_2EDTA \cdot 2H_2O$	2.44	8.29 µM
Vitamin stock		
Thiamine- HCl	0.1	297 nM
Biotin	0.002	4.09 nM
B_{12}	0.001	1.47 nM

REFERENCES

Al-Medhi A.B., Shuman H., Fisher A.B., 1997. Oxidant generation with K+ - induced depolarization in the isolated perfused lung. *Free Radical Biology Medicine*, **23**: 47-56.

Amoroso G., Sültemeyer D.F., Thyssen C., Fock H.P., 1998. Uptake of HCO^{3-} and CO_2 in cells and chloroplasts from microalgae *Chlamydomonas reinhardtii* and *Dunaliella tertiolecta*. *Plant Physiology*, **116**: 193-201.

Anderson D.M., Morel F.M.M., 1978. Copper sensitivity of *Gonyaulax tamarensis*. *Limnology and Oceanography*, **23**: 283-295.

Andersson A., Halcky P., Hagstrom A., 1994. Effect of temperature and light on the growth of micro-, nano-, and pico-plankton: impact on algal succession. *Marine Biology* **120**: 511-520.

Asada K., Takahashi M., 1987. Production and scavenging of active oxygen in photosynthesis. *In*: Kyle D. J., Osmond C., Arntzen C. J. (Eds) Photoinhibition. Elsevier, New York, pp. 227-297.

Babu T.S., Marder J.B., Tripuranthakam S., Dixon D.G., Greenberg B.M., 2001. Synergistic effects of a photooxidized polycyclic aromatic hydrocarbon and copper on photosynthesis and plant growth: evidence that in vivo formation of reactive oxygen species is a mechanism of copper toxicity. *Environmental Toxicology and Chemistry*, **20**: 1351-1358.

Barranguet C., Kromkamp J., 2000. Estimating primary production rates from photosynthetic electron transport in estuarine microphytobenthos. *Marine Ecology Progress Series*, **204**: 39-52.

Beardall J., Beer S., Raven J. A., 1998. Biodiversity of marine plants in an era of climate change: some predictions on the basis of physiological performance. *Botanica marina* **41**: 113-123.

Beardall J., Heraud P., Roberts S., Shelly K., Stojkovic S., 2002. Effetcs of UVB radiation on inorganic carbon acquisition by the marine microalga *Dunaliella tertiolecta* (Chlorophyceae). *Phycologia*, **41** (3): 268-272.

Beardall J., Quigg A., Raven J.A., 2003. Oxygen consumption: photorespiration and chlororespiration. *In*: Photosynthesis in Algae, (Larkum, A.W.D. Duglas, S.E. Raven, J.A. editors), 157-181. Kluwer Academic Publishers.

Beardall J., Raven J.A., 2004. The potential effects of global climate change on microbial photosynthesis, growth and ecology. *Phycologia*, **43**: 26-40.

Beherenfield M.J., Lean D.R.S., Lee H., 1995. Ultraviolet-B radiation effects on inorganic nitrogen uptake by natural assemblages of oceanic plankton. *Journal of Phycology*, **31**: 25-36.

Behrenfeld M. J., Esaias W. E., Turpie K. R., 2002. Assessment of primary production at the global scale. *In*: Phytoplankton productivity. Carbon assimilation in marine and freshwater ecosystems. (Ed. By P. J. Williams, D. N. Thomas, C. S. Reynolds), pp. 156-186. Blackwell Science, Oxford.

Behrenfeld M. J., Randerson J. T., McClain C. R., Feldman G. C., Los S. O., Tucker C. J., Falkowski P. G., Field C. B., Frouin R., Esaias W. E., Kolber D. D., Pollack N. H., 2001. Biospheric primary production during an ENSO transition. *Science*, **291**: 2594-2597.

Bendall D.S., Manasse R.S., 1995. Cyclic photophosphorylation and electron transport. *Biochimica et Biophysica Acta*, **1229**: 23-38.

Berges J.A., Franklin D.J., Harrison P., 2001. Evolution of an artificial seawater medium: improvements in enriched seawater, artificial water over the last two decades. *Journal of Phycology*, **37**: 1138-1145.

Bischof K., Hanelt D., Wiencke C., 2000. Effects of ultraviolet radiation on photosynthesis and related enzyme reactions of marine macroalgae. *Planta*, **211(4)**: 555-562.

Blank H., Wallin G., Wangberg S.A., 1984. Species-dependent variation in algal sensitivity to chemical compounds. *Ecotoxicology and Environmetal Safety*, **8(4)**: 339-351.

Blank H., Wangberg S.A., 1988. Induced community tolerance in marine priphyton established under arsenate stress. *Canadian Journal of Fisheries and Aquatic Sciences*. 45(10): 1816-1819.

Blumthaler M., Ambach W., 1990. Indication of increasing solar ultraviolet-B radiation flux in alpine regions. *Science*, **248**: 206-208.

Bolhar-Nordenkampf H.R., Long S.P., Baker N.R., Oquist G., Schreiber U., Lechner E.G., 1989. Chlorophyll fluorescence as a probe of the photosynthetic competence of leaves in the field: a review of current instrumentation. *Functional Ecology*, **3**: 497-514.

Bolhar-Nordenkampf H.R., Oquist G.O., 1993. Chlorophyll fluorescence as atool in photosynthesis research. *In*: Hall D.O., Seurlock J.M.O., Bolhar-Nordenkampf H.R., Leegood R.C., Long S.P. (Eds.), Photosynthesis and production in a changing environment: A field and laboratory manual. Chapman & Hall, London, pp. 193-206.

Boni L., Guerrini F., Pistocchi R., Cangini M., Pompei M., Cucchiari Emellina Romagnoli T., Totti C., 2005. Microalghe tossiche del Medio ed Alto Adriatico. Guida per Acquacoltori ad Operatori sanitari.

Borkowski J., 2000. Homogenisation of the Belsk UVB series (1976-1997) and trend analysis. *Journal Geophysical Research*, **105**: 4873-4878.

Boscolo P.R.S., Menossi M., Jorge R.A., 2003. Aluminium-induced oxidative stress in maize. *Phytochemistry*, **62**: 181-189.

Bradford M., 1976. A rapid and sensitive method for the quantification of microgram quantities of protein utilizing the principle of protein-dye binding. *Analytical Biochemistry*, **180**:136-139.

Brand L.E., Sunda W.G., Guillard R.R.L., 1986. Reduction of marine phytoplankton reproduction rates by copper and cadmium. *Journal of Experimental Marine Biology and Ecology*, **96**: 225-250.

Brash D. E., Franklin W. A, Sancar G. B., Haseltine W. A., 1985. *Escherichia coli* DNA photolyase reverses cyclobutane dimmers but not pyrimidine-pyrimidone (6-4) photoproducts. *Journal of Biological Chemistry*, **260**: 11438-11441.

Britt A. B., 1996. DNA-damage and repair in plants. *Annual reviews of plant physiology and plant molecular biology*, **47**: 75-100.

Buma A. G. J., Van Hannen E. J., Veldhuis M. J., Gieskes W. W. C., 1996a. UV-B induces DNA-damage and DNA-synthesis delay in the marine diatom *Cyclotella* sp. *Scientia Marina*, **60**: 101-106.

Buma A. G. J., Zemmelink H. J., Sjollema K., Gieskes W. W. C., 1996b. UVB radiation modifies protein, photosynthetic pigment content, volume and ultrastructure of marine diatoms. *Marine Ecology Progress Series*, **142**: 47-54.

Buma A.G.J., Helbling E.W., De Boer M.K., Villafane V.E., 2001. Patterns of DNA damage and photoinhibition in temperate South Atlantic picophytoplankton exposed to solar radiation. *Journal of Photochemistry and Photobiology B: biology*, **62**: 9-18.

Buma A.G.J., Van Oijen T., Van de Poll W., Veldhuis M.J.W., Gieskes W.W.L., 2000. The sensitivity of *Emiliana huxleyi* (Prymnesiophyceae) to ultraviolet-B radiation. *Journal of Phycology*, **36**: 296-303.

Burkardt S., Zondervan I., Riebesell U., Sultemeyer D., 2001. CO_2 and HCO_3^- uptake in marine diatoms acclimated to different CO_2 concentrations. Limnology and Oceanography 46: 1378-1391.

Chubarova N. Y. and Nezval Y. I., 2000. Thirty year variability of UV irradiance in Moscow. *Journal of Geophysical Research*, **105**: 12529-12539.

Cobbett C., Goldsbrough P., 2002. Phytochelatins and metallothioneins: role in heavy metal detoxification and homeostasis. *Annual Review of Plant Biology*, **53**: 159-182.

Cullen J.T., Lane T.W., Morel F.M.M, Sherrell R.M., 1999. Modulation of cadmium uptake in phytoplankton by seawater CO_2 concentration. *Nature*, **402(11)**: 165-167.

Cumming J. R., Gregory J. T., 1990. Mechanisms of metal tolerance in plants: physiological adaptation for exclusion of metal ions from the cytoplasm. *In*: Alscher R. G., Cumming J. R. (Eds) Stress Responses in plants: Adaptation and Acclimatation Mechanisms. Wiley-Liss, New York, pp. 338-355.

Daugbjerg N., Hansen G., Larsen J., Moestrup Ø., 2000. Phylogeny of some of the major genera of dinoflagellates based on ultrastructure and partial LSU rDNA sequence data, including the erection of three new genera of unarmoured dinoflagellates. *Phycologia,* **39**: 302-317.

De Brouwer J.F.C., Wolfstein K., Stal L.J., 2002. Physical characterization and diel dynamics of different fractions of extracellular polysaccharides in an axenic culture of a benthic diatom. *European Journal of Phycology*, **37**:37-44.

Dietz K.J., Bair M., Krämer U., 1999. Free radicals and reactive oxygen species as mediators of heavy metals toxicity in plants. *In*: Prasad M.N.V., Hagemeyer J. (Eds.), Heavy metal stress in plants: from molecular to ecosystems. Springer-Verlag, Berlin, pp. 73-97.

Dix T.A., Aikens J., 1993. Mechanisms and biological relevance of lipid peroxidation initiation. *Chemical Research in Toxicology*, **6**: 2-18.

Döhler G., Hagmeier E., David C., 1995. Effects of solar and artificial UV radiation on pigments and 15N ammonium and 15N nitrate by macroalgae. *Journal of photochemistry and Photobiology B. Biology*, **30**: 179-187.

Dubois M., Gilles K.A., Hamilton J.K., Rebers P.A., Smith F., 1956. Colorimetric method for determination of sugar and related substances. *Analitical Chemistry*, **28**: 350-356.

Eilers P.H.C., Peeters J.C.H., 1988. A model for the relashionship between light intensity and the rate of photosynthesis in phytoplankton. *Ecological Modelling*, **42**:199-215.

Filatov D.A. (2002). ProSeq: A software for preparation and evolutionary analysis of DNA sequence data sets. *Molecular Ecology Notes*, **2**: 621-624.

Fisher N.S., Frood D., 1980. Heavy metals and marine diatoms: influence fo dissolved organic compounds on toxicity and selection for metal tolerance among four species. *Marine Biology*, **59**: 85-93.

Fisher N.S., Jones G.J., nelson D.M., 1981. Effects of copper and zinc on growth, morphology and metabolism of *Asterionella japonica* (Cleve). *Journal of Experimental Marine Biology and Ecology*, **51**: 37-56.

Foyer C.H., Noctor G., 2000. Tansley Review No. 112. Oxygen processing in photosynthesis: regulation and signalling. *New Phytologist*, **146**: 359-388.

Franklin L. A. and Forster R. M., 1997. The changing irradiance environment: consequences for marine macrophyte physiology, productivity and ecology. *European Journal of Phycology*, **32(3)**: 207-232.

Gaur J.P, Rai L.C., 2001. Heavy metal tolerance in algae. *In*: Rai L.C., Gaur J.P. (Eds.), Algal Adaptation to environmental stresses: physiological, biochemical and molecular mechanisms. Springer-Verlag, Berlin, pp. 363-388.

Genty B., Briantais J.M., Baker N.R., 1989. The relationship between the quantum yield of photosynthetic electron transport and quenching of chlorophyll fluorescence. *Biochima Biophysica Acta*, **990**: 87-92.

Gerringa L.J.A., Rijstenbil J.W., Poortvliet T.C.W., van Drie J., Schot M.C., 1995. Speciation of copper and responses of the marine diatom *Ditylum brightwelli* upon increasing copper concentrations. *Aquatic Toxicology*, **31**: 77-90.

Gigon A., Matos A.R., Laffray D., Zuily-Fodil Y., Phamthi A.T, 2004. Effect of drought stress on lipid metabolism in the leaves of *Arabidopsis thaliana* (ecotype Columbia). *Annals of Botany*, **94**: 345-351.

Girotti A.W., 1998. Lipid hydroperoxide generation, turnover and effector action in biological systems. *Journal of Lipid Research*, **30**: 1529-1539.

Godhe A., Otta S.K., Rehnstam-Holm A.S., Karunasagar I., Karunasagar I., 2001. Polymerase chain reaction in detection of *Gymnodinium mikimotoi* and *Alexandrium minutum* in field samples from Southwest India. *Marine Biotechnology*, **3**:152-162.

Goffart A., Heco J. H., Legendre L., 2002. Changes in the development of the winter-spring phytoplankton bloom in the bay of Calvi (NW Mediterranean) over the last two decades: a response to changing climate? *Marine Ecology Progress Series*, **236**: 45-60.

Häder D. P., 1993. Risk of enhanced solar ultraviolet radiation for aquatic ecosystems. *In*: Round F. E., Chapman D. J., (Eds), Progress in Phycological Research. Biopress Bristol, UK, pp: 1-45.

Häder D.P., Herrmann H., Santas R., 1996. Effects of solar radiation and solar radiation deprived of UVB and total UV on photosynthetic oxygen production and pulse amplitude modulated fluorescence in the brown alga *Padina pavonia*. *FEMS Microbiology and Ecology*, **19**: 53-61.

Hansen, G., Daugbjerg, N., Franco, J. M, 2003. Morphology, toxin composition and LSU rDNA phylogeny of *Alexandrium minutum* (Dinophyceae) from Denmark, with some morphological observations on other European strains. *Harmful Algae*, **2**:317-335.

Heraud P., Beardall J., 2000. Changes in chlorophyll fluorescence during exposure of *Dunaliella tertiolecta* to UV radiation indicate a dynamic interaction between damage and repair processes. *Photosynthesis Research*, **63**: 123-134.

Hermes-Lima M., Willimore W.G., Storey K.B., 1995. Quantification of lipid peroxidation in tissue extracts based on Fe(III)Xilenol Orange complex formation. *Free Radical Biology & Medicine*, **19**:271-280.

Hofmann D. J., Deshler T., 1991. Evidence from balloon measurements for chemical depletion of stratospheric ozone in the Artic winter of 1989-1990. *Nature*, **349**: 300-305.

Houghton J. T., Ding Y., Griggs D. J., Noguer M., Van der Linden P. J., Dai X. Maskell L., Jhonson C. A., 2001. Climate change 2001: the scientific basis. Cambridge University Press, Cambridge. 881 pp.

Houghton J. T., Jenkins G. J., Ephraums J. J., 1990. Climate change. The IPCC scientific assessment. Cambridge University Press, Cambridge. 365 pp.

Hughes K. A., Overpeck J. T., Peterson L. C., Trumbore S., 1996. Rapid climate changes in the tropical atlantic region during the last deglaciation. *Nature*, **380**: 51-54.

Ishii N., Goto S., Hartman P.S., 2002. Protein oxidation during aging of the nematode *Caeonorhabditis elegans*. *Free Radicals in Biology and Medicine*, **33**: 1021-1025.

Iturbe-Ormaetxe I., Escuredo P.R., Arrese-igor C., Becana M., 1998. Oxidative damage in Pea plants exposed to water deficit or paraquat. *Plant Physiology*, **116**: 173-181.

Izard J., Limberger R.J., 2003. Rapid screening method for quantitation of bacterial cell lipids from whole cells. *Journal of Microbiological Methods*, **55**: 411-418.

Jansen M.A.K., Gaba V., Greenberg B.M., 1998. Higher plants and UVB radiation: balancing damage, repair and acclimation. *Trends Plant Science*, **3**: 131-135.

Jeffrey S.W., Humphrey G.F., 1975. New spectrophotometric equations for determining chlorophylls *a*, *b*, c_1, and c_2 in higher plants, algae and natural phytoplankton. *Biochemical Physiology Plants*, **167**: 191-194.

Jeffrey W. H., Aas P., Lyons M. M., Coffin R. B., Pledger R. J., Mitchell D. L., 1996. Ambient solar radiation-induced photodamage in marine bacterioplankton. *Photochemistry and photobiology*, **64**: 419-427.

Juneau P., Popovic R., 1999. Evidence for the rapid phytotoxicity and environmental stress evaluation using the PAM fluorometric method: Importance and future application. *Ecotoxicology*, **8**: 449-455.

Karentz D., Cleaver J. E., Mitchell D. L., 1991. Cell survival characteristics and molecular responses of Antarctic phytoplankton to ultraviolet-B radiation. *Journal of Phycology*, **27**: 326-341.

Kautsky H., Hirsch A., 1931. Neue Versuche zur Kohlensäure-assimilation. *Naturwissenschaften*, **19**: 964.

Klatt P., Lamas S., 2000. Regulation of protein function by S-glutathione in response to oxidative and nitrosative stress. *European Journal of Biochemistry*, **267**: 4928-4944.

Knight J.A., Shauna A:, Rawle J.M., 1972. Chemical Basis of the Sulfo-phospho-vanillin method for estimating total serum lipids. *Clinical Chemistry*, **18**: 199-203.

Kriedemann P.F., Graham R.D., Wiskich J.T., 1985. Photosynthetic dysfunction and *in vivo* chlorophyll *a* fluorescence from manganese-deficient wheat leaves. *Australian Journal Agricultural Research*, **36**: 157-169.

Krieger-Liszkay A., 2004. Singlet oxygen production in photosynthesis. *Journal of Experimental Botany*, **56(411)**: 337-346.

Krompkamp J., Peene J., 1999. Estimation of phytoplankton photosynthesis and nutrient limitation in the Eastern Scheldt estuary using variable fluorescence. *Aquatic Ecology*, **33**: 101-104.

Kumar S., Tamura K., Nei M. 2004. MEGA3.1: Integrated software for Molecular Evolutionary Genetics Analysis and sequence alignment. Briefings; *Bioinformatics*, **5**: 150-163.

Lage O.M., Parente A.M., Soares H.M.V., Vasconcelos M.T.S.D., Salema R., 1994. Some effects of copper on the dinoflagellates *Amphidinium carterae* and *Prorocentrum micans* in batch culture. *European Journal of Phycology*, **29**: 253-260.

Lao K., Glazer A. N., 1996. Ultraviolet-B photodestruction of a light-harvesting complex. *Proceedings of the National Academy of Sciences*, USA, **93**: 5258-5263.

Lavorel J., Etienne A.L., 1977. In vivo chlorophyll fluorescence. *In*: Primary processes of photosynthesis (J.Barber editor), Vol. II: 203-68. Elsevier/ North-Holland Biomedical Press, Amsterdam.

Lee J.G., Roberts S.B., Morel F.M.M., 1995. Cadmium: a nutrient for the marine diatom *Thalassiosira weissflogii*. *Limnology and Oceanography*, **40(6)**: 1056-1063.

Lee M.Y., Shin H.W., 2003. Cadmium-induced changes in antioxidant enzymes from the marine alga *Nannochloropsis oculata*. *Journal of Applied Phycology*, **15**: 13-19.

Lesser M.P., Cullen J.J., Neale P.J., 1994. Carbon uptake in a marine diatom during acute exposure to ultraviolet B radiation: relative importance of damage and repair. *Journal of Phycology*, **30**: 183-192.

Levine R.L., Garland D., Oliver C.N., Amici A., Climent I., Lenz A.G., Ahn B., Shaltiel S., Stadtman E.R., 1990. Determination of carbonyl content in oxidatively modified proteins. *Methods in Enzymology*, **186**.

Little C., 2000. The biology of soft shores and estuaries. New York Oxford University Press.

Lundholm N., Daugbjerg N., Moestrup O., 2002. Phylogeny of the Bacillariaceae with emphasis on the genus *Pseudo-nitzschia* (Bacillariophyceae) based on partial LSU rDNA. *European Journal of Phycology*, **37**:115-134.

Lyndsay M.A., Giembycz M.A., 1997. Signal transduction and activation of the NADPH oxidase in eosinophils. *Memorias do Instituo Osvaldo Cruz-On line*, 2: 115-123.

Mallick N., 2004. Copper-induced oxidative stress in the chlorophycean microalga *Chlorella vulgaris*: response of the antioxidant system. *Journal Plant Physiology*, **162**: 591-597.

Mallick N., Mhon F.H., 2003. Use of chlorophyll fluorescence in metal-stress research: a case study with the green microalga *Scenedesmus*. *Ecotoxicology and Environmetal Safety*, **55**: 64-69.

Mallick N., Mohn F.H., 2000. Reactive oxygen species: response of algal cells. *Journal of Plant Physiology*, **157**: 183-193.

Malloy K.D., Holman M.A., Mitchell D., Detrich H. W., 1997. Solar UVB-induced DNA damage and photoenzymatic DNA repair in Antarctic zooplankton. *Proceedings of the National Academy of Sciences*, USA, **94**: 1258-1263.

Malone T.C., 1977. Light-saturated photosynthesis by phytoplankton size fractions in the New York Bight, U.S.A. *Marine Biology*, **42**: 281-292.

Masojìdek J., Grobbelaar J.U., Pechar L., Koblizek M., 2001. Photosystem II electron transport rates and oxygen production in natural waterblooms of freshwater cyanobacteria during a diel cycle. *Journal of Plankton Research*, **23**: 57-66.

Matoo A. K., Edelman M., 1987. Intramembrane translocation and post-translational palmitylation of the chloroplast 32K-Da herbicide-binding protein. *Proceedings of the National Academy of Sciences*, USA, **84**: 1497-1501.

McCord J.M., Fridovich I., 1969. Superoxide Dismutase: an enzymatic reaction for erythrocuprein (hemocuprein). *Journal of Biological Chemistry*, **244**: 6049-6055.

McKenzie R. L., Björn L. O., Bais A., Lyasd M., 2003. Changes in biologically active ultraviolet radiation reaching the Earth's surface. *Photochemistry Photobiology Science,* **2**: 5-15.

Melis A., Nemson J. A., Harrison M. A., 1992. Damage to functional components and partial degradation of photosystem II reaction center proteins upon chloroplast exposure to ultraviolet-B radiation. *Biochimica and Biophysica Acta*, **1100**: 312-320.

Miller A.G., Turpin D.H., Canvin D.T., 1984. Growth and photosynthesis of the cyanobacterium *Synechococcus teopoliensis* in HCO_3^-- limited chemostat. *Plant Physiology*, **75**: 1064-1070.

Miserocchi, S., Frascari, F., Guerzoni, S., Langone, L., 1990. Inquinamento da mercurio ed altri metalli pesanti (Pb, Cu, Zn) nei sedimenti delle valli ravennati (Pialassa della Baiona). *Acqua-Aria,* **4**: 361-370.

Mitchell D. L., Nairn R. S., 1989. The biology of the (6-4) photoproduct. *Annual Reviews of Photochemistry and Photobiology*, **49**: 805-819.

Monteiro De Paula F., Pham Thi A.T., Vieira Da Silva J., Justin A.M., Demandre C., Mazliak P., 1990. Effects of water stress on the molecular species composition of polar lipids from *Vigna unguiculata* L. leaves. *Plant Science*, **66**: 185-193.

Neale P.J., 2000. Spectral weighting functions for quantifying effects of UV radiation in marine ecosystems. *In*: The effects of UV radiation in the marine environment (De Mora, SJ. Demers, S. Vernet, M. editors), 72-100. Cambridge University Press, Cambridge.

Okamoto K., Colepicolo P., 1998. Response of Superoxide Dismutase to pollutant metal stress in the marine dinoflagellate *Gonyaulax polyedra*. *Comparative Biochemistry and Physiology*, **119C(1)**: 67-73.

Otero S., Núñez-Olivera E., Martinez-Abaigar J., Tomás R., Arróniz-Crespo M., Beaucourt N., 2006. Effects of cadmium and enhanced UV radiation on the

physiology and the concentration of UV-absorbing compounds of the aquatic liverwort *Jungermannia exsertifolia subsp. cordifolia*. *Photochemical Photobiological Sciences*, **5**: 760-769.

Palmqvist K., Sundblad L.G., Wingsle G., Samuelsson G., 1990. Acclimation of photosynthetic light reactions during induction of inorganic carbon accumulation in the green alga *Chlamydomonas reinhardtii*. *Plant Physiology*, **94**: 357-366.

Peletier H., Gieskes W.W.C., Buma A.G.J., 1996. Ultraviolet-B radiation resistance of benthic diatoms isolated from tidal flats in the Dutch Wadden Sea. *Marine Ecology Progress Series*, **135**: 163-168.

Pérez P., Esteve-Blanco P., Beiras R., Fernández E., 2006. Effect of copper on the photochemical efficiency, growth and chlorophyll a biomass of natural phytoplankton assemblages. *Environmetal Toxicology and Chemistry*, **25**:137-143.

Pinto E., Sigaud-Kutner T. C. S., Leitao M. A. S., Okamoto O. K., Morse D., Colepicolo P., 2003. Heavy metal-induced oxidative stress in algae. *Journal of Phycology*, **39**: 1008-1018.

Pistocchi R., Guerrini F., Balboni V., Boni L., 1997. Copper toxicity and carbohydrate production in the microalgae Cylindrotheca fusiformis and Gymnodiium sp. *European Journal of Phycology*, **32**: 125-132.

Platt T., Gallegos C.L., Harrison W.G., 1980. Photoinibition of photosynthesis in natural assemblages of marine phytoplankton. *Journal of Marine Research*, **38**: 687-701.

Popovic R., Dewez D., Junaeu P., 2003. Applications of chlorophyll flurescence in ecotoxicology: heavy metals, herbicides, and air pollutants. *In*: Practical applications of chlorophyll fluorescence in plant biology; ed. DeEll J.R. and Toivonen P.M.A., Kluwer, Boston, pp. 151-184.

Pospelova V., Chmura G. L., Boothman W. S., Latimer J. S., 2002. Dinoflagellate cyst records and human disturbance in two neighboring estuaries, NewBedford Harbor and Apponagansett Bay, Massachussetts. *Science of the Total Environment*, **298**: 81-102.

Prasad M., Zeeshan M., 2005. UV-B radiation and cadmium induced changes in growth, photosynthesis and antioxidant enzymes of cyanobacterium *Plectonema boryanum*. *Biologia Plantarum*, **49**: 229-236.

Quesada A., Vincent W. F., 1997. Strategies of adaptation by Antarctic cyanobacteria to ultraviolet radiation. *European Journal of Phycology*, **32**:335-342.

Rai L.C., Tyagi B., Rai P.K., Mallick N., 1998. Interactive effects of UVB and heavy-metals (Cu and Pb) on nitrogen and phosphorus metabolism of a N2-fixing cyanobacterium Anabaena doliolum. *Environmetal and Experimental Botany,* **39**: 221-231.

Rauser W. E., 1995. Phytochelatins and related peptides. *Plant Physiology*, **109**: 1141-1149.

Raven J. A., Evans M. C. W., Korb R. E., 1999. The role of trace metals in photosynthetic electron transport in O_2-evolving organisms. *Photosynthesis Research*, **60**: 111- 149.

Raven J. A., Kobler J. E., Beardall J., 2000. Put out the light and then put out the light. *Journal of the Marine Biological Association of the United kingdom*, **80**: 1-25.

Raven J. A., Samuelsson G., 1986. Repair of photoinhibitory damage in *Anacystis nidulans* 625 (Synechococcus 5301): relating catalytic capacity for and energy supply to protein synthesis and implications for P_{max} and the efficiency of light limited growth. *New Phytologist*, **103**: 625-643.

Raven J.A., 1997b. Inorganic carbon acquisition by marine autotrophs. *Advances in Botany Research*, **27**: 85-209.

Raven J.A., 1997c. Putting the C in Phycology. *European Journal of Phycology*, **32**: 319-333.

Rijstenbil J.W., Poortvliet T.C.W., 1992. Copper and zinc in estuarine water: chemical speciation in relation to bioavailability to the marine planktonic diatom *Ditylum brightwelli*. *Environmental Toxicology Chemistry*, **11**: 1615-1625.

Rijstenbil J.W., Wijnholds J.A., 1996. HPLC analyses of nonprotein thiols in planktonic diatoms: pool size, redox state and response to copper and cadmium exposure. *Marine Biology*, **127**: 45-54.

Rijstenbil J.W., 2001. Effects of periodic, low UVA radiation on cell characteristics and oxidative stress in the marine planktonic diatom *Dytilum brightwellii*. *European Journal of Phycology*, **36**:1-8.

Rijstenbil J.W., 2002. Assessment of oxidative stress in the planktonic diatom *Thalassiosira pseudonana* in response to UVA and UVB radiation. *Journal of Plankton Research*, **24**: 1277-1288.

Rijstenbil J.W., 2003. Effects of UVB radiation and salt stress on growth, pigments and antioxidative defence of the marine diatom *Cylindrotheca closterium*. *Marine Ecology Progress Series*, **254**: 37-48.

Rijstenbil J.W., 2005. UV- and salinity-induced oxidative effects in the marine diatom *Cylindrotheca closterium* during simulated emersion. *Marine Biology*, **147**:1063-1073.

Rosen B., 1996. Bacterial resistance to heavy metals and metalloids. *Journal of the Biological Inorganic Chemistry*, **1**: 273-277.

Salawitch R. J., 1998. A greenhouse warming connection. *Nature,* **392**: 551-552.

Sanders J.G., Cibik S.J., 1988. Response of Chesapeake Bay phytoplankton communities to low levels of toxic substances. Marine Pollution Bulletin, **19**: 439-444.

Sanità di Toppi, Gabbrielli R., 1999. Response to cadmium in higher plants. *Environmental Experimental Botany*, **41**: 105-130.

Scholin C.A., Herzog M., Sogin M., Anderson D.M. (1994). Identification of group- and strain specific genetic markers for globally distributed *Alexandrium* (Dinophyceae). II.Sequence analysis of a fragment of the LSU rRNA genes. *Journal of phycology,* **30**: 999-1011.

Schreiber U., Schliwa U., Bilger W., 1986. Continous recording of photochemical and non-photochemical chlorophyll fluorescence quenching with a new type of modulation fluorometer. *Photosynthesis Research*, **10**: 51-62.

Scully N.M., Lean D.R.S., 1994. The attenuation of ultraviolet radiation in temperate lakes. Ergebn. *Limnology*, **43**: 135-144.

Shiraiwa Y., Miyachi S., 1985. Effects of temperature and CO_2 concentration on induction of carbonic anhydrase and changes in efficiency of photosynthesis in *Chlorella vulgaris*. *Plant Cell Physiology*, **26**: 543-549.

Shukla U.C, Kakkar P., 2002. Effect of dual stress of ultraviolet B radiation and cadmium on nutrient uptake of wheat seedlings. Commun. Soil Sci Plant Anal, **33**: 1737-1749.

Shukla U.C., Prasad C.J., Kakkar P., 2002. Synergistic action of Ultraviolet-B radiation and cadmium on the growth of wheat seedlings. *Ecotoxicology and Enivronmental Safety*, **51**: 90-96.

Sigaud-Kutner T.C.S., Pinto E., Neto A.M.P., Colepicolo P., 2005. Changes in antioxidant enzyme activities, malondialdehyde, and glutathione contents in the dinoflagellate *Lingulodinium polyedrum* (Dinophyceae) grown in batch cultures. *Phycological Research*, **53**: 209-214.

Smirnoff N., 1993. Transley Review n. 52. The role of active oxygen in the response of plants to water deficit and dessication. *New Phytologist*, **125**: 27-58.

Stohs S. J., Bagchi D., 1995. Oxidative mechanisms in the toxicity of metal ions. *Free Radical Biology and Medicine,* **18**: 321-336.

Stumm W., Morgan J. J., 1981. Aquatic chemistry: an introduction emphasizing chemical equilibria in natural waters. Wiley, New York, 780 pp.

Sunda W. G., 1988. Trace metal interactions with marine phytoplankton. *Biology Oceanography*, **6**: 411-442.

Sunda W., Guillard R.R.L., 1976. The relashionship between cupric ion activity and the toxicity of copper to phytoplankton. *Journal of marine research*, **134**: 511-529.

Sunda W.A., Huntsman S.A., 1983. Effect of competitive interactions between manganese and copper on cellular manganese and growth in estuarine and oceanic species of the diatom *Thalassiosira*. *Limnology and Oceanography*, **28**: 924-934.

Suzuki Y., Takahashi M., 1995. Growth responses of several diatoms isolated from various environments to temperature. Journal of Phycology, 31: 880-888.

Talling J. F., 1985. Inorganic carbon reserves of natural waters and ecophysiological consequences of their photosynthetic depletion by microalgae. *In*: Inorganic carbon uptake by aquatic photosynthetic organisms (Eds. By Lucas W. J., and Berry J. A.), p. 403-420. American Society of Plant Physiologists, Rockville, Maryland.

Thomas D. J., Thomas J. B., Prier S. D., Nasso N. E., Hebert S. K., 1999. Iron superoxide dismutase protects against chilling damage in the cyanobacterium *Synechococcus* species PCC7942. *Plant Physiology*, **120**: 275-282.

Thompson J.D., Gibson T.J., Plewniak F., Jeanmougin F., Higgins D.G., 1997. The ClustalX windows interface: flexible strategies for multiple sequence alignment aided by quality analysis tools. *Nucleic Acids Research*, **25**: 4876-4882.

Tortell P. D., DiTullio G. R., Digman D. M., Morel E. M. M., 2002. CO_2 effects on taxonomic composition and nutrient utilization in an Equatorial Pacific phytoplankton assemblage. *Marine Progress Series*, **236**: 37-43.

Tripathi B.N., Mehta S.K., Amar A., Gaur J.P., 2006. Oxidative stress in *Scenedesmus* sp. during short- and long-term exposure to Cu^{2+} and Zn^{2+}. *Chemosphere*, **62**: 538-544.

Underwood G.J.C., Kromkamp J.C., 1999. Primary production by phytoplankton and microphytobenthos in estuaries. *Advances in Ecological Research*, **29**: 93-152.

Van Ho A., Ward D. M., Kaplan J., 2002. Transition metal transport in yeast. *Annual Review Microbiology*, **56**: 237-261.

Vass I., 1997. Adverse effects of UVB light on the structure and function of the photosynthetic apparatus. *In:* Handbook of Photosynthesis. Ed. Pessarakli, pp931-949. Marcel Dekker, New York.

Vassiliev I.R., Prasil O., Wyman K.D., Kolber Z.K., Hanson A.K., Prentice J.E., Falkowski P.G., 1994. Inhibition of PSII photochemistry by PAR and UV radiation in natural phytoplankton communities. *Photosynthesis Research,* **42**: 51.

Vavilin D.V., Polynov V.A., Matorin D.N., Venediktov P.S., 1995. Sublethal concentrations of copper stimulate photosystem II photoinhibition in *Chlorella pyrenoidosa*. *Journal of Plant Physiology*, **146**: 609-614.

Vincent W. F., Roy S., 1993. Solar ultraviolet radiation and aquatic primary production: damage, protection and recovery. *Environmental Reviews*, **1**: 1-12.

Vosjan J. K. and Pauptit E., 1992. Penetration of photosynthetically available light (PAR), UV-A and UV-B in Admirably Bay, King Georges Island, Antarctica. Circumpol. Journal, 1-2: 50-58.

Wang W. X., Dei R. C. H., 2001a. Metal uptake in a costal diatom influenced by major nutrients (N, P and Si). *Water Research*, **35**: 315-321.

Wang W. X., Dei R. C. H., 2001b. Effects of major nutrient additions on metal uptake in phytoplankton. *Environmental Pollution*, **111**: 233-240.

West L.J.A., Greenberg B.M., Smith R.E.H., 1999. Ultraviolet radiation effects on a microscopic green alga and the protective effects of natural dissolved organic matter. *Photochemistry and Photobiology*, **69(5)**: 536-544.

West L.J.A., Li K., Greenberg B.M., Mierle G., Smith R.E.H., 2003. Combined effects of copper and ultraviolet radiation on a microscopic green alga in natural soft lake waters of varying dissolved organic carbon content. *Aquatic Toxicology*, **64**: 39-52.

Winterbourn C. C., 1982. Superoxide-dependent formation of hydroxyl radicals in the presence of iron salts is a feasible source of hydroxyl radicals in vivo. *Biochemical Journal Letters*, **205**: 461-463.

Withers K., Tunnel J.W., 1998. Identification of tidal flat alterations and identification of effects on biological productivity of these habitats within the coastal bend. Corpus Christi Bay National Estuary Program, publication CCBNEP 26.

Wu J.T., Hsieh M.T., Kow L.C., 1998. Role of praline accumulation in response to toxic copper in *Chlorella* sp. (Chlorophyceae) cells. *Journal of Phycology*, **34**: 113-117.

Wundram M., Selmer D., Bahadir M., 1996. The *Chlamydomonas* test: a new phytotoxicity test based on the inhibition of algal photosynthesis enables the assessment of hazardous leachates from waste disposals in salt mines. *Chemosphere*, **32**: 1623-1631.

Zerefos C., Balis D. S., Bais A. F., Gillotay D., Simon P. C., Mayer B. and Seckmeyer, 1997. Variability of UVB at four stations in Europe. *Geophysical Research Letters*, **24**: 1363-1366.